

LB/DORU/07/2018

DEVELOPMENT OF A PROSTHETIC HAND FOR POWER GRASPING APPLICATIONS

LIBRARY
UNIVERSITY OF MORATUWA, SRI LANKA
MORATUWA

Herath Mudiyansele Chathura Madhubhashitha Herath

(138109J)

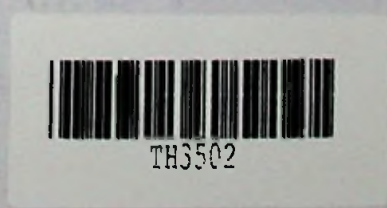
Thesis submitted in partial fulfillment of the requirements for the
Master of Engineering in Manufacturing Systems Engineering

Department of Mechanical Engineering

TH3502+
CD ROM

University of Moratuwa
Sri Lanka

October 2017



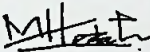
621 "17"
621.7 (043)

TH3502

DECLARATION

I declare that this is my own work and this thesis does not incorporate without acknowledgement any material previously submitted for a Degree or Diploma in any other University or institute of higher learning and to the best of my knowledge and belief it does not contain any material previously published or written by another person except where the acknowledgement is made in the text.

Also, I hereby grant to University of Moratuwa the non-exclusive right to reproduce and distribute my thesis/dissertation, in whole or in part in print, electronic or other medium. I retain the right to use this content in whole or part in future works (such as articles or books).

Signature: 

Date: 07/10/2017

The above candidate has carried out research for the Masters thesis under my supervision.

Name of the supervisor: Dr. Ruwan Gopura

Signature of the supervisor:  Date: 09/10/2017

Name of the co-supervisor: Dr. Thilina Lalitharatne

Signature of the co-supervisor:  Date: 09/10/2017

DEDICATION

To the most courageous two persons who guided me to great achievements: my beloved father *Somadasa Herath* and mother *Kumari Dissanayake*

ACKNOWLEDGEMENT

As a graduate student of the Faculty of Engineering, University of Moratuwa, I have to complete a research project for the partial fulfillment of the requirements for the MEng. in Manufacturing Systems Engineering. For that, I selected the topic “Development of a Prosthetic Hand for Power Grasping Applications”. I am highly indebted to University of Moratuwa for the opportunity. Exclusively I would like to express my gratitude towards Dr. Ruwan Gopura for his guidance and constant supervision as well as for providing necessary information regarding the project and for his support in completing the research project. His kind co-operation and encouragement inspired me in completion of this project. Further, I acknowledge Dr. Thilina Lalitharatne for his valuable comments on my research. I would like to express my special gratitude and thanks to University of Ruhuna for giving me such information, time and engineering workshop facilities. My thanks and appreciation go to my colleagues in developing the project and people who have willingly helped me out with their abilities.

ABSTRACT

The human hand is an exceptionally significant part of the human body with a very complex biological system having bones, joints, and muscles, to provide many degrees of freedom. Among all the grasp patterns of hand, power grasping plays a crucial role in daily activities of a human. During the past few years, there was a rapid development in prosthetic limb technology to be used for the upper limb amputees. In this research, a prosthetic terminal device has been developed to assist the power grasping activities of daily living of upper limb amputees. The designed terminal device includes four fingers, which generates eight degrees of freedom. In order to generate finger movements, a novel linkage mechanism has been proposed. Notably, the proposed mechanism can be characterized as a combination of parallel and series links. The mobility of the system has been analyzed according to Chebychev-Grübler-Kutzbach criterion for a planar mechanism. By considering the easy fabrication, the linkage finger mechanism was redesigned based on the design for manufacturing guidelines. With the intention of verifying the effectiveness of the mechanism, kinematics analysis has been carried out by means of the geometric representation and Denavit-Hartenberg parameter approaches. Subsequently, a Matlab program has been developed, in order to proceed with the numerical study. Furthermore, the motion simulation and static structural analysis proved that the mechanism is capable of generating the required finger movements for power grasping. Furthermore, trajectories and the configuration space of the proposed finger mechanism has been determined by using the motion simulations inbuilt with Solidworks software package. The movements of the finger mechanism, which is fabricated by 3D printing was experimentally tested. Experimental results proved the effectiveness of the proposed mechanism to accomplish the expected motion generation. In addition, the finite element simulations exhibited that the finger is sturdy to withstand the standard finger forces.

Key words: Prosthetic hand, Linkage finger mechanism, Kinematic analysis, Power grasp

TABLE OF CONTENTS

	Page
Declaration	i
Dedication	ii
Acknowledgement	iii
Abstract	iv
Table of content	v
List of figures	viii
List of tables	xi
List of appendices	xii
List of abbreviations	xiii
CHAPTER 01: INTRODUCTION	1
1.1 Thesis Overview	2
CHAPTER 02: LITERATURE REVIEW	4
2.1 Types of Prosthesis	4
2.1.1 Electrically-Powered Prosthesis	5
2.1.2 Cosmetic Restoration	5
2.1.3 Body-Powered Prosthesis	5
2.1.4 Activity-Specific Prosthesis	5
2.1.5 Hybrid Prosthesis	5
2.2 Materials for Prostheses	5
2.3 Biomechanics of the Human Upper Extremity	6
2.3.1 Anatomy of the Hand and Wrist	6
2.3.2 Muscles of the Forearm, Wrist and Hand	8

2.3.3	Grasp Types of Human Hand	11
2.3.4	Power Grasping	11
2.3.5	Hand Forces and Strength	12
2.3.6	Fingertip Trajectories of Grasp	15
2.4	Hand Anthropometry	17
2.5	Upper Limb Prosthetics	19
2.6	Passive Prosthetic Hands	20
2.7	Recent Technological Advances in Hand Prosthetics	21
2.7.1	Commercial Prosthetic Hands	22
2.7.2	UoM Transradial Prosthetic Arm	23
2.7.3	Amrita Prosthetic Hand	24
2.7.4	Ondokuz Mayıs Prosthetic Hand	24
2.7.5	Evolution of Prosthetic Hands	25
2.8	Summary of Literature Review	27
CHAPTER 03: MECHANISM AND MECHANICAL DESIGN		28
3.1	Mechanism	29
3.2	Grasping Sequence	31
3.3	Ergonomics in Design	32
3.4	Design for Manufacture	33
3.5	Fabrication of the Finger Mechanism	33
3.5.1	Material used for Fabrication	35
3.6	Actuation of the Finger	36
CHAPTER 04: KINEMATIC ANALYSIS		39
4.1	Kinematics of the Human Hand	40
4.2	Kinematics of the Prosthetic Hand	41

4.3	Geometric Representation	43
4.4	Forward Kinematics	48
4.5	Finger Positions	53
CHAPTER 05: SIMULATION AND RESULTS		55
5.1	Motion Simulation	55
5.2	Validation of the Kinematic Analysis	57
5.3	Work Envelop	58
5.4	Grasps of the Prosthetic Hand	60
5.5	Experimental Results	64
5.6	FEA Simulation	67
CHAPTER 06: DISCUSSION		73
CHAPTER 07: CONCLUSION		74
PUBLICATIONS		75
REFERENCES		76
APPENDIX I		83
APPENDIX II		84
APPENDIX III		85
APPENDIX IV		88

LIST OF FIGURES

Figure 2.1: Bones and joints of the right hand [18]	7
Figure 2.2: Anterior muscles of the right hand [24]	9
Figure 2.3: Posterior muscles of the right hand [24]	9
Figure 2.4: Basic grasping patterns of a human hand [25]	11
Figure 2.5: Maximum finger push strength (males) [29]	13
Figure 2.6: Maximum pinch-pull strength (males) [29]	13
Figure 2.7: Maximum hand grip strength (males) [29]	14
Figure 2.8: Maximum horizontal wrist-twisting strength (males) [29]	14
Figure 2.9: Mean maximum opening strength (males) [29]	14
Figure 2.10: Maximum strength vertical handle (males) [29]	14
Figure 2.11: Maximum strength horizontal handle (males) [29]	15
Figure 2.12: Convex of the thumb workspace [30]	15
Figure 2.13: Trajectory of tip of index finger [30]	16
Figure 2.14: The fingertip trajectories for five different activation levels [31]	16
Figure 2.15: Basic hand measurements of Sri Lankans defined in Table 2.3 [33]	18
Figure 2.16: Classification of passive prostheses for replacement of the hand [38]	20
Figure 2.17: Examples of passive prosthetic tools [38]	21
Figure 2.18: Ottobock prosthetic hands and cosmetics	22
Figure 2.19: UoM transradial prosthesis [2]	24
Figure 2.20: Amrita prosthetic hand grasps and mimicking postures [44]	24
Figure 2.21: Ondokuz Mayıs prosthetic hand and grasps [45]	25
Figure 2.22: Research level prosthetic devices [46]	25
Figure 3.1: CAD Model of the prosthetic hand	28

Figure 3.2: Linkage finger mechanism	29
Figure 3.3: Links and joints of the finger	30
Figure 3.4: Basic activation steps of the finger mechanism	30
Figure 3.5: Grasping sequence of the hand	31
Figure 3.6: Dimensions of the prosthetic hand side view	32
Figure 3.7: Dimensions of the prosthetic hand top view	32
Figure 3.8: Finger design for manufacture	33
Figure 3.9: Slic3r software interface	34
Figure 3.10: Fabricated finger mechanism	35
Figure 3.11: Passive dynamic finger mechanism	37
Figure 3.12: Adaptive finger actuation method	37
Figure 3.13: Adaptive finger actuation device	38
Figure 4.1: Kinematic structure of human hand	40
Figure 4.2: Kinematics structure of the developed prosthesis	41
Figure 4.3: Simplified kinematics structure of the developed prosthesis	42
Figure 4.4: Geometric representation of the novel finger mechanism	43
Figure 4.5: Link frame assignment of finger	49
Figure 4.6: Position of point D with respect to CD and DG distance	54
Figure 4.7: Position of point G with respect to CD and DG distance	54
Figure 4.8: Position of point K with respect to CD and DG distance	54
Figure 5.1: Trajectory of point K with respect to change of CD	55
Figure 5.2: Trajectory of point K with respect to change of DG	56
Figure 5.3: Trajectory of point K with respect to change of CD, DG	56
Figure 5.4: Trajectories of the point K	56
Figure 5.5: PIP joint angle with respect to CD distance	57

Figure 5.6: DIP joint angle with respect to DG distance	58
Figure 5.7: Trajectory of the fingertip and joints	59
Figure 5.8: Work envelop of the finger	59
Figure 5.9: Cylindrical grasp of the prosthetic hand	60
Figure 5.10: View orientations for 75mm diameter cylindrical grasp	60
Figure 5.11: Grasp sequence for small cylinder	61
Figure 5.12: View orientations for 100mm diameter cylindrical grasp	61
Figure 5.13: Grasp sequence of large cylinder	62
Figure 5.14: Spherical grasp of the prosthetic hand	62
Figure 5.15: View orientations for 85mm diameter spherical grasp	63
Figure 5.16: Grasp sequence of small sphere	63
Figure 5.17: View orientations for 110mm diameter spherical grasp	64
Figure 5.18: Grasp sequence of large sphere	64
Figure 5.19: Sequence of the finger motion with respect to change of DG	65
Figure 5.20: Sequence of the finger motion with respect to change of CD	65
Figure 5.21: Sequence of the finger motion with respect to change of CD, DG	65
Figure 5.22: Fiji ImageJ software interface during measuring	66
Figure 5.23: Von mises stress of finger	70
Figure 5.24: Resultant displacement of finger	71
Figure 5.25: Equivalent strain of the finger	71
Figure 5.26: Factor of safety of the finger	71
Figure 5.27: Variation of maximum stress with respect to the one over mesh size	72

LIST OF TABLES

Table 2.1: Extrinsic muscles of the hand and wrist [18]	10
Table 2.2: Hand anthropometric dimensions of male [32]	17
Table 2.3: Hand measurements of Sri Lankans [33]	18
Table 2.4: Features of commercially available prosthetic hands [6]	23
Table 2.5: General characteristics of modern prosthetic hands [46] [47] [48]	26
Table 3.1: Uni-Print 3D printer settings	35
Table 3.3: Specification of the finger material	36
Table 3.4: General characteristics of the PLA material [49]	36
Table 4.1: D-H link parameters	49
Table 4.2: Link parameter values for the prototype finger	53
Table 5.1: PIP joint angle with respect to CD distance	57
Table 5.2: DIP joint angle with respect to DG distance	58
Table 5.3: Comparison for experimental and simulation results	67
Table 5.4: Load and fixtures for FEA simulation	68
Table 5.5: Material properties for FEA simulation	69
Table 5.6: Mesh information and FEA results	70
Table 5.7: Mesh size, number of elements and stress	72

LIST OF APPENDICES

Appendix I: Components of the linkage mechanism	83
Appendix II: Components of the finer mechanism	84
Appendix III: Matlab codes used to generate 3D plots	85
Appendix IV: Detail drawing of the finger	88
Appendix V: Compact disc	

LIST OF ABBREVIATIONS

Abbreviation	Description
ADL	Activities of daily living
CMC	Carpometacarpal
CNC	Computer numerical control
DFM	Design for manufacture
DIP	Distal inter phalangeal
DoF	Degrees of freedom
DP	Distal phalanx
EDM	Electrical discharge machining
EMG	Electromyography
FDM	Fused deposition modeling
FEA	Finite element analysis
IPB	Intermediate phalanx bottom
IPM	Intermediate phalanx middle
IPT	Intermediate phalanx top
MCP	Metacarpo phalangeal
PIP	Proximal interphalangeal
PLA	Polylactic acid
PPB	Proximal phalanx bottom
PPM	Proximal phalanx middle
PPT	Proximal phalanx top

CHAPTER 01: INTRODUCTION

The hand is the most frequently symbolized part of the human body. It is one of the most complex and beautiful pieces of natural engineering which gives human not only a powerful grip but also allows them to manipulate small objects with great precision. This ability sets human apart from other creatures. The large number of muscles and joints of the hand obviously enable numerous and varied patterns of movement which are vital for human daily activities [1].

However, the people incur an illness or experience an accident result in loss of a limb. Besides some may also have been born with a congenital condition in which one or more of their limbs are missing [2]. Fortunately, there are artificial limbs that enable those people to still do things such as running, walking, reaching, and gripping. These apparatuses are known as prosthetics [1] [3] [4].

A significant portion of the injuries treated in the emergency rooms around the globe involve upper extremities [5] [6]. The majority of them occur at home, during work, or when performing sports. Considering that almost all our daily activities depend on manipulation by the hands, severe hand injuries can truly be devastating. Consequences of such incidents can lead to long term disabilities, also affecting the mental and social state, with difficult reintegration in the society [7] [8].

The severe consequences of upper limb loss have been recognized centuries ago, and the ideas of artificial substitution have been since then very appealing [9]. Transition from simple cosmetic prostheses to a more functional solution was inevitable and high in demand, resulting in the development of early body-powered and cable-driven systems [10]. These simple devices proved themselves to be very useful and, with modern materials, are still currently in use. The first pneumatic hand was developed at the beginning of the 20th century, soon followed by the first electric-powered hand. Advances in micromachining and material design have enabled construction of versatile lightweight prosthetic hands and wrists. Greater understanding of the human neuromuscular system yielded new surgical and reconstructive techniques, which now provides access to high-quality and intuitive electromyography (EMG) sources even

in high-level amputations [5]. Currently there is an explosion in the number of devices being developed for interaction with the human body, especially in the field of robotics. This activity results from several recent technological advances in control techniques and sensor technology. For example, allowing devices to be more sensitive to the actions of the user. It is also due to the introduction of compliant mechanisms using variable impedance actuators (VIA), or software based elasticity generated by the control mechanism, in robotic structures. These developments have led to a matching of the physical and motor characteristics of robots with those of the human body, making the robots safer and therefore promoting the development of closer physical exchanges [5].

Looking in to the Sri Lankan context, the development in the field of prosthetics and orthotics in the past six decades has been very slow especially in comparison with its South Asian neighbors [11]. Disability requiring prosthetics and orthotics intervention is increasing due to population, ageing and ongoing conflict. Improved orthopaedic services will demand more access to prosthetics and orthotics. It is essential that a concentrated effort be taken by all stakeholders using available international guidelines to provide quality prosthetics and orthotics services and increase awareness about the benefits of such services. Subsequently this study proposed a modest prosthetic hand with a novel finger mechanism which may be capable of generating the motion patterns and the finger forces required for an authentic power grasp. The mechanical design and the mechanism of the proposed prosthetic hand is deliberated in the thesis. Consequently, the kinematic analysis, motion simulations and the experimental investigations also presented.

1.1 Thesis Overview

The thesis consists of six other chapters. The content of the remaining chapters are constructed as below.

Chapter 2: Literature Review

This chapter deliberates the background information and literature review related to human hand and hand prosthesis. At the beginning of the chapter, the existing types of prosthesis are categorized. Afterward the biomechanics of the human upper extremity

and anatomy of the hand are described. In addition, grasp types of human hand and fingertip trajectories of grasp are also presented. The chapter also classifies the human hand anthropometry and hand forces. The classification will be followed by a review of recent technological advances in hand prosthetics.

Chapter 3: Mechanism and Mechanical Design

The chapter demonstrates the working principle of the novel hand prosthesis. Initially, the mechanism of the proposed finger mechanism is explained, which is followed by the illustration of the grasping sequence of the prosthetic hand. Next section of the chapter expresses the concerns on design for ergonomics and design for manufacture. Moreover, the fabrication of the finger mechanism and the materials used for fabrication are elaborated. Finally, the actuation process of the finger is clarified.

Chapter 4: Kinematic Analysis

This chapter presents the details of the kinematic studies of the mechanisms. First the kinematics of the human hand is discussed followed by the kinematics of the proposed prosthesis. In addition, mobility analyses of the mechanisms are also presented. The geometric representation and forward kinematics of the novel finger mechanism are clarified. Lastly the finger positions are illustrated which are mapped based on the kinematic analysis.

Chapter 5: Simulation and Results

This chapter covers the simulation and experimental results related to the prosthesis. At first the outcomes of the motion simulations are presented, resulting the validation of the kinematic analysis. Moreover, the work envelop of the finger and the grasps functionality of the prosthetic hand are deliberated. Notably the next section of the chapter presents experimental results of the finger mechanism during motion generation. Additionally the chapter provides the details of the finite element analysis for finger mechanism.

Chapter 6: Conclusion

The final chapter summarizes the contributions of the thesis, the conclusion, a brief discussion, and future directions.

CHAPTER 02: LITERATURE REVIEW

The history of prosthetics is rich and exciting. Since the beginning of time, humans have felt the need to replace lost limbs for cosmetic, functional and psycho-spiritual reasons. The great civilizations of Greece, Rome and Egypt fostered the development of science and medicine leading to the development of the first prosthetics. The oldest prosthetic care began in the fifth Egyptian Dynasty (2750-2625 BC) since archeologists discovered the oldest known splint. [12] Recent development of the prostheses was influenced by the World War I and II, which resulted in a remarkable loss of man power in USA and Europe. In 1948, the concept of Cybernetics, i.e., the study of control and communication between human and machine [13], played a significant role later on for the improvement of the prostheses. Samuel Anderson developed the first electrically powered arm prosthesis, with the support of the US government and IBM in 1949 [14]. Russians in 1958 developed the first myoelectric arm and soon after, Ottobock Company came up with a commercially available arm prosthesis for common application, which was the first finished versions of the Russian design [14]. Researchers have been making effort to develop a prosthetic system, which will mimic the exact human motion, power requirement and anatomical/cosmetic features. However, still there are some technological limitations that do not allow researchers to develop such a system. Studies on development of prostheses and their supporting technologies are among the emerging research topics globally.

2.1 Types of Prosthesis

There are six basic prosthetic options to consider for the upper extremity amputee. The type of prosthesis needed depends on the level of amputation, the condition of the residual limb, individual goals and work requirements, and other variables. An individual often needs more than one prosthesis to accomplish all of his or her goals. Personal requirements may be function-related, cosmetic or psychological in nature [15].

2.1.1 Electrically-Powered Prosthesis

This category of prosthesis uses small electrical motors in the terminal device (hand or hook), wrist and elbow. A rechargeable battery system powers the motors. Because electric motors operate the hand function, its grip force is significantly increased [15].

2.1.2 Cosmetic Restoration

Cosmetic restoration, or duplication of the contralateral arm or hand, is a popular prosthetic option. This involves replacing what was lost from amputation or congenital deficiency with a prosthesis similar in appearance to the non-affected arm or hand and provides simple aid in balancing and carrying [15].

2.1.3 Body-Powered Prosthesis

A body-powered (or conventional) prosthesis is powered and controlled by gross body movements of the shoulder, upper arm, chest, etc. The movements are captured by a harness system attached to a cable and connected to a terminal device (hook or hand). Some levels of amputation or deficiency allow an elbow system to be added for improved function [15].

2.1.4 Activity-Specific Prosthesis

An activity-specific prosthesis is designed for an activity that requires some function or durability that other prostheses cannot provide. Often created for recreational activities such as fishing, swimming, golfing, hunting, bicycle riding and weight lifting prostheses have also been designed for music or work-related tasks [15].

2.1.5 Hybrid Prosthesis

A hybrid prosthesis combines body power and electrical power. Most hybrid prostheses are used for individuals with transhumeral (above the elbow) amputations or deficiencies [15].

2.2 Materials for Prostheses

In the 1900s, prostheses started to look and feel more realistic because they were beginning to be made from materials such as plastic, silicone, and PVC. This allowed

them to be stronger and lighter. Today, most prostheses are made out of plastic that encases the interior structure, and they are attached by straps and sock. This sock cushions and protects the stump. If the socket is not fixed by straps, it is fixed via suction to the stump. Most prosthetic feet are made with wood. However, now they consist of foam and plastic as well [16] [4]. The most commonly used materials in current prosthetic devices are leather, metal, wood, thermoplastic and thermosetting materials, foamed plastics, and viscoelastic polymers. Five characteristics are considered when deciding what materials to use to construct a prosthesis: strength, stiffness, durability, density, and corrosion resistance. Strength, which is determined by the amount of weight that the material can withstand, is important in lower appendage prostheses. Stiffness is the amount of bending that is allowed when the material is loaded. For example, a stiffer material is desired for a rigid prosthetic frame, but a more flexible material is desired for a flexible transfemoral prosthetic socket. Durability, or fatigue resistance, is determined by its ability to withstand repeated loading and unloading. Density, the weight per unit of volume, is important because it is a determinant of energy cost while a person is wearing the prosthesis. If a material is susceptible to corrosion, it is vulnerable to be damaged by chemicals. Prosthetic limbs are often made from materials that preserve heat, thereby creating the problem of perspiration. This is why it is better to make prostheses out of materials which are resistant to moisture; prostheses that are made of materials that are resistant to moisture are more readily cleaned than porous substances [17] [4].

2.3 Biomechanics of the Human Upper Extremity

Biomechanics is mechanics, the science that deals with forces and their effects, applied to biological systems. Biomechanical principles can be applied to a system of bodies at rest, termed statics, or to a system of bodies in motion, termed dynamics. In such systems, bodies may be pushed or pulled by actions termed forces [18].

2.3.1 Anatomy of the Hand and Wrist

The human hand has 27 bones divided into three groups where 8 carpal bones in the wrist, 5 metacarpal bones, and 14 phalanges of the fingers. The carpal bones are



arranged in two rows and have names reflecting their shapes as shown in Figure 2.1 [18].

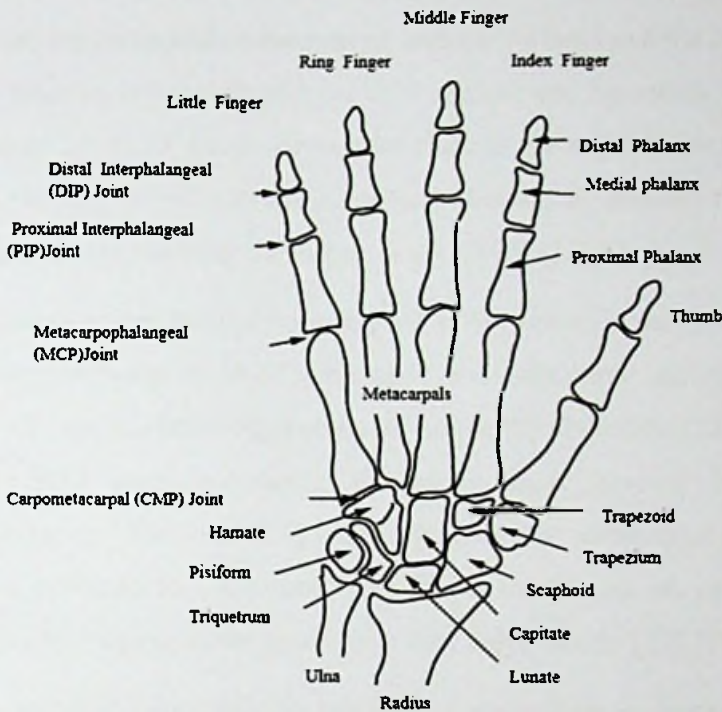


Figure 2.1: Bones and joints of the right hand [18]

There are three phalanges for each digit and two for the thumb for a total of 14 bones. They are labeled proximal, middle, and distal phalanges (with the middle one missing in the thumb), according to their positions and become progressively smaller. The heads of the proximal and middle phalanges are bicondylar, facilitating flexion and extension and circumduction. The shafts are semicircular in cross section (the palmar surface is almost flat), as opposed to the cylindrical metacarpals. The axes of the distal phalanges of the index, ring, and little fingers are, respectively, deviated ulnarly, radially, and radially from the axes of the middle phalanges [18] [19].

There are four joints in each finger, in sequence from the proximal to distal which are carpometacarpal (CMC), metacarpo phalangeal (MCP), proximal interphalangeal (PIP), and distal inter phalangeal (DIP) joints. The CMC joints are formed by the bases of the four metacarpals and the distal carpal bones and are stabilized by interosseous

ligaments to form a relatively immobile joint. However, a major function of the CMC joint is to form the hollow of the palm and allow the hand and digits to conform to the shape of the object being handled [20] [18].

The MCP joints are composed of the convex metacarpal head and the concave base of the proximal phalanx and stabilized by a joint capsule and ligaments. Flexion of 90° and extension of 20° to 30° from neutral take place in the sagittal plane. The range of flexion differs among fingers with the index finger having the smallest flexion angle of 70° and the little finger showing the largest angle of 95° [18] [21].

Radial and ulnar deviation of approximately 40° to 60° occurs in the frontal plane, with the index finger showing up to 60° abduction and adduction, the middle and ring fingers up to 45° , and the little finger about 50° of mostly abduction [22]. The range of motion at the MCP joint decreases as the flexion angle increases because of the bicondylar metacarpal structure [23] [18]. There is also some axial rotation of the fingers from a pronated to a supinated position as the fingers are extended. In the reverse motion, the fingers crowd together as they enter flexion [22] [18].

The IP joints, as hinge joints, exhibit only flexion and extension. Each finger has two IP joints, the PIP and the DIP, except the thumb, which has only one. Volar and collateral ligaments, connected with expansion sheets of the extensor tendons, prevent any side-to-side motion. The largest flexion range of 100° to 110° is found in the PIP joints, while a smaller flexion range of 60° to 70° is found in the DIP joints. Hyperextension or extension beyond the neutral position, due to ligament laxity, can also be found in both DIP and PIP joints [22] [18].

2.3.2 Muscles of the Forearm, Wrist and Hand

The muscles producing movement of the fingers are divided into two groups extrinsic and intrinsic based on the origin of the muscles. The extrinsic muscles originate primarily in the forearm, while the intrinsic muscles originate primarily in the hand. Therefore, the extrinsic muscles are large and provide strength, while the intrinsic muscles are small and provide precise coordination for the fingers. Each finger is innervated by both sets of muscles, requiring good coordination for hand movement [18].

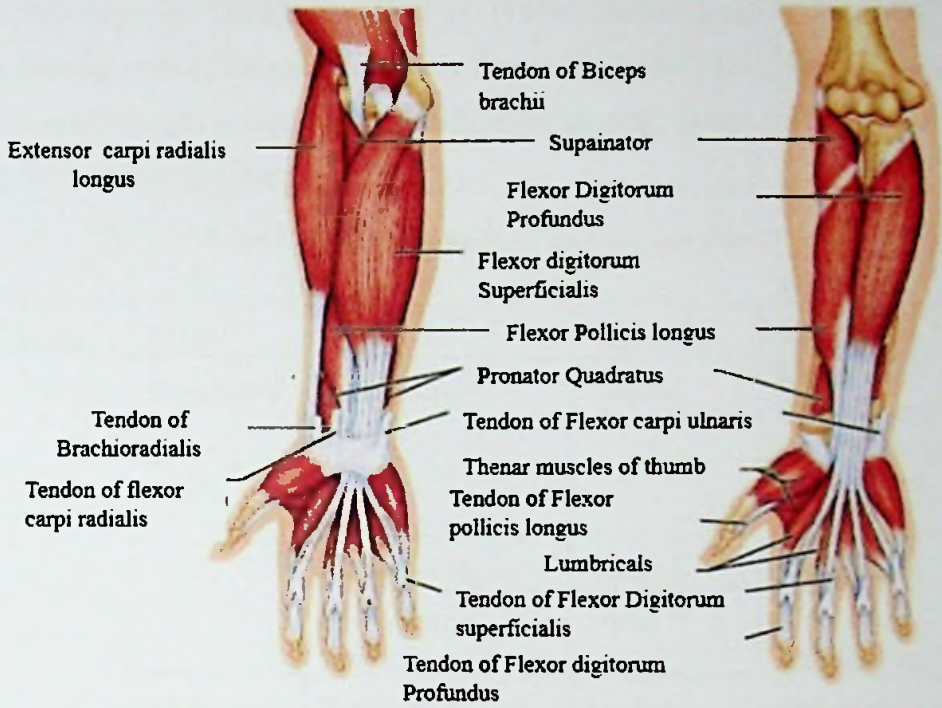


Figure 2.2: Anterior muscles of the right hand [24]

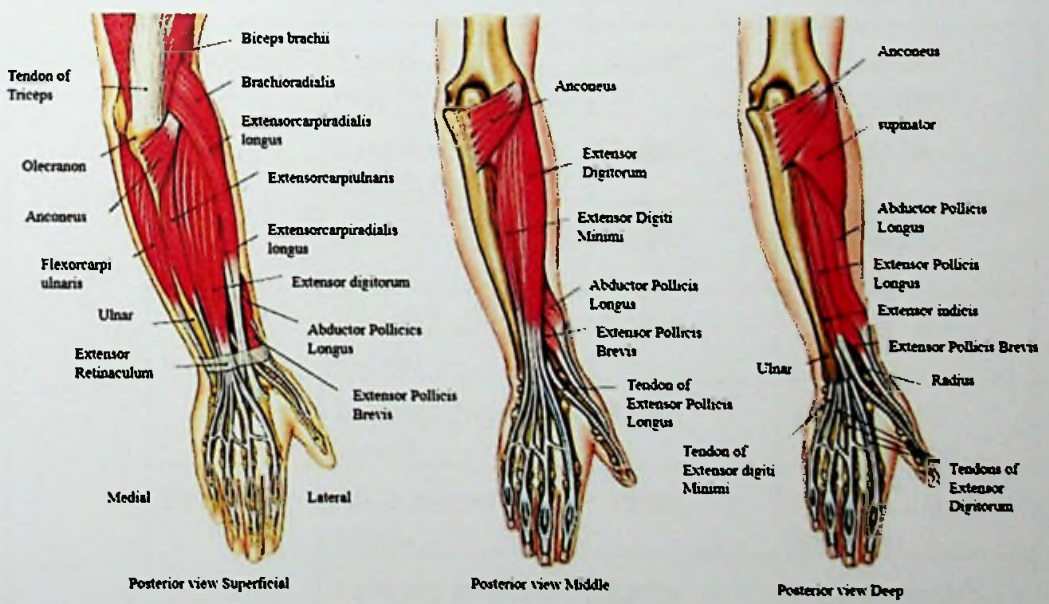


Figure 2.3: Posterior muscles of the right hand [24]

The flexor digitorum profundus (FDP) and flexor digitorum superficialis (FDS) are the main finger flexor muscles and are involved in most repetitive work. Using

electromyography (EMG), Long et al. (1970) identified the FDP as the muscle performing most of the unloaded finger flexion, while the FDS comes into play when additional strength is needed, with the FDP comprising about 12% of the total muscle capability below the elbow.

Table 2.1: Extrinsic muscles of the hand and wrist [18]

Group	Layer	Name	Nerve	Function
Anterior	Superficial	Flexor carpi radialis	Median	Flexes and adducts hand Aids in flexion / pronation of forearm
		Palmaris longus	Median	Flexes hand
		Flexor carpi ulnaris	Ulnar	Flexes and adducts hand
	Middle	Flexor digitorum superficialis	Median	Flexes phalanges and hand
	Deep	Flexor digitorum profundus	Median, Ulnar	Flexes phalanges and hand
Posterior	Superficial	Extensor carpi radialis longus	Radial	Extends and abducts hand
		Extensor carpi radialis brevis	Radial	Extends hand
		Extensor digitorum	Radial	Extends little finger
		Extensor digiti minimi	Radial	Extends little finger
		Extensor carpi ulnaris	Radial	Extends and adducts hand
	Deep	Abductor pollicis longus	Radial	Abducts thumb and hand
		Extensor pollicis brevis	Radial	Extends thumb
		Extensor pollicis longus	Radial	Extends thumb
		Extensor indicis	Radial	Extends index finger

2.3.3 Grasp Types of Human Hand

Understanding the basic grasp patterns are important for rehabilitation and prosthesis. These grasps are primarily defined by the object that the hand interacts with. There are two basic categories power and precision. The basic grasping patterns of a human hand are shown in Figure 2.4.

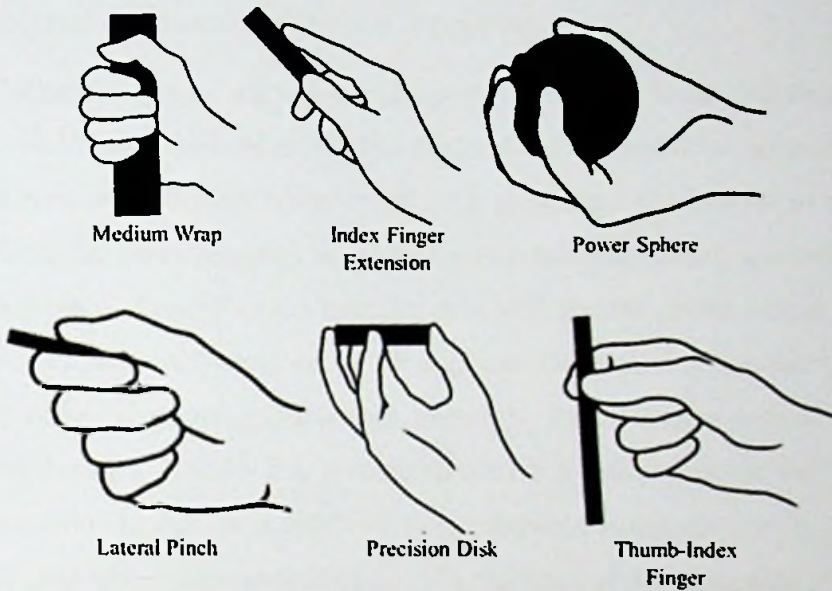


Figure 2.4: Basic grasping patterns of a human hand [25]

2.3.4 Power Grasping

Power grip is the mostly employed grasping pattern with a frequency of 35% of ADL [26] [27]. The power grasp is demonstrated by the fingers and sometimes palm clamping down on an object with the thumb making counter pressure. Examples of the power grip are gripping a hammer, opening a jar using both your palm and fingers and during pullups. There are two factors that affect the ability to generate force with a power grip:

- Wrist orientation - deviations from a normal posture reduce the maximum grip force.
- Grip span - spans that are too small or large will reduce grip strength.

The power of grasp is derived from two groups of muscles, the extrinsic and the intrinsic. The extrinsic muscles in the forearm provide the major power of the hand.

The intrinsic muscles within the hand are of fundamental importance, since they are largely responsible for the refinement and delicate control of digital movements. These small muscles achieve their control by modifying and moderating the actions of the long extrinsic muscles. Opening the hand and then closing it around an object is a very complicated motion. Simultaneous contraction to varying degrees of the 35 muscles in the forearm and hand will create a grasping motion. And also it leads to several patterns of handling that can be achieved by power grasping,

- Cylindrical grasp: the entire palmar surface of the hand grasping around a cylindrical-shaped object. For this finger flexors, intrinsic muscles, and thumb flexors and abductors are involved. (e.g. grasping a baseball bat or a hammer)
- Spherical grasp: cupping the thenar and hypothenar eminences with varying degrees of finger flexion muscles involved for the above action are finger flexors, especially from 4th or 5th digits, and interossei (e.g. holding a ball)
- Hook grasp: gripping like a hook formed by flexed fingers without the thumb involvement. Usually it is a static nature for a period of time. For this flexor digitorum profundus is involved. (e.g. carrying a suitcase)
- Conoid grasp: cone-shaped grasp with the apex at the ulnar side of the palm. (e.g. using a knife or other tools)

Power grasp is an important area of research in the emerging area of analysis and control of whole arm or whole-hand manipulation systems. A power grasp is characterized by multiple points of contact between the object grasped and the surfaces of the fingers and palm. It maximizes the load carrying capability of a grasping system and is inherently highly stable because of the enveloping nature of the grasp which provides form-closure [28].

2.3.5 Hand Forces and Strength

Hand force measurements consist total of six different force exertions as described below [29].

- Finger push strength – pushing with the pad of the thumb and index finger in a forward and downward direction.

- Pinch-pull strength – pinching and pulling with one hand at three pinch distances. There are two types. Pulp pinch (pad of the thumb in opposition to pad of the index finger) and chuck pinch (pad of the thumb in opposition to the pads of both the index and middle fingers).
- Hand grip strength – one and two-handed strength when gripping a series of three rectangular handles of varying size.
- Wrist-twisting strength – torque (clockwise) using one hand on a series of six handles and controls.
- Opening strength – torque (anti-clockwise) on a series of replica jars with smooth and knurled textured lids of various diameters.
- Push and pull strength – pushing and pulling with one and two hands on a cylindrical bar, and pulling with one hand only on a convex knob.

The maximum strength of males for all six measurements are shown in below figures [29].

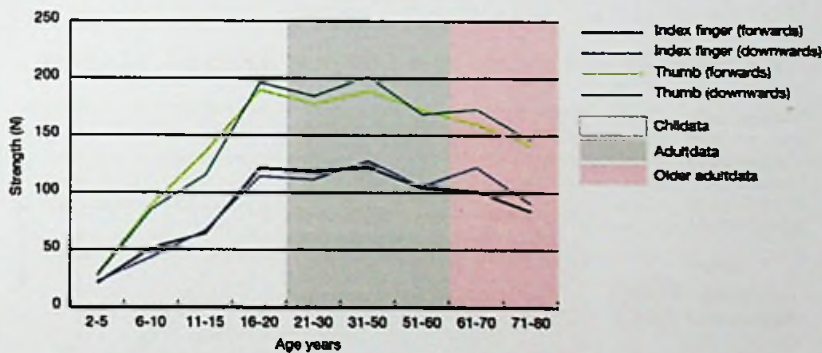


Figure 2.5: Maximum finger push strength (males) [29]

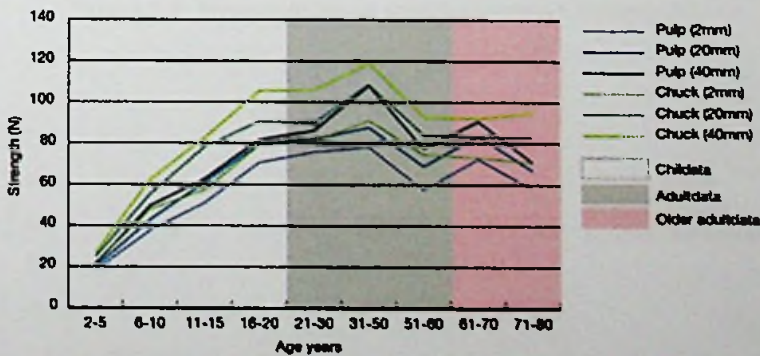


Figure 2.6: Maximum pinch-pull strength (males) [29]

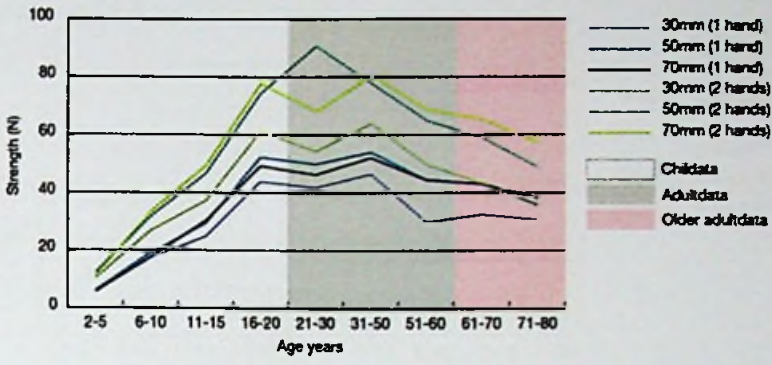


Figure 2.7: Maximum hand grip strength (males) [29]

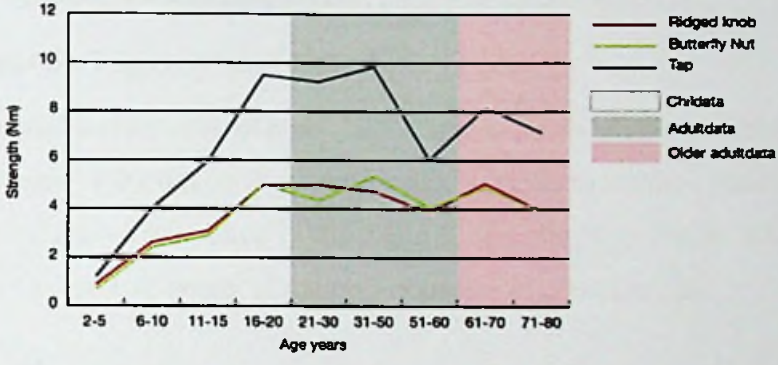


Figure 2.8: Maximum horizontal wrist-twisting strength (males) [29]

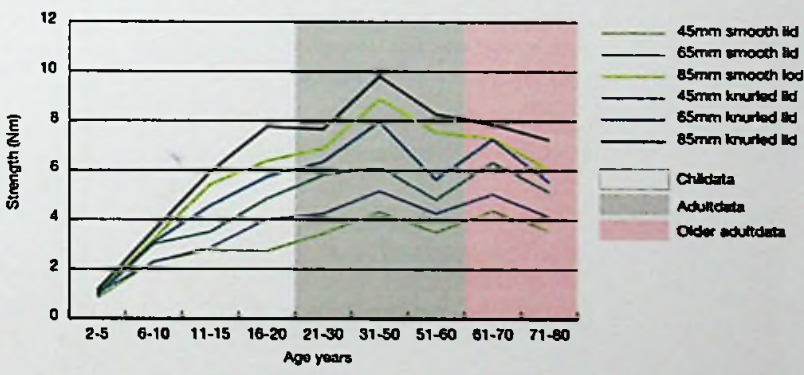


Figure 2.9: Mean maximum opening strength (males) [29]

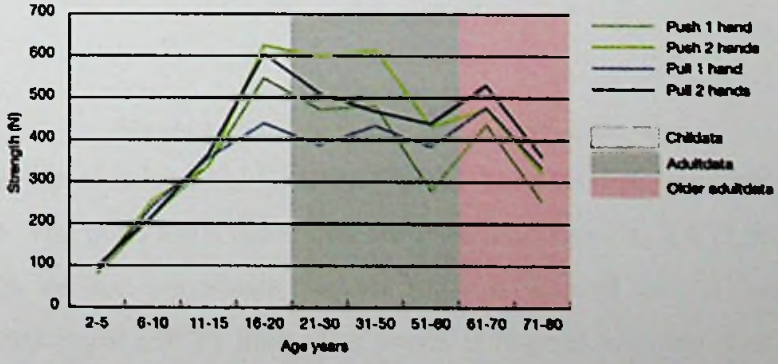


Figure 2.10: Maximum strength vertical handle (males) [29]

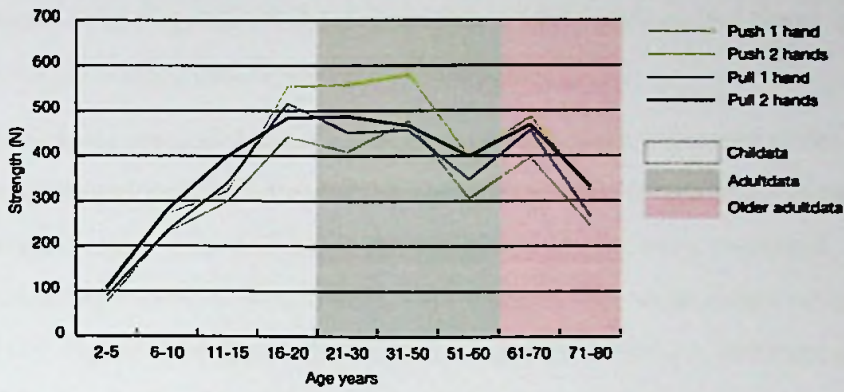


Figure 2.11: Maximum strength horizontal handle (males) [29]

2.3.6 Fingertip Trajectories of Grasp

The human hand is comprised of many joints that permit an infinite number of different trajectories to move the fingers from one location in space to another. Researchers have attempted to characterize motion of the digits during grasping. Figure 2.12 shows the estimation of volume of potential thumb workspace of a human [30].

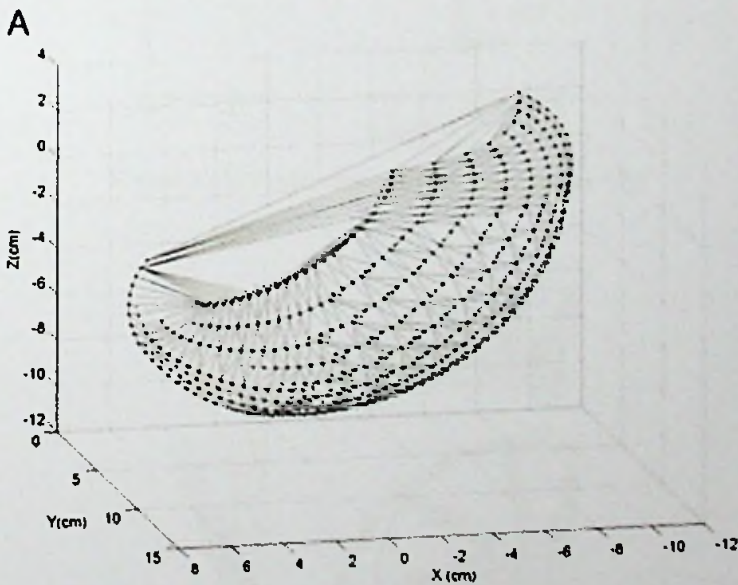


Figure 2.12: Convex of the thumb workspace [30]

Trajectory of tip of index finger in the x-y plane for three different trials is shown in Figure 2.13. The three trials illustrated are grasping a marker, a CD, and a playing card. Origin of the coordinate system (0,0) is located at the center of the metacarpophalangeal (MCP) joint. The y-axis is aligned with the first metacarpal, while the x-axis is perpendicular to the palm. Thus negative x values denote

movements of the fingertip on the palmar side of the hand. Actual finger posture is shown for a particular point along the trajectory.

Researchers have studied the motion analysis of fingertip trajectory under different levels of lumbrical muscle activation by using four fresh-frozen cadaver hands. The finger motion under five different Lum activation levels were measured. The five different loading 0.00N, 0.49N, 0.98N, 1.47N and 1.96N were achieved by a static weight [31]. Figure 2.14 shows the fingertip trajectories for five different activation levels of the Lum when the FDP was pulled in one specimen.

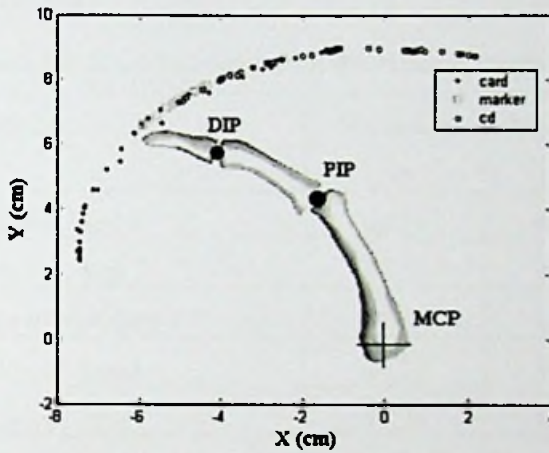


Figure 2.13: Trajectory of tip of index finger [30]

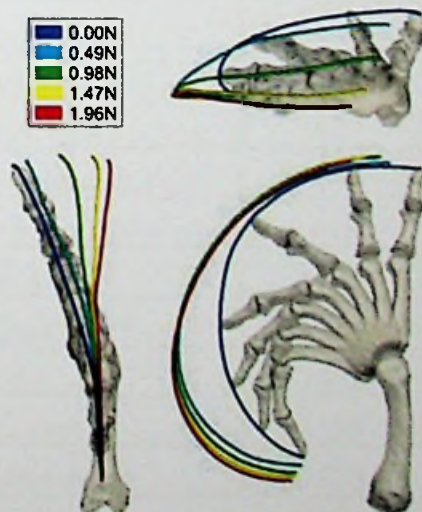


Figure 2.14: The fingertip trajectories for five different activation levels [31]

2.4 Hand Anthropometry

Anthropometric data provides information on static dimensions of the human body in standard postures. Anthropometric measurement of human limbs plays an important role in design of workplace, clothes, hand tools and many products for human use. To design any product for human use, human factors engineers/ergonomists have to rely on anthropometric data, otherwise the output product may turn out to be non-ergonomically designed product or the product may turn out to be ergonomically incompatible [32]. With respect to the basic hand anthropometric dimensions of male are shown in Table 2.2 [32].

Table 2.2: Hand anthropometric dimensions of male [32]

No	Hand dimensions	Minimum (mm)	Maximum (mm)	Mean (mm)
1	Fingertip to root digit 5	49.79	68.10	59.13
2	First joint to root digit 5	27.31	41.58	34.23
3	Second joint to root digit 5	12.93	22.55	17.52
4	Fingertip to root digit 3	69.79	90.80	79.05
5	First joint to root digit 3	43.76	60.51	52.06
6	Second joint to root digit 3	19.46	32.41	25.53
7	Breadth at tip digit 5	10.62	15.84	12.97
8	Breadth at first joint digit 5	12.72	17.60	15.10
9	Breadth at second joint digit 5	14.73	19.79	17.06
10	Breadth at tip digit 3	12.85	18.56	15.79
11	Breadth at first joint digit 3	15.07	19.64	17.35
12	Breadth at second joint digit 3	17.90	22.45	20.21
13	Depth at tip digit 5	9.46	13.86	11.37
14	Depth at first joint digit 5	11.22	16.31	13.70
15	Depth at second joint digit 5	13.84	19.97	16.50
16	Depth at tip digit 3	10.32	15.35	12.99
17	Depth at first joint digit 3	12.83	17.85	15.51
18	Depth at second joint digit 3	16.53	22.30	19.08
19	Grip span	82.32	114.66	98.07
20	Max. breadth of the hand	95.00	110.00	101.83
21	Breadth of the knuckles	78.00	92.00	84.85

22	Hand length	170.00	202.00	185.77
23	Palm length	94.00	118.00	105.59
24	Depth of the knuckles	24.00	32.00	28.04
25	Max. depth of the hand	35.00	54.00	44.62
26	Fist length	89.00	113.00	100.05
27	First phalanx digit 3 length	60.00	74.00	65.85
28	Fist circumference	252.00	305.00	277.65
29	Hand circumference	225.00	265.00	243.82
30	Maximum hand circumference	310.00	379.00	344.50
31	Index finger circumference	60.00	77.00	67.28
32	Wrist circumference	149.00	185.00	164.54
33	Arm length	692.00	847.00	771.16

With respect to the Figure 2.15 basic hand dimensions of Sri Lankan population are shown in Table 2.3 [33].

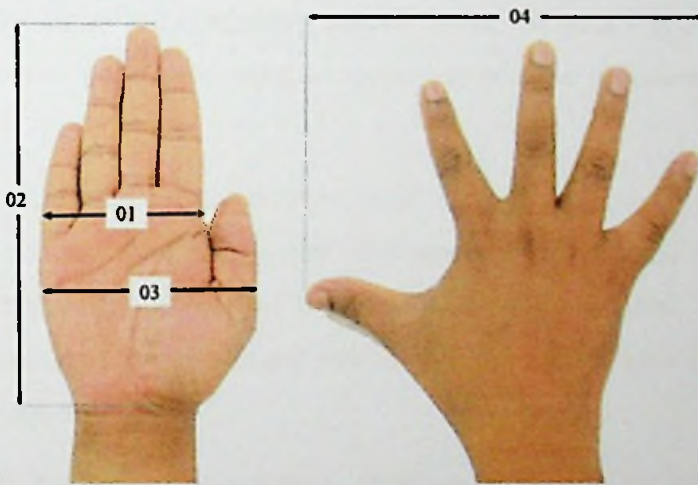


Figure 2.15: Basic hand measurements of Sri Lankans defined in Table 2.3 [33]

Table 2.3: Hand measurements of Sri Lankans [33]

No	Measurement	Mean for Females (mm)	Mean for Men (mm)
01	Hand Grith	176.57	196.19
02	Hand Length	166.59	179.38
03	Hand Breadth	88.59	99.50
04	Finger Span	184.33	207.64

2.5 Upper Limb Prosthetics

People, especially young, active persons, who are disabled following an acquired or congenital amputation of an upper limb, are usually fitted with an external prosthesis, or orthoprosthesis [34] [35]. The primary etiologies which lead to surgical amputation are trauma (road traffic accidents, accidents at work, or war injuries), malignant tumors, vascular accidents or infections, and diabetes [34] [36]. Whatever the cause of the amputation, the loss of one or both upper limbs have huge consequences on the person's capacity to carry out activities of daily living as well as affecting their professional life and autonomy.

Three different types of prostheses are currently available to patients. Non-functional (cosmetic) prostheses, and functional ones, among which mechanical prostheses (controlled by the remaining joints or the opposite limb via a cable) and myoelectric prostheses which use surface electromyograms (sEMG) of the voluntary electrical activity of the residual muscles of the stump to control the electrical actuators of the prosthesis. The latter are commonly placed under the term "robotic" prostheses although "robotic" prostheses relate to recent myoelectric prostheses that integrate automation.

Commercial companies mostly propose hand and forearm prostheses for forearm amputations (the most common upper limb amputation), as well as a few elbow prostheses. Naturally, because of the small size of the market, there are fewer prostheses available for transhumeral (above the elbow), and even fewer for higher levels of amputation.

Most research institutes and companies focus on improving the hardware of hand devices, the design of which is coming closer to that of humanoid robotics limbs [37] [34] Several polydigital myoelectric hand prostheses, with greater degrees of freedom than the traditional opening or closing hand, are already commercially available. Nonetheless, rigorous clinical studies of the performance and advantages offered by these devices are still lacking.

2.6 Passive Prosthetic Hands

The wide range of prostheses for replacement of the hand can be divided into active and passive prostheses. The force to control the grasping mechanism of active prostheses is applied to this mechanism internally, for example, by an electric actuator or a body powered cable. In passive prosthesis, the force to adjust the grasping mechanism is applied externally [38]. There are various types of passive prostheses. The group of passive prostheses for replacement of the hand consists of prosthetic hands and prosthetic tools. Prosthetic hands offer a lifelike appearance and are used for a variety of activities. Prosthetic tools have a mechanical appearance and are mostly designed for one specific activity which needs to be performed two handedly. Some prosthetic tools, such as a passive prosthetic hook, can be used for a variety of activities.

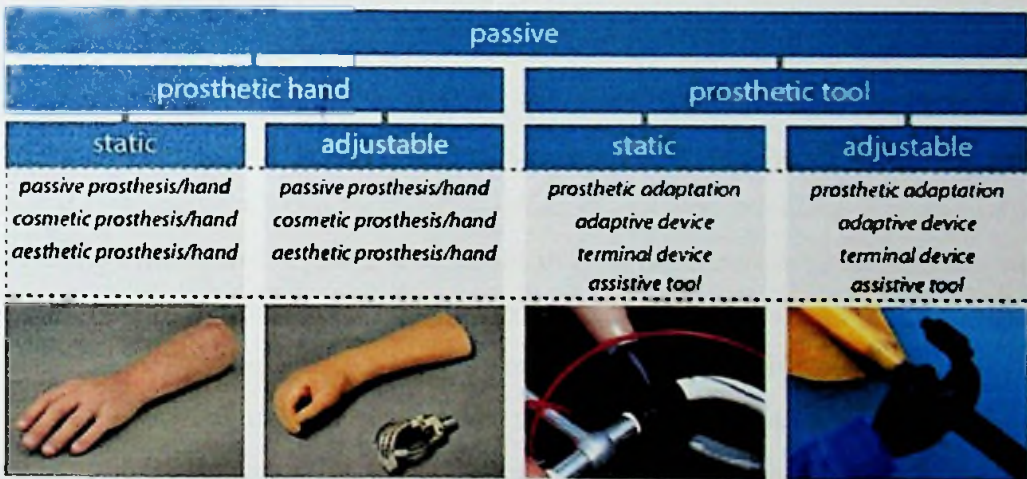


Figure 2.16: Classification of passive prostheses for replacement of the hand [38]

Both passive prosthetic types can be either static or adjustable. Static prostheses cannot be moved at all [39]. Adjustable prostheses feature an adjustable grasping mechanism or parts of the prosthesis can be adjusted to multiple orientations. Research on passive prosthetic tools primarily focus on sport, recreation, and vehicle driving. However, prosthetic tools are also very useful for ADLs such as using cutlery or riding a bicycle. Some examples of prosthetic tools are shown in Figure 2.17 [38].

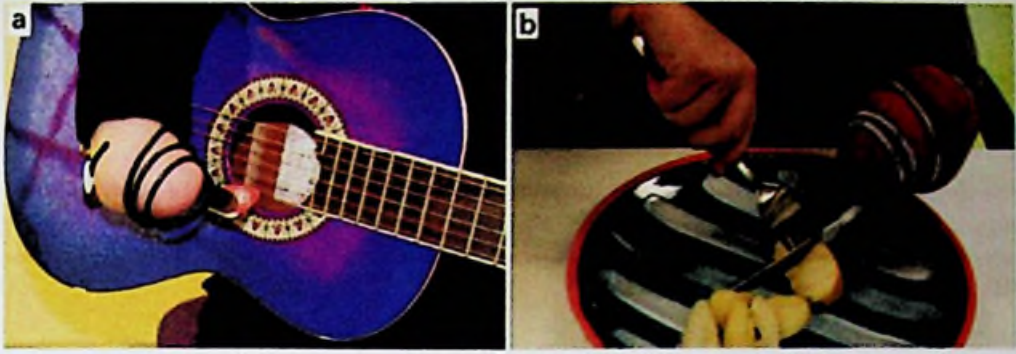


Figure 2.17: Examples of passive prosthetic tools [38]

(a) Playing a musical instrument and (b) Eating

2.7 Recent Technological Advances in Hand Prosthetics

Beyond improvements in hardware, significant progress has been made both in devices developed by research laboratories and in commercial prosthetics. The additional progress has been in the areas of control techniques, sensory feedback, and the development of new materials. Researchers from the Rehabilitation Institute of Chicago (RIC) have developed an innovative surgical technique called “targeted muscle reinnervation.” This technique involves the surgical rerouting of motor nerves of the sectioned limb to a group of surgically deinnervated muscles in the thoracic wall [40]. Following a learning process, the subject control these muscles exactly as he/she controlled the missing limb. Electrodes are implanted within the muscles in order to capture the EMG signal sent by the brain, which thinks it is controlling the arm. This signal is then used to drive the prosthesis. This method can be used to control prostheses with a large number of active joints, avoiding sequential control (joint by joint). More recently, electrodes have been implanted in the cortex of the brain of tetraplegia patients with a total loss of mobility. During these short-term trials (one month for ethical-legal reasons), including an intensive learning phase, the patients were able to use an external robotic arm to carry out activities of daily living [41].

Sensory information is essential for the performance of motor activities (in neurosciences the term sensory-motor control is used, rather than motor control). Much research is therefore focused on restoring the sensations of interaction of the prosthesis with the environment. The aim is to improve fine control (such as the degree of force exerted by the hand), and to reduce the necessity for intense visual control.

The technique involves placing force/pressure sensors in the prosthetic fingers and returning the information to the patient via another modality (usually vibro-tactile) to the residual part of the limb [42]. An alternative invasive approach has recently been tested on one patient. Information on touch and interaction forces measured on a prosthetic hand was translated into electrical stimulations sent to electrodes directly implanted into the peripheral nerves of an amputated patient. Using this sensory feedback, the blindfolded patient was able to recognize different objects by their feel and shape and to adapt his grasping strategy accordingly [43].

Several less “robotic” innovations have also improved the quality of prostheses, as well as their comfort. The use of new materials (plastics, composites, light metal alloys) has significantly reduced the weight of prostheses compared with old fashioned ones made of steel, PVC, and until recently, wood and leather. Silicon suction sockets simplify donning of the prosthesis (in some cases, avoiding the use of harnesses and straps), providing a better fit and limiting problems relating to irritation around the stump. The use of silicon as an alternative to PVC, which is usually used to line prostheses, has the advantage of being able to create ultra-realistic and customizable prostheses, reducing the visibility of the disability [34].

2.7.1 Commercial Prosthetic Hands

Some of the current common characteristics of the most promising commercial hand products i-limb Quantum by Touch Bionics, RSL Steeper’s BeBionic v3, and Ottobock’s Michelangelo are presented in Table 2.4 [6].



Figure 2.18: Ottobock prosthetic hands and cosmetics

(From left to right): small System Inner Hand, small MyoHand VariPlus Speed, and medium Michelangelo hand [6]

Table 2.4: Features of already established commercially available prosthetic hands [6]

Product name	Established devices			Emerging devices		
	Child Myoelectric Hand by Centri	Transcarpal Hand	Select Electric Hand	i-Limb Quantum	BeBionic v353	Michelangelo59
Vendor	Hosmer Dorrance Corp.	Ottobock Healthcare	Liberating Technologies	Touch Bionics	RSL Steeper	Ottobock Healthcare
Weight (g)	238	308	470–520	474	570–590	420–510
Size (mm)	171	184–210	184–210	154–182	190–200	177–210
Full closing time (s)	0.35	0.91	0.90	0.80	1.00	0.37
Maximal grip force (N)	63	90	–	136	140.1	70
Thumb rotation properties	Static	Static	Static	Passive and motorized	Passive	Motorized
Digit dexterity	First two digits coupled	First two digits coupled	First digit active	Four individually motorized	Four individually motorized	First two digits coupled
Wrist options	Passive rotation	Passive flexion and active rotation	Passive rotation	Active and passive rotation and passive flexion	Passive in all directions	Active and passive rotation and passive flexion

2.7.2 UoM Transradial Prosthetic Arm

University of Moratuwa (UoM) has designed an underactuated anthropomorphic transradial prosthetic arm as shown in Figure 2.19. In their design, a novel wrist mechanism is proposed based on the parallel prismatic manipulators in order to generate the wrist flexion/extension and ulna/radial deviation. The proposed prosthetic hand supports seven DoF with three actuation modules that are dedicated to thumb, index finger and remaining three fingers linked to one another. Moreover, the hand mechanism is capable of providing the grasping adaptation. For the finger movements, modified crossbar mechanism is implemented by introducing a link-spring construction. Thereby, prosthetic hand can adapt and achieve various grasping patterns to grip objects with different geometries [2].

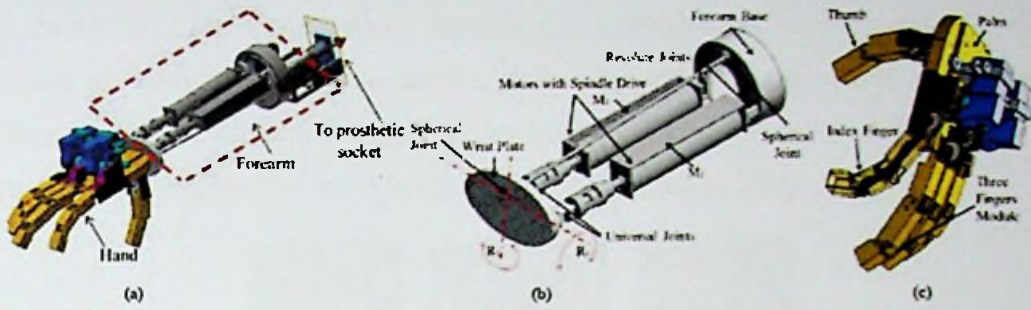


Figure 2.19: UoM transradial prosthesis [2]

(a) proposed transradial prosthesis (b) parallel manipulator wrist (c) hand

2.7.3 Amrita Prosthetic Hand

Amrita University has designed and manufactured a myoelectric multi-fingered anthropomorphic prosthetic hand using 3D printing technique. The hand is able to achieve 5 DoF with individually actuated fingers. EMG signal is used for the control and coordination of five fingers. The developed hand is designed to lift 2kg load and actuated by polymer string or fishing line along with metal gear servo motors. Various grasps and mimicking postures of the prosthetic hand is shown in Figure 2.20 [44].

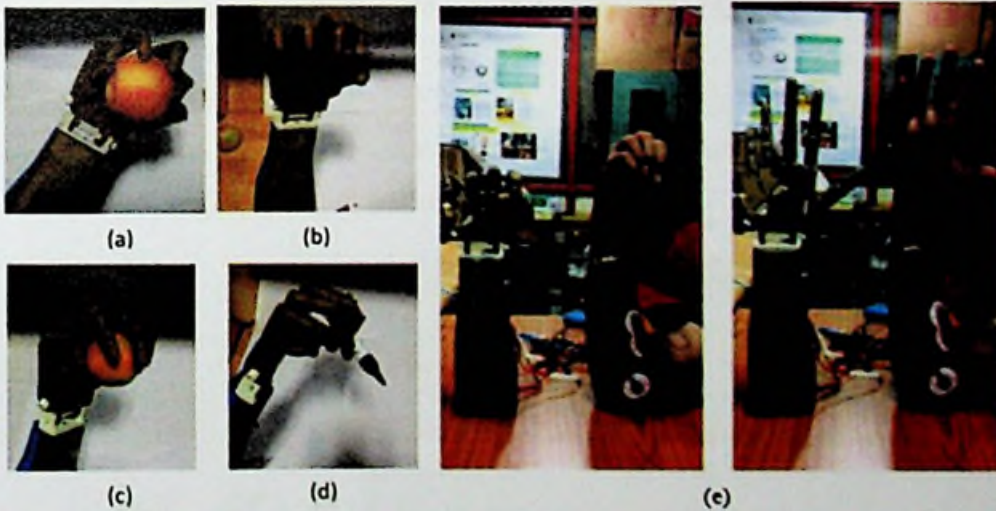


Figure 2.20: Amrita prosthetic hand grasps and mimicking postures [44]

(a) Spherical (b) Cylindrical (c) Power (d) Precision (e) mimicking human hand

2.7.4 Ondokuz Mayıs Prosthetic Hand

Ondokuz Mayıs University has developed a multifunctional, two channels myoelectric prosthetic hand which is operated for biomedical and control engineering laboratory as an experimental apparatus. Various analog signal processing steps are implemented

to the surface EMG signals which received on the triceps and biceps muscles. Those signals are conveyed to microcontroller and compared with a threshold value. One function of five different functions is selected by the received signal from triceps muscles and this function is activated by the biceps muscles [45].

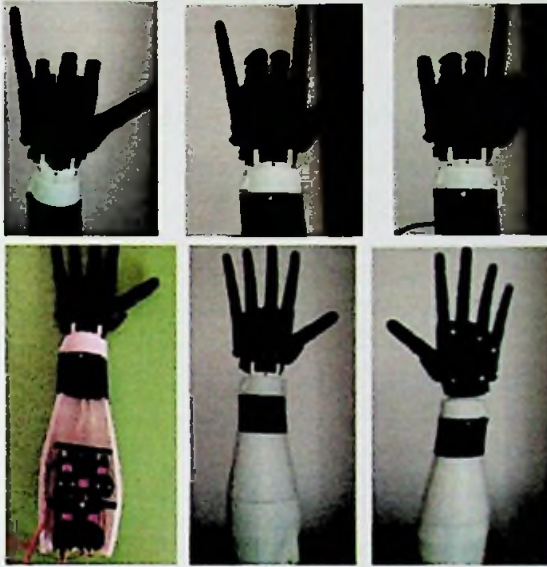


Figure 2.21: Ondokuz Mayıs prosthetic hand and grasps [45]

2.7.5 Evolution of Prosthetic Hands

Many researchers have developed different prosthetic hands with various functionalities and mechanisms as presented in Figure 2.22.

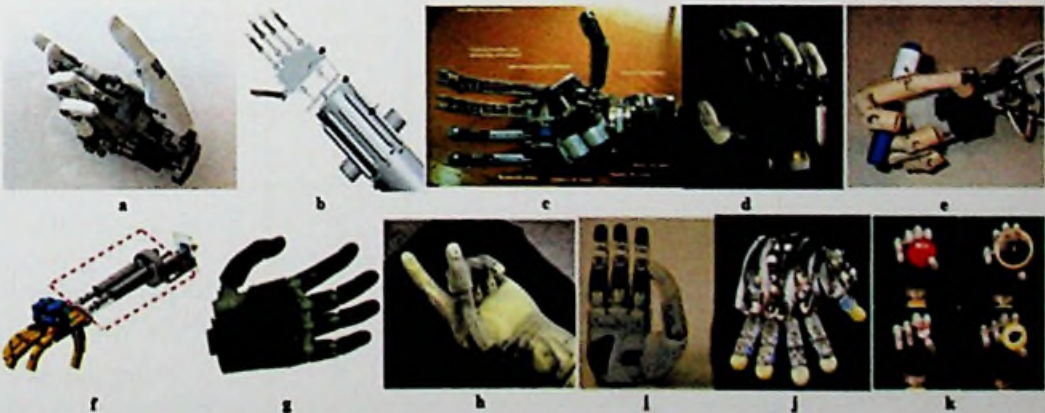


Figure 2.22: Research level prosthetic devices [46]

(a) UNB Hand, (b) 3D model of uGrip II Hand, (c) MANUS Hand, (d) FluidHand HI, (e) LUCS Haptic Hand III, (f) UoM transradial prosthesis, (g) Vanderbilt Multigrasp Hand, (h) DEKA RC Gen 3 Hand, (i) DLR/HIT II Hand, (j) Keio Hand, (k) SmartHand.

Latest technological advances may enable the prosthetic developers to derive an ideal replacement in future. In order to realize this task, it is essential to have a better understanding on the performance capabilities and design characteristics of existing transradial prostheses. Table 2.5 describe both hardware and control systems of modern transradial prostheses at research-level developed during the last decade [46].

Table 2.5: General characteristics of modern prosthetic hands at research level [46] [47] [48]

Name	DoF	No. of actuators	Finger movement mechanism	Actuation Method
MANUS Hand (2004)	7	2	Tendon based mechanism and crossed-bar mechanism	Brushless DC motors
LUCS Haptic Hand III (2008)	12	6	Tendon based mechanism	RC servo motors
DLR/HIT II Hand (2008)	15	15	Belt drives and gears based mechanism	Brushless DC motors with harmonic drive
Keio Hand (2008)	20	20	Wire driving method using elastic elements	Ultrasonic motor
FluidHand III (2008)	8	5	Flexible fluidic actuators	Pressurized fluid
Vanderbilt Multigrasp Hand (2009)	9	4	Tendon and torsion spring based mechanism	Brushless DC servomotors
Smart Hand (2009)	16	4	Tendon and torsion spring based mechanism	DC motors with using worm gears
UNB Hand (2010)	5	3	Linkage based mechanism	DC motors
DEKA RC Gen3 arm (2012)	6	4	Linkage based mechanism	Both brushless and brushed DC motors
uGrip II (2013)	5	5	Pneumatic artificial muscles (PAMs)	Pneumatic
UOM Transradial Prosthesis (2014)	7	3	Cross-bar mechanism	Brushless DC motors with gear drives
MoBio (2017)	5	4	Ball and screw mechanism	Brushed DC motors and BLDC motor
UoM Prosthetic Hand (2017)	-	4	Four bar linkages, torsion spring	DC Motors

2.8 Summary of Literature Review

The hand is the most frequently symbolized part of the human body containing a large number of muscles and joints which enable numerous patterns of movement essential for activities of daily living (ADL). However, the people incur an illness or experience an accident result in loss of their hand. Consequently, the researchers have been making effort to develop prosthetics to mimic the motion, anatomy, cosmetic and the power of the human hand.

The wide range of prostheses for replacement of the human hand can be categorized as prosthetic hands and prosthetic tools. Prosthetic hands offer a realistic appearance and are used for a variety of activities where the prosthetic tools have a mechanical appearance and are mostly designed for one specific activity. Most of the passive prosthetic tools has been primarily designed for the activities such as using cutlery, performing sports, entertaining and driving. Besides, the researchers have developed different prosthetic hands with various functionalities and mechanisms. Several companies have been focused on improving the commercial hardware devices such as, Child Myoelectric Hand, Transcarpal Hand, Select Electric Hand, i-Limb Quantum, BeBionic v353 and Michelangelo59 which are closer to human hand. The universities and research institutes have been developed hands such as UoM Transradial Prosthesis, Amrita Hand Ondokuz Mayıs Hand, LUCS Haptic Hand III and Keio Hand. Mostly those hands are powered by electric motors and various finger movement mechanisms are used such as tendon based mechanisms, crossed-bar mechanism, belt or gears based mechanisms, wire driving methods using elastic elements, flexible fluidic actuators, torsion spring based mechanisms and linkage based mechanisms. Most of those prosthetics are made with five fingers and each finger may flex, extend, abduct and adduct. Furthermore, those are capable of wrist flexion extension and ulna radial deviation which may beneficial for various hand functions.

CHAPTER 03: MECHANISM AND MECHANICAL DESIGN

It has been identified that, power grasp is the most frequently employed grasping pattern with a frequency of 35% of the ADL and generally, it can be categorized in to cylindrical and spherical grasps. In consideration of power grasping applications with a high workload and finger contact forces, prosthetic hands have a need of powerful actuators to be placed inside the fingers, which will create an excessive weight, which should bear by the amputee. This research proposes a novel linkage based finger mechanism, which is mostly applicable for the grasping applications with a high workload and finger contact force. Besides, the proposed mechanism causes to move by the cables, can be made with less in weight since there is no need to place any actuator inside the finger. Subsequently, a self-adaptive actuation method is presented. The mechanical design and the functionality of the developed prosthesis is described in this chapter. Figure 3.1 shows the basic components of the prosthetic hand which is 3D modeled using Solidworks CAD package.

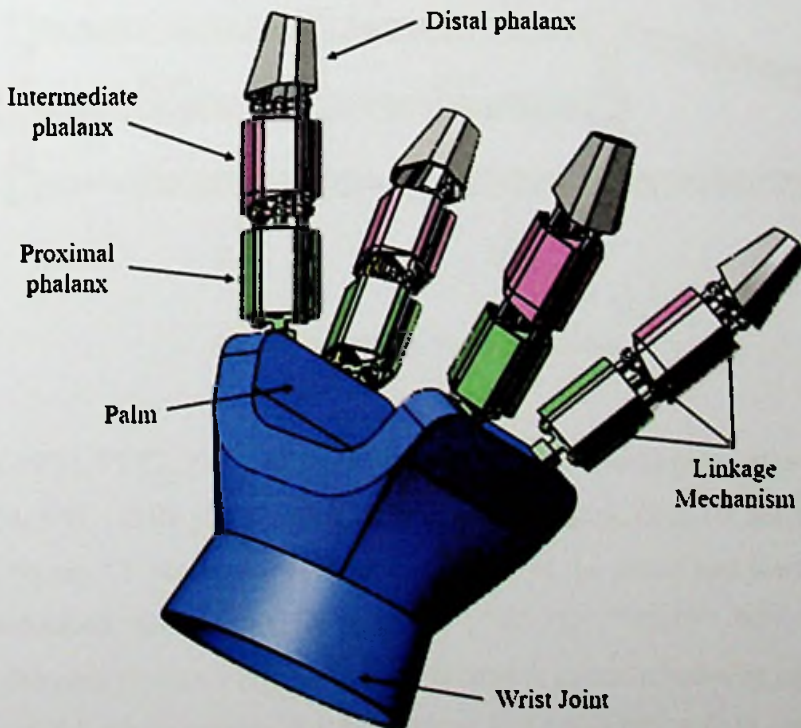


Figure 3.1: CAD Model of the prosthetic hand

The prosthesis can be fixed below the wrist joint of the amputee. Design of the palm is altered from the human hand as it is designed specifically to carry out power grasping activities. There are four finger modules which are same in design. Each finger consist of Proximal phalanx, Intermediate phalanx and Distal phalanx. In order to achieve the required finger motions with the adequate forces, a novel linkage mechanism is proposed. Since the design is only for a special type of grasping applications, the metacarpophalangeal (MCP) joint of the finger is not actuated. However, the proximal interphalangeal (PIP) joint, and distal inter phalangeal (DIP) joint is designed to be set in motion by any linear actuator based on the active or passive dynamics.

3.1 Mechanism

As descried in the previous section the PIP and the DIP joints of the finer is actuated by a novel linkage mechanism as shown in Figure 3.2. There are 12 different links. The isometric views of individual links are illustrated in Appendix I.

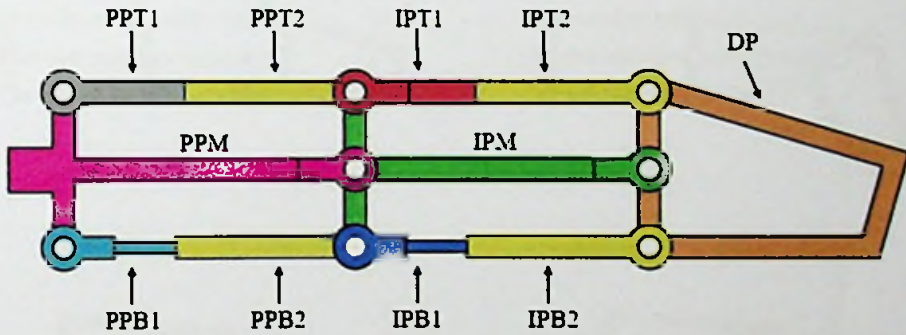


Figure 3.2: Linkage finger mechanism

The links PPT1, PPT2, PPM, PPB1, PPB2 placed in the Proximal phalanx and IPT1, IPT2, IPM, IPB1, IPB2 placed in the Intermediate phalanx. Link DP act as the Distal phalanx. Figure 3.3 presents the sematic diagram of the joints and the links of the finger mechanism. Accordingly, the points “C”, “E”, “D”, “B”, “F”, “G”, “H” and “I” illustrate the rotary joints. Further there are prismatic joints in between point C-D, E-F, D-G, and F-I. Consequently, E-F be made of PPT1 and PPT2, C-D made of PPB1 and PPB2, F-I made of IPT1 and IPT2, D-G made of IPB1 and IPB2.

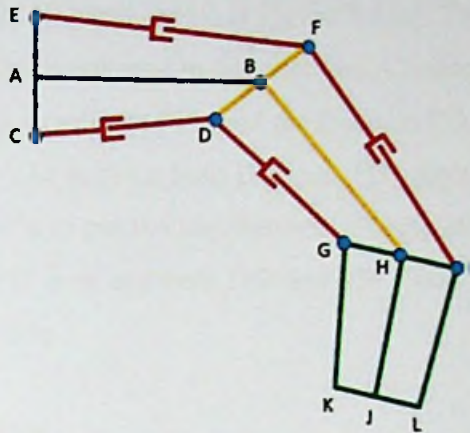


Figure 3.3: Links and joints of the finger

Distance AB, BH, HJ, CE, DF, GI, LK, GK and IL are fixed length where CD, EF, DG and FI are adjustable lengths. The four basic activation steps of the finger is presented in Figure 3.4.

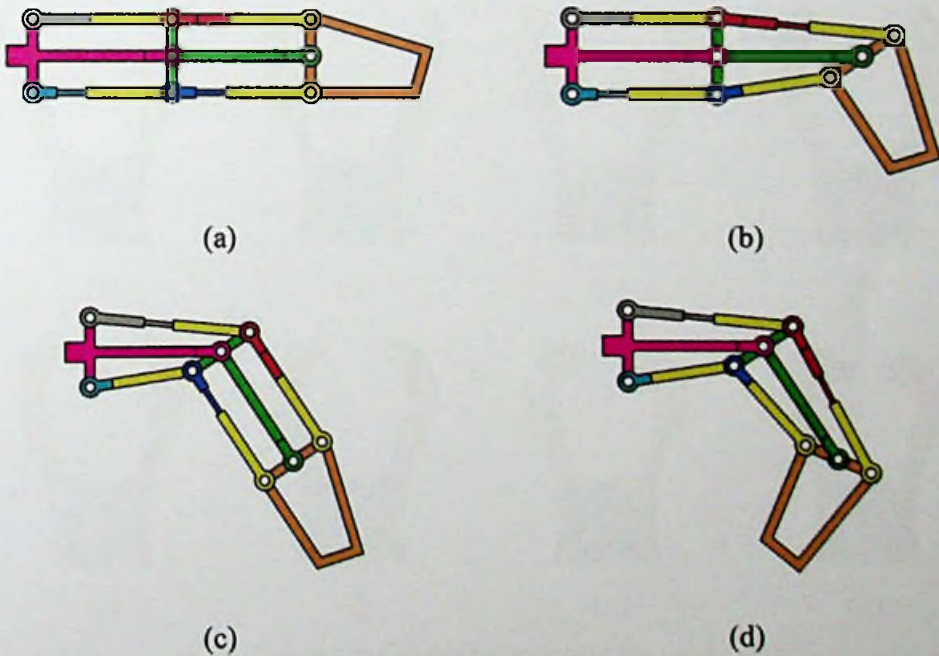


Figure 3.4: Basic activation steps of the finger mechanism

(a) Initial position (b) Rotation of DIP joint (c) Rotation of PIP joint (d) Rotation of both DIP and PIP joints

The initial position of the finger is shown in Figure 3.4 (a). To achieve the full rotation DIP joint the distance DG is adjusted to its minimum. Consequently, FI will extend to its maximum. Similarly, to activate PIP joint the distance CD is reduced where the EF draw out automatically. To activate both DIP and PIP joints at once the lengths CD and DG should be shorten as per the requirement of angle of rotation. The maximum rotation of DIP joint, PIP joint and both DIP and PIP joints are shown in Figure 3.4 (b), (c) and (d) respectively.

3.2 Grasping Sequence

The basic gasping patterns of the human hand is mainly categorizing as power and precision. The developed prosthetic hand is specifically designed for power grasping applications. The hand is capable of accomplishing cylindrical grasp and spherical grasp. Furthermore, it can be used to perform hook grasp for larger diameters. Figure 3.5 demonstrate the sequence of the grasping in eight steps.

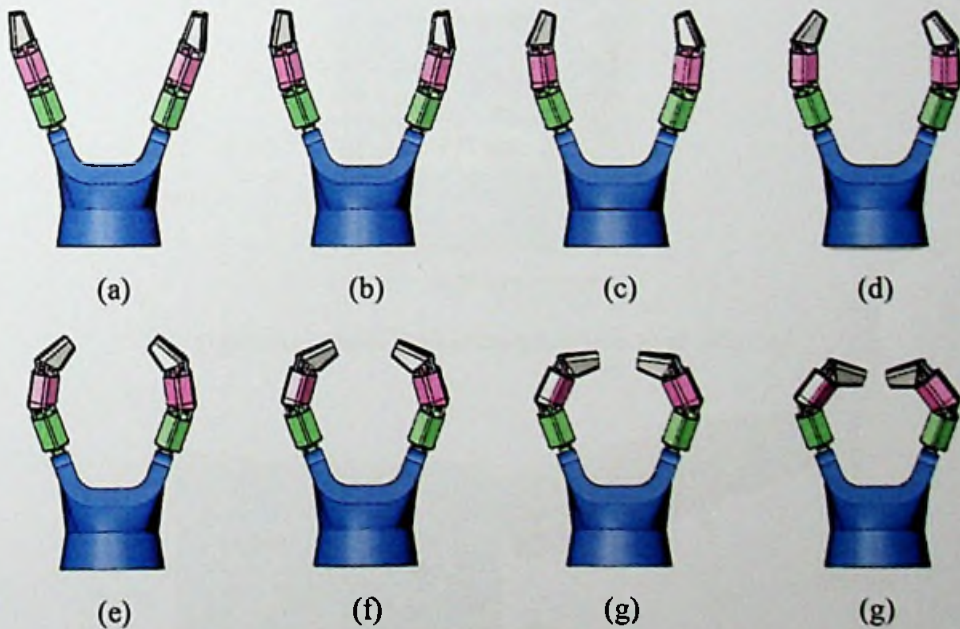


Figure 3.5: Grasping sequence of the hand
(a) - (g) Initial step to final step

3.3 Ergonomics in Design

The transradial prosthetic hand has been designed by considering the anthropometric data of the Sri Lankan population. Furthermore, it is designed to withstand the standard loads applied on each part of the hand as it is defined in ergonomics data for use in the design of safer products. The dimensions of the prosthesis terminal device are shown in Figure 3.6 and Figure 3.7.

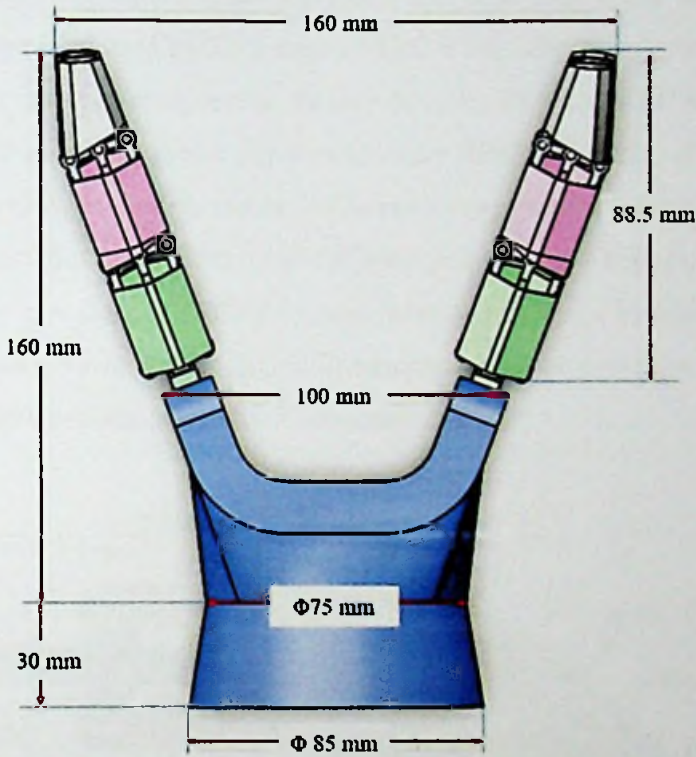


Figure 3.6: Dimensions of the prosthetic hand side view

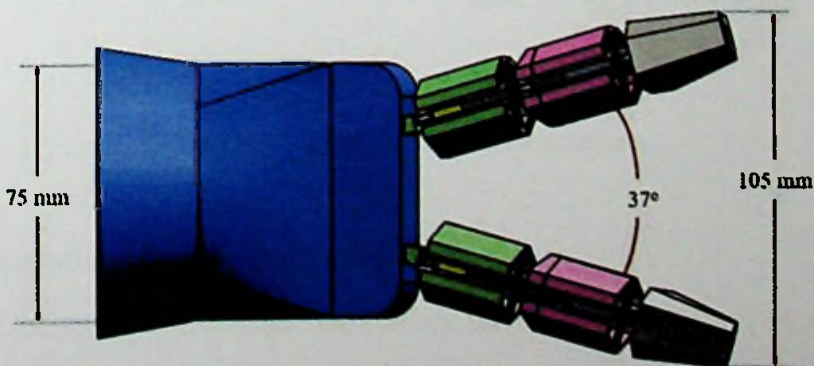


Figure 3.7: Dimensions of the prosthetic hand top view

3.4 Design for Manufacture

Since the designed finger mechanism consists of millimeter scale links with prismatic and rotary joints, advanced manufacturing processes have been required for the fabrication. Necessary CNC milling and EDM processes are expensive and time consuming. In order to study the finger motion experimentally, the finger mechanism is redesigned by considering the design for manufacture (DFM) guidelines. Redesigned finger for experimental analysis is shown in Figure 3.8. All the links are redesigned to be fabricated by 3D printing additive manufacturing process. PPM and IPM were split in to two components for easy printing. PPM1 and PPM2 were printed in two separate parts and joined together to make PPM. Similarly, IPM1 and IPM2 were used to make IPM. Furthermore, DP is made by joining DP1 and DP2 together. Appendix II provides the isometric view of each part designed with Solidworks CAD package. In the new design, all the prismatic joints were altered by adding copper rod inserters that act as linear guides (LGs). The animation of the prototype finer design is shown in Video 01 of the Appendix V (compact disc).

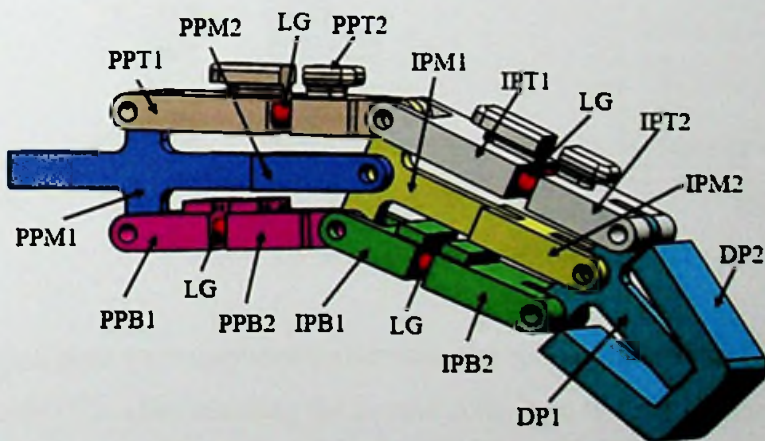


Figure 3.8: Finger design for manufacture

3.5 Fabrication of the Finger Mechanism

First, all the links of the finger mechanism were 3D printed with PLA polymer material. Secondly, 3mm copper rods were inserted as linear guides. Finally, the compartments were assembled together with 3mm nut and bolts.

The components developed in Solidworks software package were converted into STL file format and then uploaded to Slic3r package to generate required G-codes for printing. The generated G-codes were used to operate the Uni-Print 3D printer which is connected to sandyBox motion controller that is controlled by Machinekit control application. Figure 3.9 presents the Slic3r software interface which is used for G-code generation. The tool Slic3r is utilized to convert the 3D model into printing instructions for Uni-Print 3D printer. It cut the model into horizontal slices (layers) and generated toolpaths to fill. Further software is used to calculate the amount of material to be extruded. The Uni-Print 3D printer is set up according the prearranged settings presented in the Table 3.1.

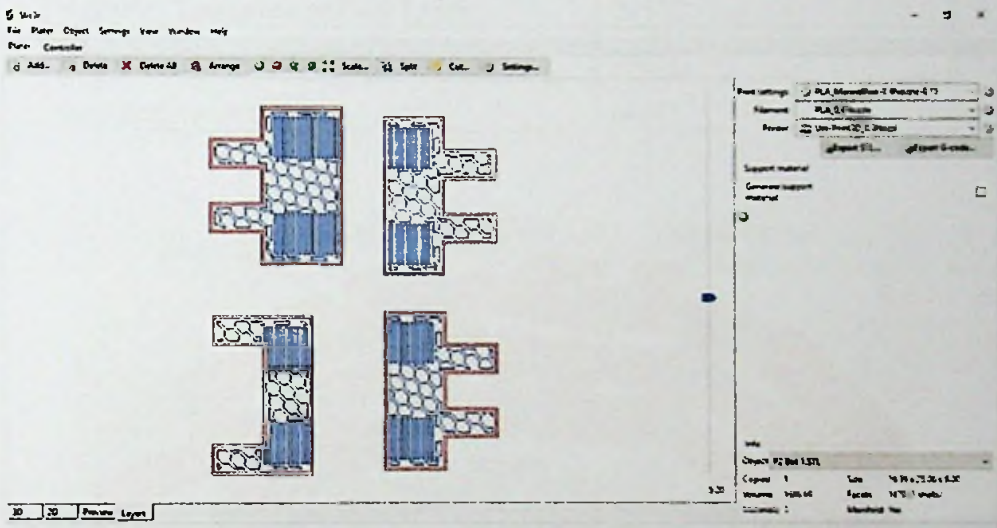


Figure 3.9: Slic3r software interface

The 3D printed parts were upgraded by inserting the copper rods to perform the action of linear guide. The after inserting the copper rods in to the plastic parts, glue was applied to make the bond stronger. Subsequently all the parts were assembled by using 3mm diameter nut and bolts. Rubber loops were placed in between PPT1 and PPT2, IPT1 and IPT2 to achieve the spring back effect. Finally, the nylon strings are threaded through the holes in the bottom of the proximal phalanges (PPB1 and PPB2) then through the holes across the bottom of the Intermediate phalange (IPB1 and IPB2). The fabricated finger is shown in Figure 3.10 and the operation of the prototype finer is shown in Video 02 of the Appendix V (compact disc).

Table 3.1: Uni-Print 3D printer settings

Parameter	Settings
Layer Height	0.15mm
Infill Density	40%
Infill Pattern	Honeycomb
Support Material	For first layer
Perimeters Print Speed	50 mm/s
Infill Print Speed	80 mm/s
Non Print Move Speed	110 mm/s
Filament Diameter	1.75 mm
Extruder Temperature First Layer	215°C
Extruder Temperature Other Layers	205 °C
Bed Temperature	60 °C



Figure 3.10: Fabricated finger mechanism

3.5.1 Material used for Fabrication

The test finger is fabricated with “colorFabb” red transparent pure Polylactic Acid (PLA) material. As provided by the manufacturer Table 3.2 pointed out the specification of the material.

There is a vast array of applications of Polylactic Acid. As it has low glass transition temperature, PLA is widely used for 3D printing. PLA undergoes more of a phase-change when heated and becomes much more liquid. If actively cooled, much sharper details can be seen on printed corners without the risk of cracking or warp. The

increased flow can also lead to stronger binding between layers, improving the strength of the printed part. Printed objects will generally have a glossier look and feel than ABS. Further, it can also be sanded and machined as per the requirement. General characteristics of the PLA material is shown in Table 3.3.

Table 3.2: Specification of the finger material

Property	Value / Description
Brand Name	ColorFabb PLA
Model	Red Transparent
Type	Filament
Effective Diameter	1.75mm
Diameter Tolerance	± 0.05 mm
Density	1.210-1.430 g/cm ³
Glass Transition Temperature	55°C

Table 3.3: General characteristics of the PLA material [49]

Property	Value	Unit
Solid density	1.252	g/cm ³
Elastic modulus	3500	MPa
Shear modulus	1287	MPa
Poisson's ratio	0.36	-
Yield strength	70	MPa
Notch izod impact	26	J/m
Rockwell hardness	88	HR
Ultimate tensile strength	73	MPa
Young's modulus	1280	MPa

3.6 Actuation of the Finger

The finger mechanism designed for experimental investigation is actuated based on the passive dynamics by pulling the links by nylon string.



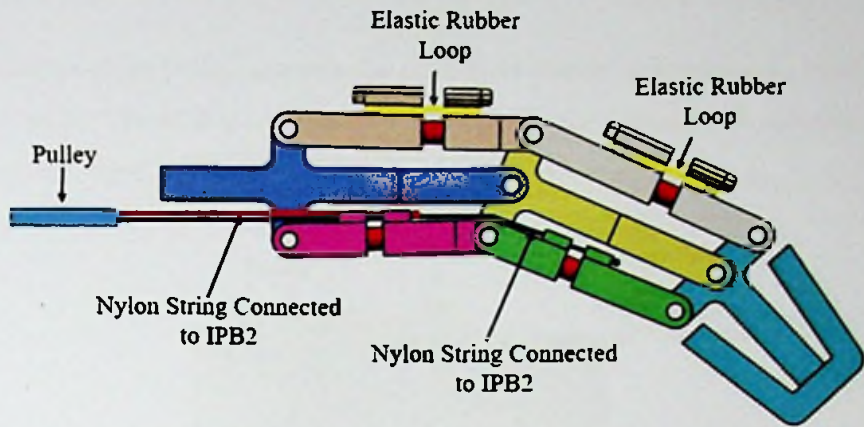


Figure 3.11: Passive dynamic finger mechanism

As presented in Figure 3.11 nylon strings are threaded through the holes in the bottom of the proximal phalanges (PPB1 and PPB2) then through the holes across the bottom of the Intermediate phalange (IPB1 and IPB2). The holes are clearly visible in the Figure 3.8. Then the strings are tightly tied around using a knot and two pairs of small long nose plier are used to ensure the knot is tight. An elastic rubber loop is placed between PPT1 and PPT2, IPT1 and IPT2. Those rubber loops act as springs to obtain the reverse actuation and bring the finger the initial position.

Further a simple mechanism is proposed in order to achieve adaptive finger motion during grasping. Figure 3.12 illustrate the schematic representation of the proposed mechanism. There are two pulleys. One end of the nylon string that goes around pulley A is connected to PPB2, where the other end is connected to IPB2. Similarly, the string goes around pulley B is also connected to PPB2 and IPB2. As there are two pulleys the forces are equally distributed among the both and it benefits reduce the lateral motions.

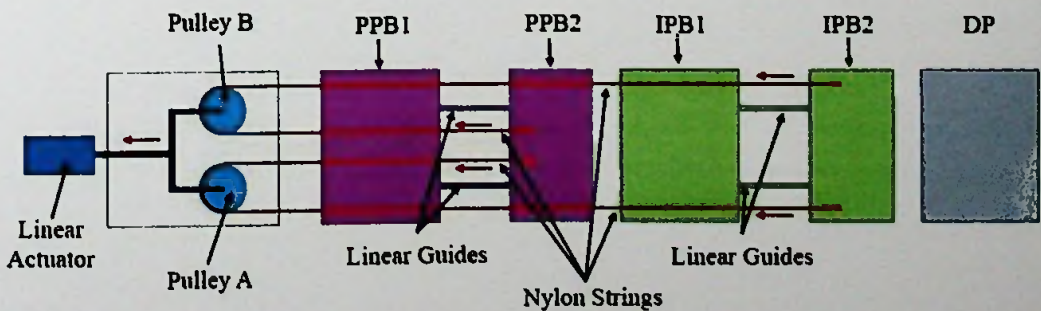


Figure 3.12: Adaptive finger actuation method

The pulleys can be pulled towards the directions shown in Figure 3.11 with aid of a linear actuator. Unless it is capable to actuate passively without any actuators. Figure 3.13 presents the CAD model of the adaptive finger actuation device.

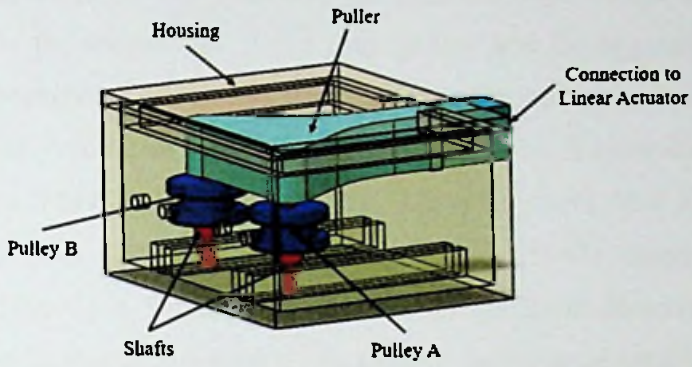


Figure 3.13: Adaptive finger actuation device

CHAPTER 04: KINEMATIC ANALYSIS

Understanding the kinematics of the hand prosthesis and the novel finger mechanism is important to achieve the finest motions of the artificial hand. In the last 150 years, several approaches have been proposed for the calculation of the mobility of the mechanisms. In the second half of the 19th century and the beginning of the 20th century the Chebychev–Grübler–Kutzbach criterion for multi-loop mechanisms were set up. Different versions of these formula were proposed all along the 20th century by Dobrovolski (1949 - 1951), Artobolevskii (1953) Kolchin (1960) Rössner (1961), Boden (1962), Ozol (1963), Manolescu and Manafu (1963), Bagci (1971), Hunt (1978), Tsai (1999) [50]. Significantly, the criterion can break down for mechanisms with special geometries and particularly for the over-constrained parallel mechanisms. The Chebychev–Grübler–Kutzbach criterion explicit the relationship between the mobility and the structural parameters of the mechanism [51]. Furthermore, kinematic analysis is essential to yield the improved performance of the mechanical design and to develop appropriate control algorithms. Chen et al. have presented the kinematic and dynamic characteristics of the human finger as a preliminary step towards the development of robotic and prosthetic fingers that imitate the human finger functions [52]. Several approaches have been deliberated by the researches, in order to analysis the kinematics of the diverse finger mechanisms. For instance, Licheng et al. have considered positional kinematics of the finger at different stages and the kinematic analysis of the equivalent mechanism of each stage has been carried out, for their fully rotational finger [53]. Furthermore, Screw theory has been used to establish the general kinematic both of series and parallel manipulators. Through the screw theory, Hunt et al. have shown that, a workpiece grasped by a fully-in- series manipulator can only lose freedom while a workpiece grasped by a fully-in-parallel manipulator can only gain freedom [54]. According to the comparison carried out by Rocha et al., the main feature of the screw-based kinematic modelling is the uniformity. In addition, screw-based modelling is advantageous in differential kinematics [55]. However, The Denavit–Hartenberg (D-H) approach is more popular and widely adopted in research than the Screw theory [56-61]. D-H conventions model has been originally applied

into single loop chains but now almost universally applied to open loop serial chains [62].

4.1 Kinematics of the Human Hand

Human wrist provides two DoF termed flexion/extension and ulnar/radial deviation. Radial means the motion towards the thumb and the ulnar means the motion towards the little finger. Additionally, hand provides three DoF for the thumb and other four DoF for each other finger. The thumb moves in a unique way compared to other four fingers. MP joint and IP joint of the thumb flex and extend. CMC Joint of the thumb is highly specialized and allows several unique movements termed circumduction, abduction, adduction, repropulsion that are possible with other fingers. Circumduction is moving around in a circle, abduction and adduction are the thumb's motion out of and into the palm, respectively and repropulsion is lifting the thumb off a table while keeping the hand flat. All other four fingers termed index, middle, ring, and small can be controlled individually. DIP, PIP and MCP joints of each finger are capable of flexion and extension. In addition the MCP joint of each finer provides abduction and adduction movements. Equivalent kinematic structure of the human hand is shown in Figure 4.1.

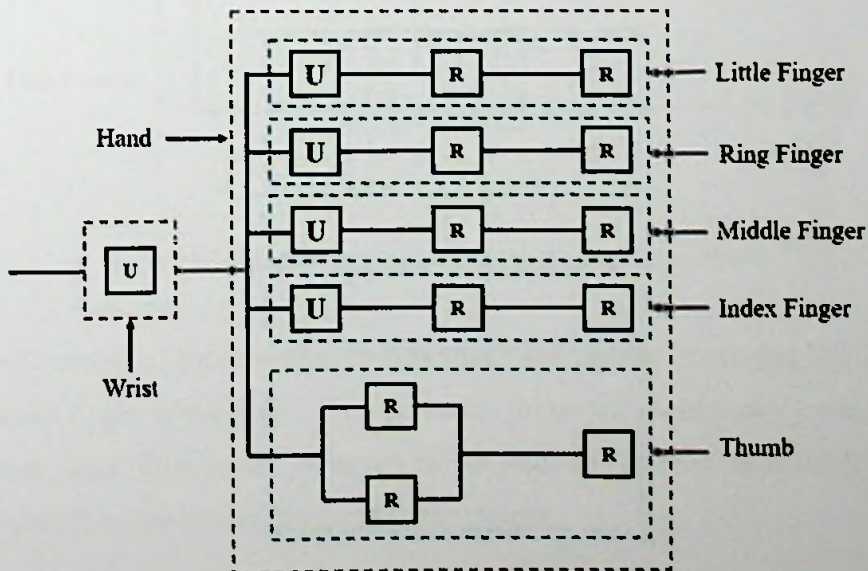


Figure 4.1: Kinematic structure of human hand

4.2 Kinematics of the Prosthetic Hand

The novel linkage mechanism presented in this paper can be identified as a combination of parallel and series links. The kinematics structure of the developed prosthesis is shown in Figure 4.2.

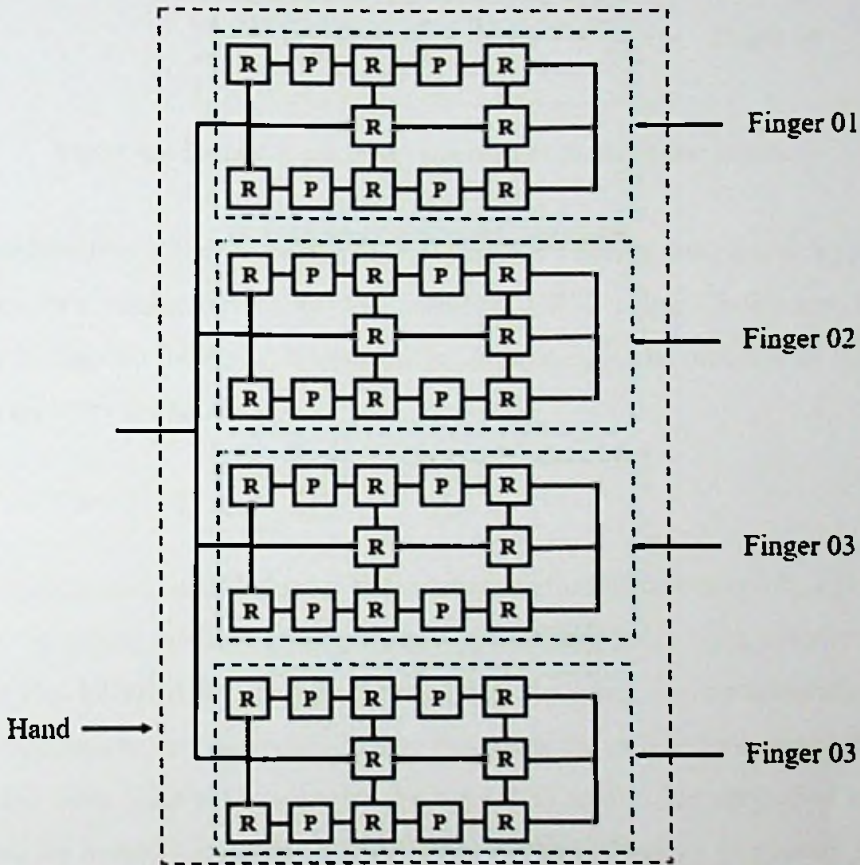


Figure 4.2: Kinematics structure of the developed prosthesis

The hand consists of four identical fingers which are capable of rotating DIP and PIP joints. Each finger is made up of two prismatic joints and eight rotary joints. Unlike the human finger three rotary joints act as PIP joint and another three for DIP joint. All together there are eleven links and twelve joints.

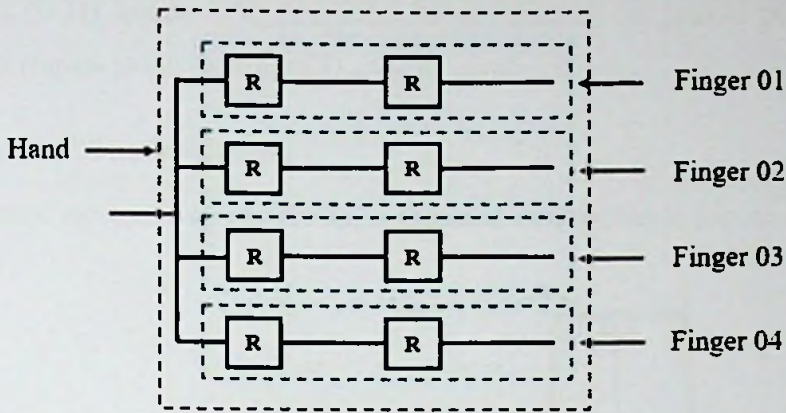


Figure 4.3: Simplified kinematics structure of the developed prosthesis

The consideration of the mobility is also an important design criterion. It is possible to compare two configurations of the modified CBM using Chebychev–Grübler–Kutzbach criterion for a planar mechanism. Accordingly, the mobility of the system will be given by the equation,

$$F = 3(n - j - 1) + \sum_{i=1}^j f_i \quad 4.01$$

Where n is the number of links, j is the number of kinematic pairs and f_i is DoF of the i th pair. However, mobility criteria are not applicable to many types of recent parallel robots [50]. Intended for analysis the mobility, the kinematic representation of the finger mechanism has been simplified by assuming the middle links act as the bones where the outer links act as muscles. Figure 4.3 illustrates the simplified kinematic structure for mobility analysis. The PIP joint is represented by one rotary joint and correspondingly DIP as well. For the initial configuration without length varying links n equals 3, j equals 2 and $\sum f_i$ equals 2. Therefore, the DoF of the mechanism is equal to 2. Thus, without length varying links the mechanism is capable of generating only two motion configuration with a fixed set of joint angles. Furthermore, kinematic analysis of the mechanism has been carried out in two steps. In the first phase, the geometric representation has been depicted with the intention to initiate the relationships between the joint angles and the link lengths. Subsequently, in the second phase, the forward kinematic analysis has been carried out by means of Denavit-

Hartenberg (D-H) approach, to determine the positions of the critical points on the finger with respect to the different CD and DG distances.

4.3 Geometric Representation

The geometric representation of the finger mechanism is shown in Figure 4.4.

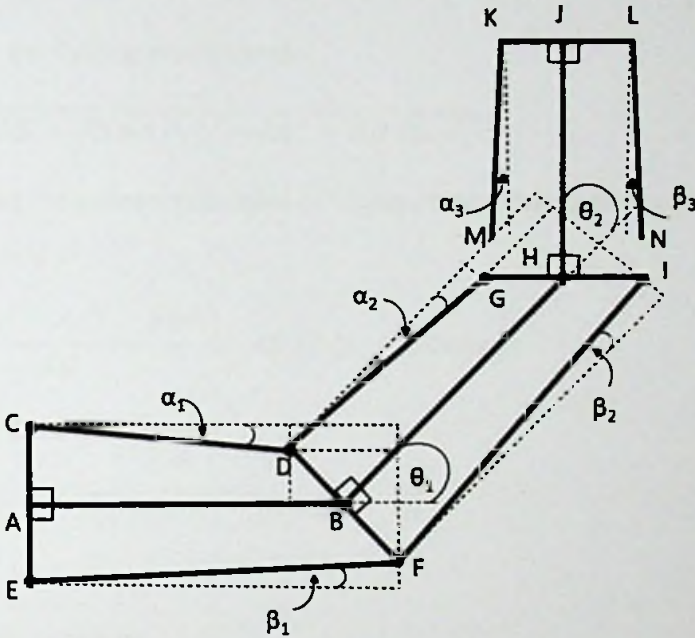


Figure 4.4: Geometric representation of the novel finger mechanism

Accordingly, PIP joint angle is θ_1 and the DIP joint angle is θ_2 . Rotation angles of links CD, EF, DG and FI are α_1 , β_1 , α_2 and β_2 respectively.

According to the geometry the design, following distances are equal.

$$AC = AE = BD = BF = GH = HI \quad (4.02)$$

Let us consider the links of the proximal phalanx. According to the geometry,

$$EF \cos \beta_1 - AB = BF \sin \theta_1 \quad (4.03)$$

$$AB - CD \cos \alpha_1 = BD \sin \theta_1 \quad (4.04)$$

By considering, equation (4.02), (4.03) and (4.04) it can be derived that,

$$2AB = EF \cos \beta_1 + CD \cos \alpha_1 \quad (4.05)$$

Moreover, according to the geometry it can be established that,

$$AC = BD \cos \theta_1 + CD \sin \alpha_1 \quad (4.06)$$

$$AE = BF \cos \theta_1 + EF \sin \beta_1 \quad (4.07)$$

By considering, equation (4.02), (4.06) and (4.07) it can be derived that,

$$CD \sin \alpha_1 = EF \sin \beta_1 \quad (4.08)$$

According to the Pythagorean theorem,

$$CD = \sqrt{(AB - BD \sin \theta_1)^2 + (AC - BD \cos \theta_1)^2} \quad (4.09)$$

By considering the general principles of trigonometry and algebra, equation (4.09) can be simplified as,

$$\frac{CD^2 - AB^2 - AC^2 - BD^2}{-2BD} = AB \sin \theta_1 + AC \cos \theta_1 \quad (4.10)$$

According to the trigonometry;

$$(AB) \sin \theta_1 + (AC) \cos \theta_1 = C_1 \sin(\theta_1 + \delta_1) \quad (4.11)$$

Where;

$$C_1 = \pm \sqrt{AB^2 + AC^2} \quad (4.12)$$

$$\delta_1 = \tan^{-1} \left(\frac{AC}{AB} \right) \quad (4.13)$$

By substituting to the right hand side of the equation (4.10), from equation (4.11), (4.12) and (4.13),

$$\begin{aligned} \frac{CD^2 - AB^2 - AC^2 - BD^2}{-2BD} &= \pm \sqrt{AB^2 + AC^2} \left(\sin \left(\theta_1 + \left(\tan^{-1} \left(\frac{AC}{AB} \right) \right) \right) \right) \end{aligned} \quad (4.14)$$

Equation (4.14) can be simplified as below to establish a relationship between the angle θ_1 and the link lengths.

$$\theta_1 = \sin^{-1} \left(\frac{CD^2 - AB^2 - AC^2 - BD^2}{-2BD(\pm \sqrt{AB^2 + AC^2})} \right) - \left(\tan^{-1} \left(\frac{AC}{AB} \right) \right) \quad (4.15)$$

$$\theta_1 = \sin^{-1}(A_1) - \delta_1 \quad (4.16)$$

Where;

$$A_1 = \frac{CD^2 - AB^2 - AC^2 - BD^2}{-2BD(\pm\sqrt{AB^2 + AC^2})} \quad (4.17)$$

$$\delta_1 = \tan^{-1}\left(\frac{AC}{AB}\right) \quad (4.18)$$

According to the Pythagorean theorem it can be derived that,

$$EF = \sqrt{(AB + BF \sin \theta_1)^2 + (AE - BF \cos \theta_1)^2} \quad (4.19)$$

By substituting the θ_1 from equation (4.16), the equation (4.19) can be written as,

$$EF = \sqrt{(AB + BF \sin(\sin^{-1}(A_1) - \delta_1))^2 + (AE - BF \cos(\sin^{-1}(A_1) - \delta_1))^2} \quad (4.20)$$

By substituting the θ_1 from equation (4.16), the equation (4.06) can be written as,

$$AC = BD \cos(\sin^{-1}(A_1) - \delta_1) + CD \sin \alpha_1 \quad (4.21)$$

Equation (4.21) can be simplified as below to establish a relationship between the angle α_1 and the link lengths.

$$\alpha_1 = \sin^{-1} \frac{AC - BD \cos(\sin^{-1}(A_1) - \delta_1)}{CD} \quad (4.22)$$

By substituting the θ_1 from equation (4.16), the equation (4.07) can be written as,

$$AE = BF \cos(\sin^{-1}(A_1) - \delta_1) + EF \sin \beta_1 \quad (4.23)$$

By substituting EF from equation (4.20), the equation (4.23) can be simplified as below to establish a relationship between the angle β_1 and the link lengths.

$$\beta_1 = \sin^{-1} \frac{AE - BF \cos(\sin^{-1}(A_1) - \delta_1)}{\sqrt{(AB + BF \sin(\sin^{-1}(A_1) - \delta_1))^2 + (AE - BF \cos(\sin^{-1}(A_1) - \delta_1))^2}} \quad (4.24)$$

Let us consider the links of the intermediate phalanx. According to the geometry,

$$FI \cos \beta_2 - BH = HI \sin \theta_2 \quad (4.25)$$

$$BH - DG \cos \alpha_2 = GH \sin \theta_2 \quad (4.27)$$

By considering, equation (4.02), (4.25) and (4.27) it can be derived that,

$$2BH = FI \cos \beta_2 + DG \cos \alpha_2 \quad (4.28)$$

Moreover, according to the geometry it can be established that,

$$BD = GH \cos \theta_2 + DG \sin \alpha_2 \quad (4.29)$$

$$BF = HI \cos \theta_2 + FI \sin \beta_2 \quad (4.30)$$

By considering, equation (4.02), (4.29) and (4.30) it can be derived that,

$$DG \sin \alpha_2 = FI \sin \beta_2 \quad (4.31)$$

According to the Pythagorean theorem,

$$DG = \sqrt{(BH - GH \sin \theta_2)^2 + (BD - GH \cos \theta_2)^2} \quad (4.32)$$

By considering the general principles of trigonometry and algebra, equation (4.32) can be simplified as,

$$\frac{DG^2 - BH^2 - BD^2 - GH^2}{-2GH} = BH \sin \theta_2 + BD \cos \theta_2 \quad (4.33)$$

According to trigonometry;

$$(BH) \sin \theta_2 + (BD) \cos \theta_2 = C_2 \sin(\theta_2 + \delta_2) \quad (4.34)$$

Where;

$$C_2 = \pm \sqrt{BH^2 + BD^2} \quad (4.35)$$

$$\delta_2 = \tan^{-1} \left(\frac{BD}{BH} \right) \quad (4.36)$$

By substituting to the right hand side of the equation (4.33), from equation (4.34), (4.35) and (4.36),

$$\frac{DG^2 - BH^2 - BD^2 - GH^2}{-2GH} = \pm \sqrt{(BH^2 + BD^2)} \left(\sin \left(\theta_2 + \left(\tan^{-1} \left(\frac{BD}{BH} \right) \right) \right) \right) \quad (4.37)$$

Equation (4.37) can be simplified as below to establish a relationship between the angle θ_2 and the link lengths.

$$\theta_2 = \sin^{-1} \left(\frac{DG^2 - BH^2 - BD^2 - GH^2}{-2GH(\pm \sqrt{(BH^2 + BD^2)})} \right) - \left(\tan^{-1} \left(\frac{BD}{BH} \right) \right) \quad (4.38)$$

$$\theta_2 = \sin^{-1}(A_2) - \delta_2 \quad (4.39)$$

Where;

$$A_2 = \frac{DG^2 - BH^2 - BD^2 - GH^2}{-2GH(\pm \sqrt{(BH^2 + BD^2)})} \quad (4.40)$$

$$\delta_2 = \tan^{-1} \left(\frac{BD}{BH} \right) \quad (4.41)$$

According to the Pythagorean theorem it can be derived that,

$$FI = \sqrt{(BH + HI \sin \theta_2)^2 + (BF - HI \cos \theta_2)^2} \quad (4.42)$$

By substituting the θ_2 from equation (4.39), the equation (4.42) can be written as,

$$FI = \sqrt{(BH + HI \sin(\sin^{-1}(A_2) - \delta_2))^2 + (BF - HI \cos(\sin^{-1}(A_2) - \delta_2))^2} \quad (4.43)$$

By substituting the θ_2 from equation (4.39), the equation (4.29) can be written as,

$$BD = GH \cos(\sin^{-1}(A_2) - \delta_2) + DG \sin \alpha_2 \quad (4.44)$$

Equation (4.44) can be simplified as below to establish a relationship between the angle α_2 and the link lengths.

$$\alpha_2 = \sin^{-1} \frac{BD - GH \cos(\sin^{-1}(A_2) - \delta_2)}{DG} \quad (4.45)$$

By substituting the θ_1 from equation (4.16), the equation (4.30) can be written as,

$$BF = HI \cos(\sin^{-1}(A_2) - \delta_2) + EF \sin \beta_2 \quad (4.46)$$

By substituting FI from equation (4.43), the equation (4.46) can be simplified as below to establish a relationship between the angle β_2 and the link lengths.

$$\beta_2 = \sin^{-1} \frac{BF - HI \cos(\sin^{-1}(A_2) - \delta_2)}{\sqrt{(BH + HI \sin(\sin^{-1}(A_2) - \delta_2))^2 + (BF - HI \cos(\sin^{-1}(A_2) - \delta_2))^2}} \quad (4.47)$$

4.4 Forward Kinematics

Forward kinematics refers to the use of the kinematic equations of linkage mechanism to compute the position of the end-effector from specified values for the joint parameters. The forward kinematic analysis has been carried out by considering the Denavit-Hartenberg (DH) parameter approach. According to the DH procedure described by the Rocha et al. [55], first the links and joints should be identified. Links and joints can be numbered from 0 to n. Subsequently, it is required to define the reference frames for the internal links. Then the reference frames should be defined for the extremities links. Successively, the DH parameters for each link should be identified, where a_i is the distance between z_{i-1} and z_i , d_i is the distance between x_{i-1} and x_i , α_i is the angle between z_{i-1} and z_i measured along x_i , while θ_i is the angle between x_{i-1} and x_i , measured along z_i . Then the homogeneous transformation matrices for each joint should be determined and finally the overall homogeneous transformation matrix by premultiplication of the individual joint transformation matrices should be determined. Accordingly, Figure 4.5 illustrates the link frame assignment of the linkage finger mechanism and Table 4.1 define the Denavit-Hartenberg link parameters.

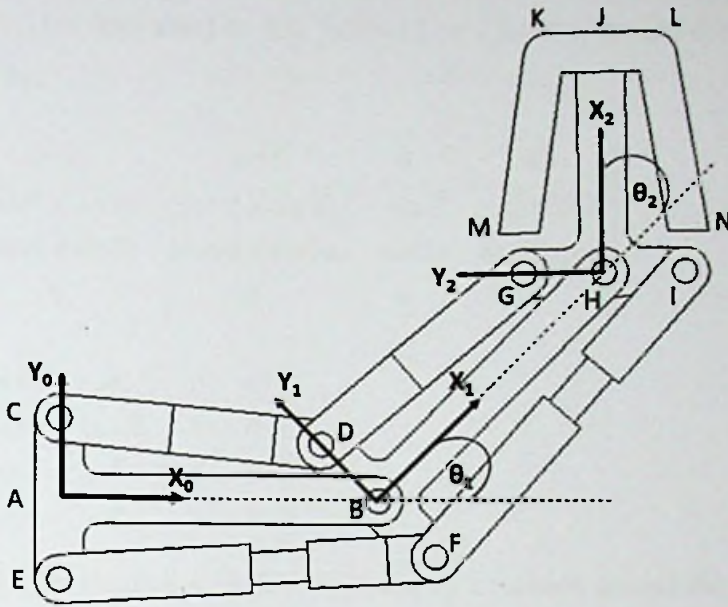


Figure 4.5: Link frame assignment of finger

Table 4.1: D-H link parameters

i	$\alpha_{(i-1)}$	$a_{(i-1)}$	d_i	θ_i
0	0	0	0	0
1	0	AB	0	θ_1
2	0	BH	0	θ_2

By referring to the link frame assignment and D-H link parameters. The rotation around the Z_0 axis can be denoted by,

$${}^0T = \begin{bmatrix} \cos 0 & -\sin 0 & 0 & 0 \\ (\sin 0)(\cos 0) & (\cos 0)(\cos 0) & -\sin 0 & (-\sin 0)(0) \\ (\sin 0)(\sin 0) & (\cos 0)(\sin 0) & \cos 0 & (\cos 0)(0) \\ 0 & 0 & 0 & 1 \end{bmatrix} \quad (4.48)$$

$${}^0T = \begin{bmatrix} 1 & 0 & 0 & 0 \\ 0 & 1 & 0 & 0 \\ 0 & 0 & 1 & 0 \\ 0 & 0 & 0 & 1 \end{bmatrix} \quad (4.49)$$

Subsequently, the translation by AB, followed by a rotation around the Z_1 axis, can be denoted by,

$${}^0_1T = \begin{bmatrix} \cos \theta_1 & -\sin \theta_1 & 0 & AB \\ (\sin \theta_1)(\cos 0) & (\cos \theta_1)(\cos 0) & -\sin 0 & (-\sin 0)(0) \\ (\sin \theta_1)(\sin 0) & (\cos \theta_1)(\sin 0) & \cos 0 & (\cos 0)(0) \\ 0 & 0 & 0 & 1 \end{bmatrix} \quad (4.50)$$

$${}^0_1T = \begin{bmatrix} \cos \theta_1 & -\sin \theta_1 & 0 & AB \\ \sin \theta_1 & \cos \theta_1 & 0 & 0 \\ 0 & 0 & 1 & 0 \\ 0 & 0 & 0 & 1 \end{bmatrix} \quad (4.51)$$

Successively, the translation by BH, followed by a rotation around the Z_2 axis, can be denoted by,

$${}^1_2T = \begin{bmatrix} \cos \theta_2 & -\sin \theta_2 & 0 & BH \\ (\sin \theta_2)(\cos 0) & (\cos \theta_2)(\cos 0) & -\sin 0 & (-\sin 0)(0) \\ (\sin \theta_2)(\sin 0) & (\cos \theta_2)(\sin 0) & \cos 0 & (\cos 0)(0) \\ 0 & 0 & 0 & 1 \end{bmatrix} \quad (4.52)$$

$${}^1_2T = \begin{bmatrix} \cos \theta_2 & -\sin \theta_2 & 0 & BH \\ \sin \theta_2 & \cos \theta_2 & 0 & 0 \\ 0 & 0 & 1 & 0 \\ 0 & 0 & 0 & 1 \end{bmatrix} \quad (4.53)$$

According to the Denavit-Hartenberg convention,

$$T = ({}^0T)({}^1T)({}^2T) \quad (4.54)$$

By substituting from the equation (4.49), (4.51) and (53), the equation (4.54) can be written as,

$${}^0_2T = \begin{bmatrix} 1 & 0 & 0 & 0 \\ 0 & 1 & 0 & 0 \\ 0 & 0 & 1 & 0 \\ 0 & 0 & 0 & 1 \end{bmatrix} \begin{bmatrix} \cos \theta_1 & -\sin \theta_1 & 0 & AB \\ \sin \theta_1 & \cos \theta_1 & 0 & 0 \\ 0 & 0 & 1 & 0 \\ 0 & 0 & 0 & 1 \end{bmatrix} \begin{bmatrix} \cos \theta_2 & -\sin \theta_2 & 0 & BH \\ \sin \theta_2 & \cos \theta_2 & 0 & 0 \\ 0 & 0 & 1 & 0 \\ 0 & 0 & 0 & 1 \end{bmatrix} \quad (4.55)$$

Subsequently, the equation (4.55) can be simplified as below,

$${}^0_2T = \begin{bmatrix} \cos(\theta_1 + \theta_2) & -\sin(\theta_1 + \theta_2) & 0 & BH \cos \theta_1 + AB \\ \sin(\theta_1 + \theta_2) & \cos(\theta_1 + \theta_2) & 0 & BH \sin \theta_1 \\ 0 & 0 & 1 & 0 \\ 0 & 0 & 0 & 1 \end{bmatrix} \quad (4.56)$$

The position of the point D with respect to the origin can be defined as,

$$D^{x_0, y_0, z_0} = {}^0_1T \begin{bmatrix} D^{x_1} \\ D^{y_1} \\ D^{z_1} \\ 1 \end{bmatrix} \quad (4.57)$$

Where;

$$\begin{bmatrix} D^{x_1} \\ D^{y_1} \\ D^{z_1} \\ 1 \end{bmatrix} = \begin{bmatrix} 0 \\ BD \\ 0 \\ 1 \end{bmatrix} \quad (4.58)$$

Substituting from equation (4.51) and (4.58), the equation (4.57) can be written as,

$$D^{x_0, y_0, z_0} = \begin{bmatrix} \cos \theta_1 & -\sin \theta_1 & 0 & AB \\ \sin \theta_1 & \cos \theta_1 & 0 & 0 \\ 0 & 0 & 1 & 0 \\ 0 & 0 & 0 & 1 \end{bmatrix} \begin{bmatrix} 0 \\ BD \\ 0 \\ 1 \end{bmatrix} \quad (4.59)$$

Furthermore, the equation (4.58) can be simplified as below to describe the position of point D with respect to the origin.

$$D^{x_0, y_0, z_0} = \begin{bmatrix} -BD \sin \theta_1 + AB \\ BD \cos \theta_1 \\ 0 \\ 1 \end{bmatrix} \quad (4.60)$$

Likewise, the position of the point G with respect to the origin can be defined as,

$$G^{x_0, y_0, z_0} = {}^0_2T \begin{bmatrix} G^{x_2} \\ G^{y_2} \\ G^{z_2} \\ 1 \end{bmatrix} \quad (4.61)$$

Where;

$$\begin{bmatrix} G^{x_2} \\ G^{y_2} \\ G^{z_2} \\ 1 \end{bmatrix} = \begin{bmatrix} 0 \\ GH \\ 0 \\ 1 \end{bmatrix} \quad (4.62)$$

Substituting from equation (4.56) and (4.62), the equation (4.61) can be written as,

$$G^{x_0, y_0, z_0} = \begin{bmatrix} \cos(\theta_1 + \theta_2) & -\sin(\theta_1 + \theta_2) & 0 & BH \cos \theta_1 + AB \\ \sin(\theta_1 + \theta_2) & \cos(\theta_1 + \theta_2) & 0 & BH \sin \theta_1 \\ 0 & 0 & 1 & 0 \\ 0 & 0 & 0 & 1 \end{bmatrix} \begin{bmatrix} 0 \\ GH \\ 0 \\ 1 \end{bmatrix} \quad (4.63)$$

Subsequently the equation (4.63) can be simplified as below to describe the position of point G with respect to the origin.

$$G^{x_0, y_0, z_0} = \begin{bmatrix} -GH \sin(\theta_1 + \theta_2) + BH \cos \theta_1 + AB \\ GH \cos(\theta_1 + \theta_2) + BH \sin \theta_1 \\ 0 \\ 1 \end{bmatrix} \quad (4.64)$$

Successively, the position of the point K with respect to the origin can be defined as,

$$K^{x_0, y_0, z_0} = {}^0_2T \begin{bmatrix} K^{x_2} \\ K^{y_2} \\ K^{z_2} \\ 1 \end{bmatrix} \quad (4.65)$$

Where;

$$\begin{bmatrix} K^{x_2} \\ K^{y_2} \\ K^{z_2} \\ 1 \end{bmatrix} = \begin{bmatrix} HJ \\ JK \\ 0 \\ 1 \end{bmatrix} \quad (4.76)$$

Substituting from equation (4.56) and (4.66), the equation (4.65) can be written as,

$$K^{x_0 y_0 z_0} = \begin{bmatrix} \cos(\theta_1 + \theta_2) & -\sin(\theta_1 + \theta_2) & 0 & BH \cos \theta_1 + AB \\ \sin(\theta_1 + \theta_2) & \cos(\theta_1 + \theta_2) & 0 & BH \sin \theta_1 \\ 0 & 0 & 1 & 0 \\ 0 & 0 & 0 & 1 \end{bmatrix} \begin{bmatrix} HJ \\ JK \\ 0 \\ 1 \end{bmatrix} \quad (4.68)$$

the equation (4.68) can be simplified as below to describe the position of point K with respect to the origin.

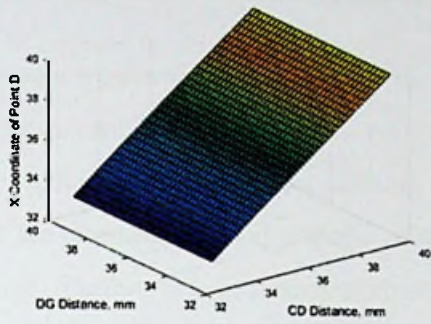
$$K^{x_0 y_0 z_0} = \begin{bmatrix} HJ \cos(\theta_1 + \theta_2) - JK \sin(\theta_1 + \theta_2) + BH \cos \theta_1 + AB \\ HJ \sin(\theta_1 + \theta_2) + JK \cos(\theta_1 + \theta_2) + BH \sin \theta_1 \\ 0 \\ 1 \end{bmatrix} \quad (4.69)$$

4.5 Finger Positions

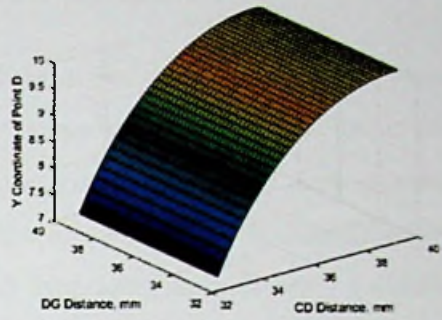
The prototype of the linkage finger mechanism has been designed with the link parameters demonstrated in Table 4.2. By considering the link parameter values and referring to the kinematic analysis, a Matlab program has been developed to plot the positions of the point D, G and K, with respect to the different CD and DG distances. By substituting for θ_1 and θ_2 from equation (4.16) and (4.39), equation (4.60), (4.64) and (4.69) the X and Y coordinates of point K, Point G and Point D has been plotted as illustrated in Figure 4.6, Figure 4.7 and Figure 4.8 respectively. Furthermore, by substituting link lengths values for the equation (4.16) and (4.39), it has been identified that, during the maximum flexion of the finger, both PIP and DIP joint angles are equal to 134.5° where CD and DG distances are at its minimum of 33mm. Contrariwise, once the CD and DG equals to 40mm the finger achieve its maximum extension where PIP and DIP joint angles are equal to 180° .

Table 4.2: Link parameter values for the prototype finger

	Constants				Variables	
Link	AC, AE, BD, BF, GH, HI	AB, BH	HJ	LJ, JK	CD, DG	EF, FI
Length (mm)	10	40	30	9	33 - 40	40 - 47



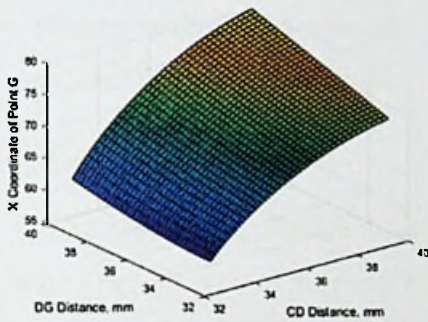
(a)



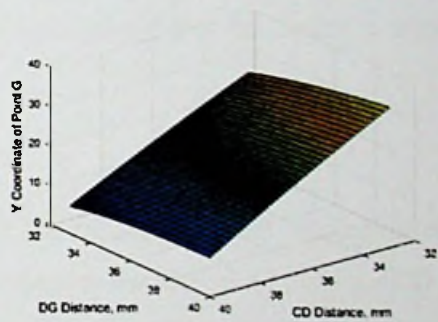
(b)

Figure 4.6: Position of point D with respect to CD and DG distance

(a) X Coordinate (b) Y Coordinate



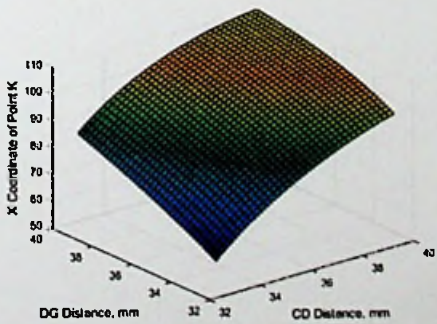
(a)



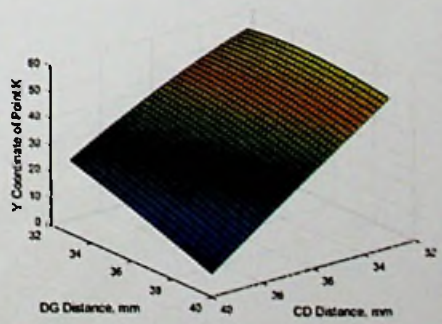
(b)

Figure 4.7: Position of point G with respect to CD and DG distance

(a) X Coordinate (b) Y Coordinate



(a)



(b)

Figure 4.8: Position of point K with respect to CD and DG distance

(a) X Coordinate (b) Y Coordinate

CHAPTER 05: SIMULATION AND RESULTS

The arm prosthesis is modeled in the Solidworks Software Package. The proposed finger mechanism is evaluated to verify that it is free of mechanical constraints that are due to joints collision or links collision. The inbuilt motion study in Solidworks showed that the expected motion patterns of the finger mechanism are accomplished by the design. Further the equations derived in the kinematic analysis were validated by comparing them with the result of motion study. Moreover, the working envelop of the finger is determined. The sequence of the finger motion is recorded during the experimental investigations. DIP and PIP joint angles were measured with respect to different CD and DG distances and compared with the motion study results. Further the finite element analysis in Solidworks Simulations proved that the finger is sturdy to withstand the standard finger forces.

5.1 Motion Simulation

Solidworks motion simulations were carried out to determine the trajectory of the fingertip. The trajectory of the point K with respect to the change of distance CD from 40mm to 32.86mm, DG from 40mm to 32.86mm, both CD and DG from 40mm to 32.86mm are shown in Figure 5.1, Figure 5.2 and Figure 5.3 respectively. The origin is placed at the metacarpophalangeal (MCP) joint and shown in the figures. The all there trajectories were plotted in x-y coordinate system as shown in Figure 5.4.

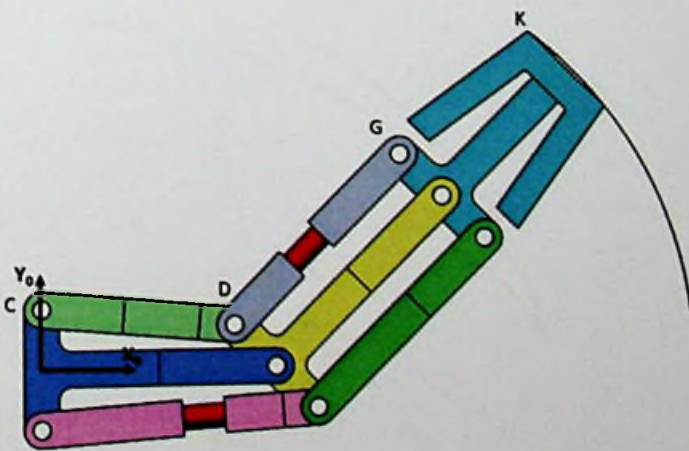


Figure 5.1: Trajectory of point K with respect to change of distance CD from 40mm to 32.86mm

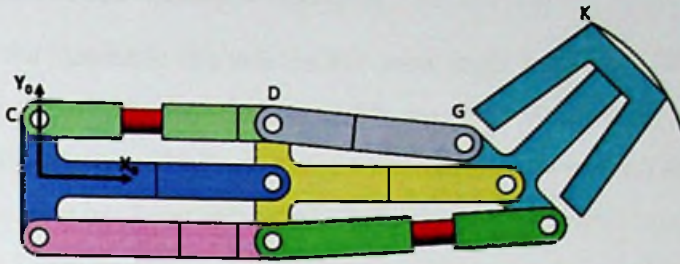


Figure 5.2: Trajectory of point K with respect to change of distance DG from 40mm to 32.86mm

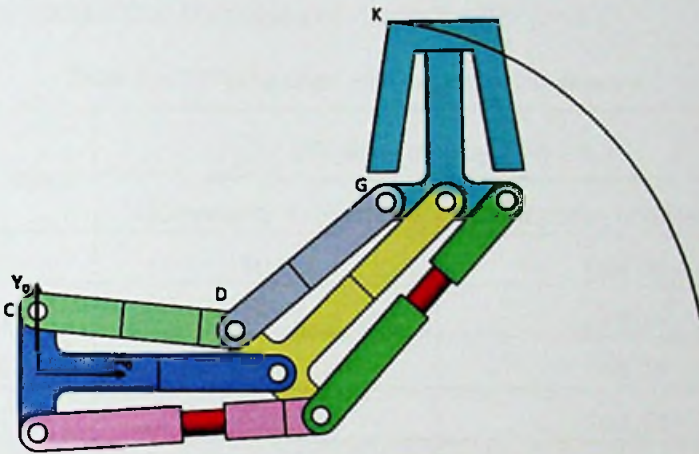


Figure 5.3: Trajectory of point K with respect to change of distance both CD and DG from 40mm to 32.86mm

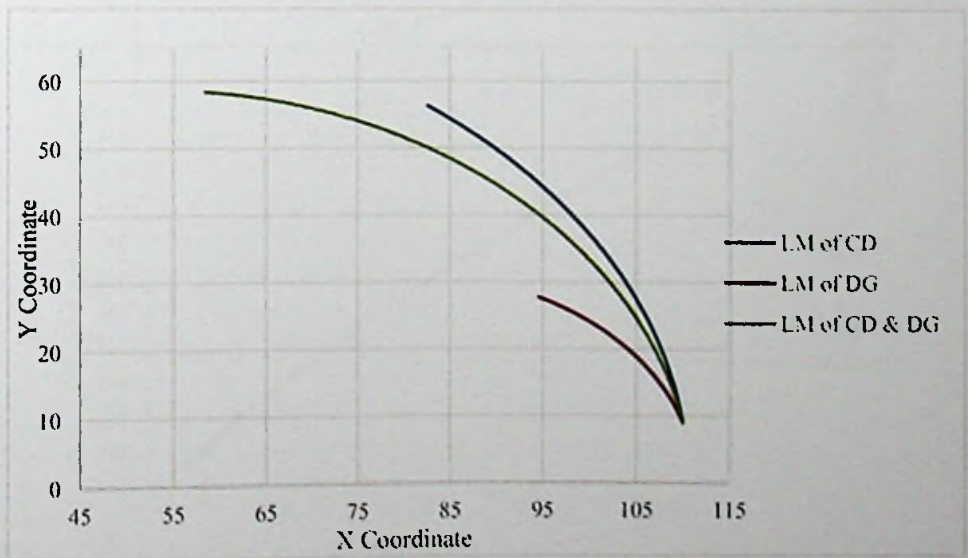


Figure 5.4: Trajectories of the point K with respect to the liner motion (LM) of CD and DG links

5.2 Validation of the Kinematic Analysis

According to the kinematic analysis the PIP joint angle equals to $(180 - \theta_1)$ and DIP joint angle equals to $(180 - \theta_2)$ where θ_1 and θ_2 are given by equation (4.16) and (4.39) respectively. Based on the link parameter values presented in the Table 4.2 different PIP and DIP angles has been calculated. Accordingly, by substituting values for CD and DG from 33mm to 40mm with 1mm steps PIP Joint Angle $(180 - \theta_1)$ and DIP Joint Angle $(180 - \theta_2)$ were determined. Same conditions were applied and generated the PIP and DIP joint angled with the aid of SolidWorks motion study. Table 5.1 and Figure 5.5 demonstrate the comparison of results for PIP joint.

Table 5.1: PIP joint angle with respect to CD distance

CD Distance	PIP Joint Angle $(180 - \theta_1)$	
	Kinematic Analysis	Solidworks Motion Study
40	180.00	180.00
39	174.26	174.34
38	168.46	168.28
37	162.53	162.54
36	156.36	156.35
35	149.83	150.03
34	142.69	143.04
33	134.47	135.5

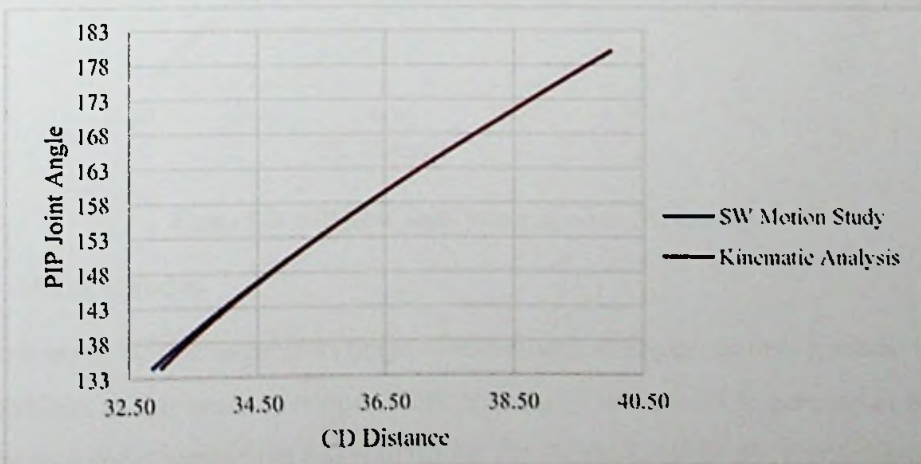


Figure 5.5: PIP joint angle with respect to CD distance

Similarly, Figure 5.5 and Figure 5.6 demonstrate the comparison of results for DIP joint. In view of that, the developed kinematic equations are validated via the motion study simulations.

Table 5.2: DIP joint angle with respect to DG distance

DG Distance	DIP Joint Angle ($180 - \theta_2$)	
	Kinematic Analysis	Solidworks Motion Study
40	180.00	180.00
39	174.26	174.34
38	168.46	168.28
37	162.53	162.54
36	156.36	156.35
35	149.83	150.03
34	142.69	143.04
33	134.47	135.5

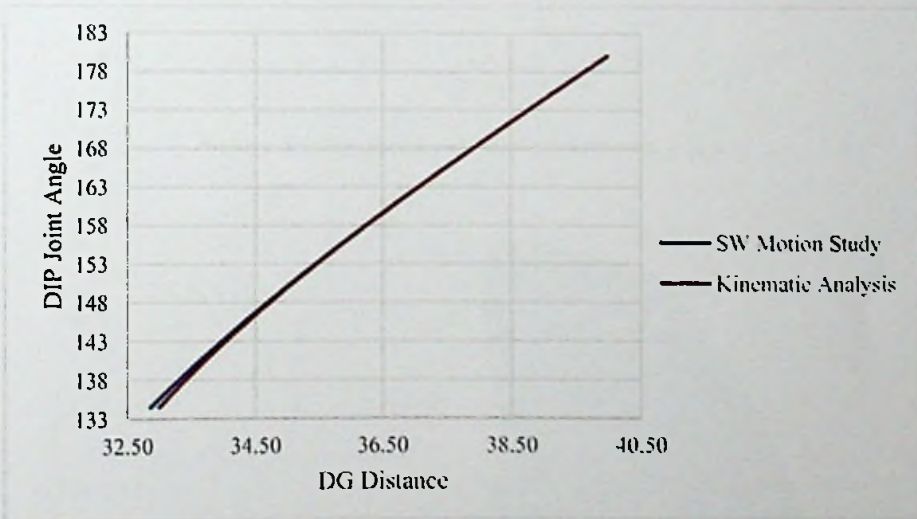


Figure 5.6: DIP joint angle with respect to DG distance

5.3 Work Envelop

A work envelope of a finger is its range of movement. A finger can only perform within the confines of this work envelope. Work envelop of the human fingers are in the 3D Workspace and it varies from finger to finger. For the designed finger, mechanism there is a specific work envelop. In order to determine the work envelop of the finger

mechanism primarily the trajectories of the points D, G and K during different motion patterns were plotted in the same graph. Afterward the boundaries of the trajectories and path of the links CD, DG and HK were considered to determine the enclosed area of finger movements which is illustrated in Figure 5.7. Based on that the work envelop of the finger mechanism is developed and presented in Figure 5.8.

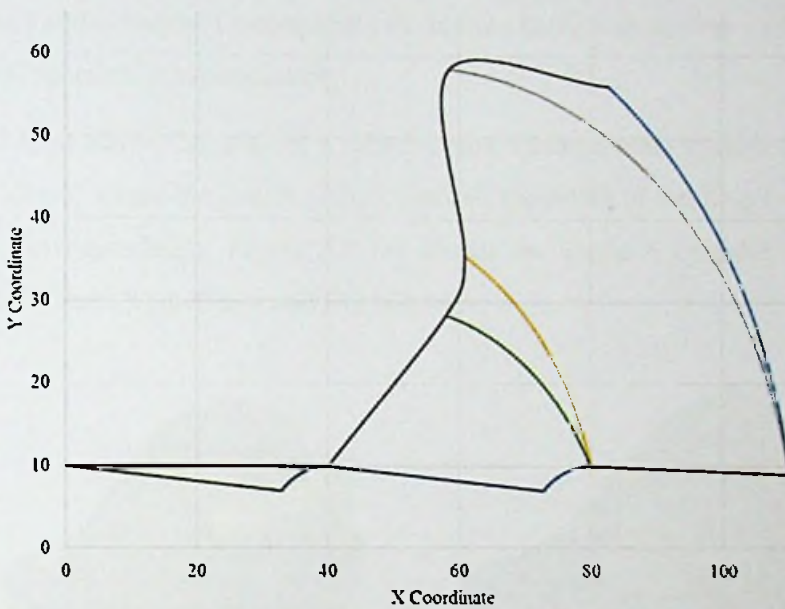


Figure 5.7: Trajectory of the fingertip and joints

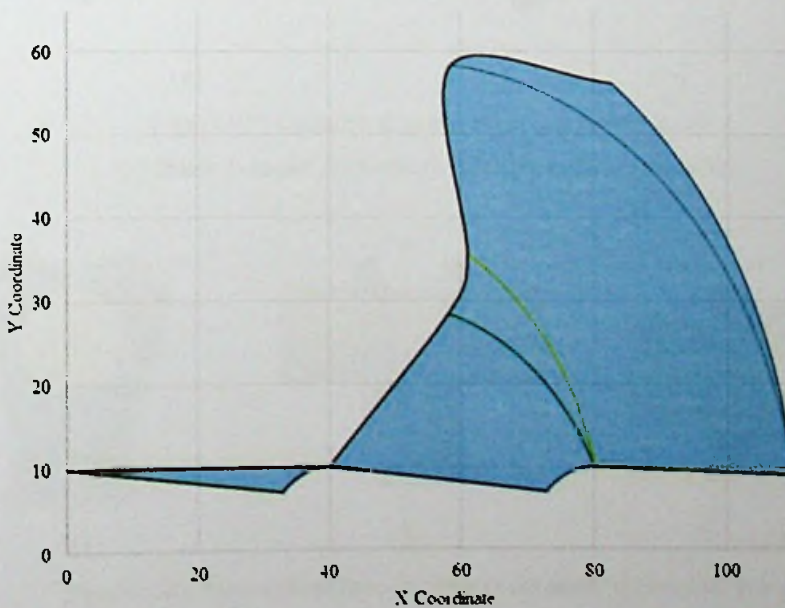


Figure 5.8: Work envelop of the finger

5.4 Grasps of the Prosthetic Hand

The Solidworks motion package was used to study the power grasp patterns of the proposed hand prosthesis. The power grasp is accomplished by the fingers and sometimes palm by clamping down on an object with the fingers making counter pressure. For all intents and purposes there are two basic power grasp types known as cylindrical and spherical. Consequently the motion study was carried out for cylindrical grasp and spherical grasp separately.

Figure 5.9 (a) shows the grasp of a cylinder with 75mm diameter using the maximum finger flexion, where the length of both links CD and DG of the finger mechanism is 33mm. Correspondingly Figure 5.9 (b) shows the grasp a cylinder with 100mm diameter, where CD is 33mm and DG is 40mm.

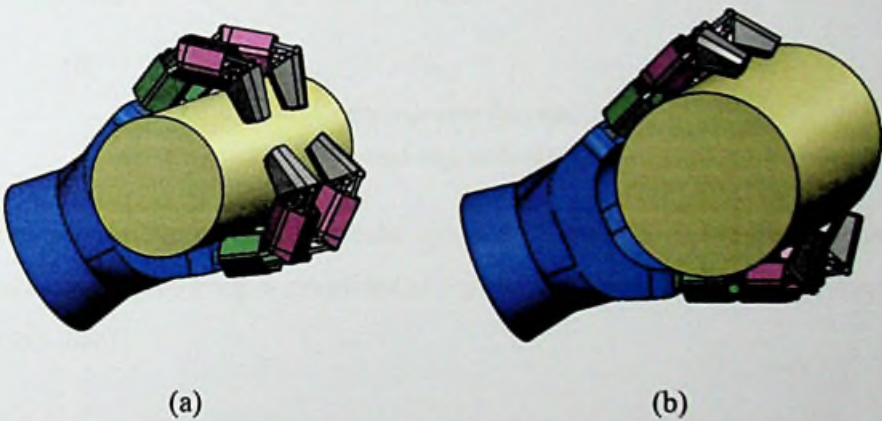


Figure 5.9: Cylindrical grasp of the prosthetic hand
(a) 75mm cylinder diameter (b) 100mm cylinder diameter

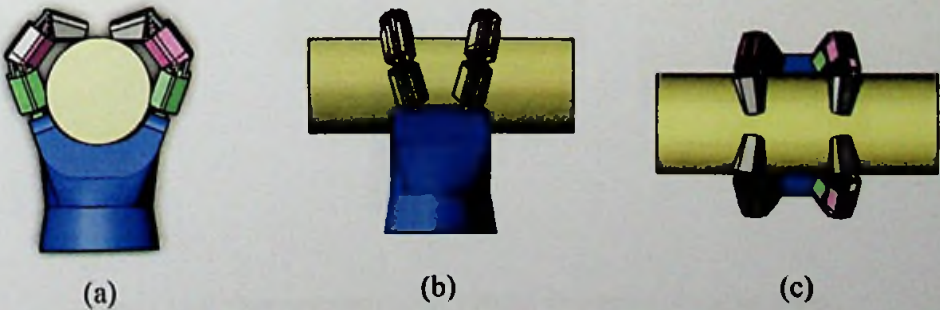


Figure 5.10: View orientations for 75mm diameter cylindrical grasp
(a) Side view (b) Top view (c) Front view

The view orientations for small cylinder grasp is illustrated in Figure 5.10 and the sequence of respective grasp is presented in Figure 5.11 and Video 03 in the Appendix V (compact disc).

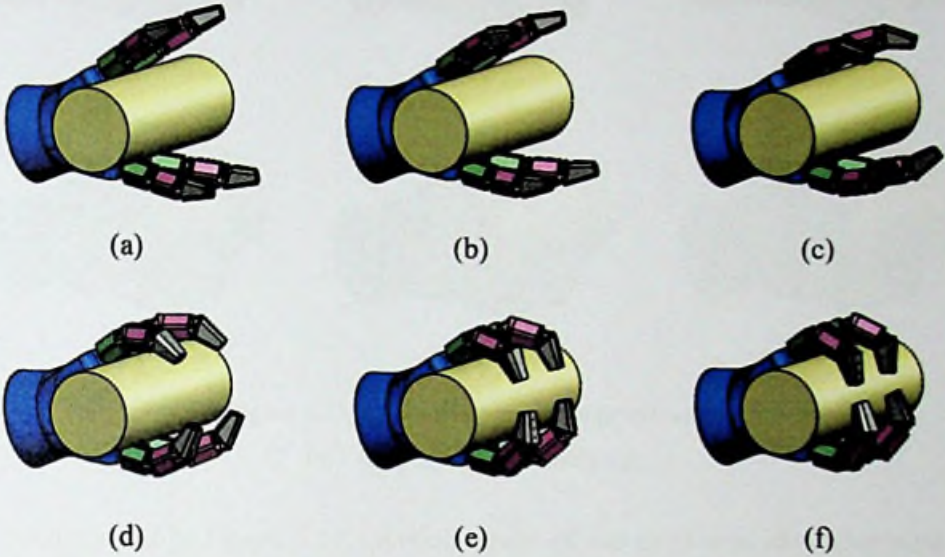


Figure 5.11: Grasp sequence for small cylinder
(a) - (f) Initial step to final step

The view orientations for large cylinder grasp is illustrated in Figure 5.12 and the sequence of respective grasp is presented in Figure 5.13 and Video 04 of the Appendix V (compact disc).

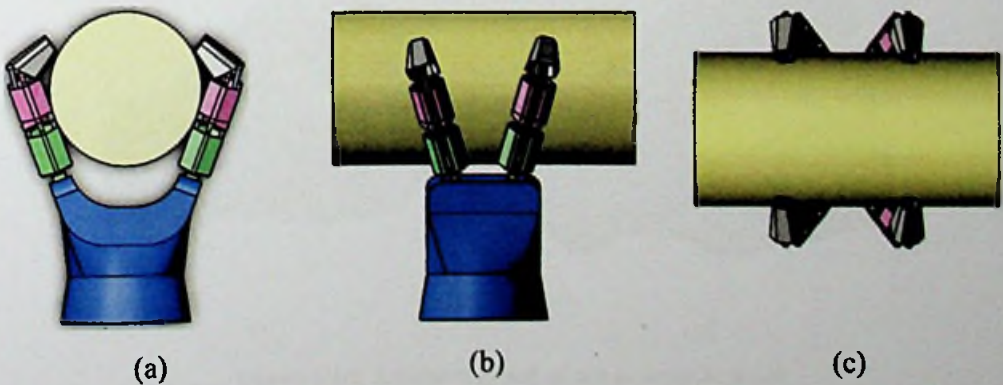


Figure 5.12: View orientations for 100mm diameter cylindrical grasp
(a) Side view (b) Top view (c) Front view

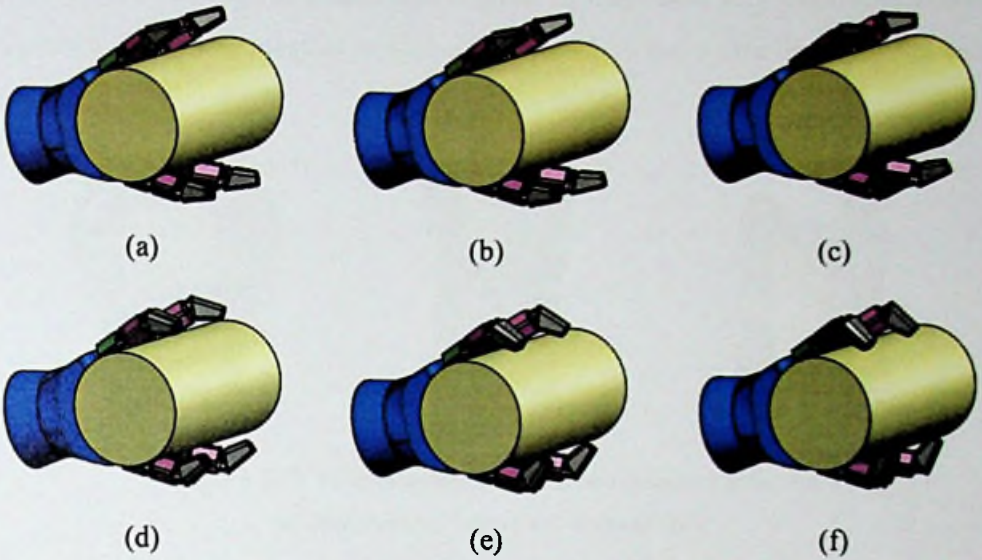


Figure 5.13: Grasp sequence of large cylinder
(a) - (f) Initial step to final step

As demonstrated in Figure 5.14 spherical grasp of the hand was identified with the minimum sphere diameter of 85mm and maximum of 110mm. 85mm sphere was grasped with maximum flexion once the CD and DG distances of the finger mechanism was 33mm. 110mm diameter sphere was perfectly grasped once the CD and DG links are shorten to 36mm and 39mm respectively.



Figure 5.14: Spherical grasp of the prosthetic hand
(a) 85mm sphere diameter (b) 110mm sphere diameter

The view orientations for small sphere grasp is illustrated in Figure 5.15 and the sequence of respective grasp is presented in Figure 5.16 and Video 05 of the Appendix V (compact disc).

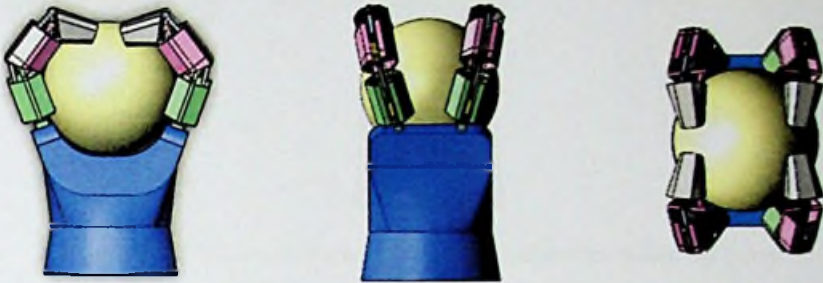


Figure 5.15: View orientations for 85mm diameter spherical grasp

(a) Side view (b) Top view (c) Front view

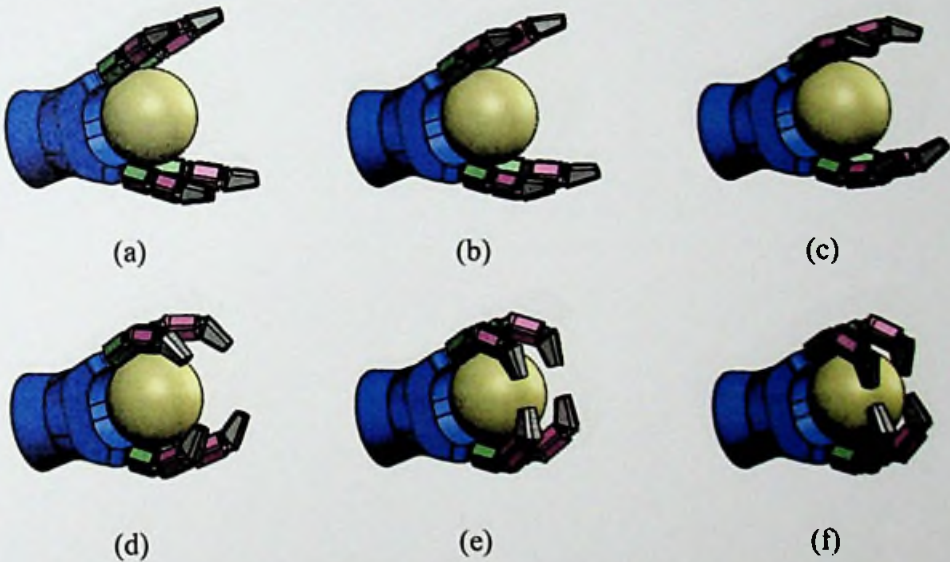


Figure 5.16: Grasp sequence of small sphere

(a) - (f) Initial step to final step

The view orientations for large sphere grasp is illustrated in Figure 5.17 and the sequence of respective grasp is presented in Figure 5.18 and Video 06 of the Appendix V (compact disc).



Figure 5.17: View orientations for 110mm diameter spherical grasp

(a) Side view (b) Top view (c) Front view

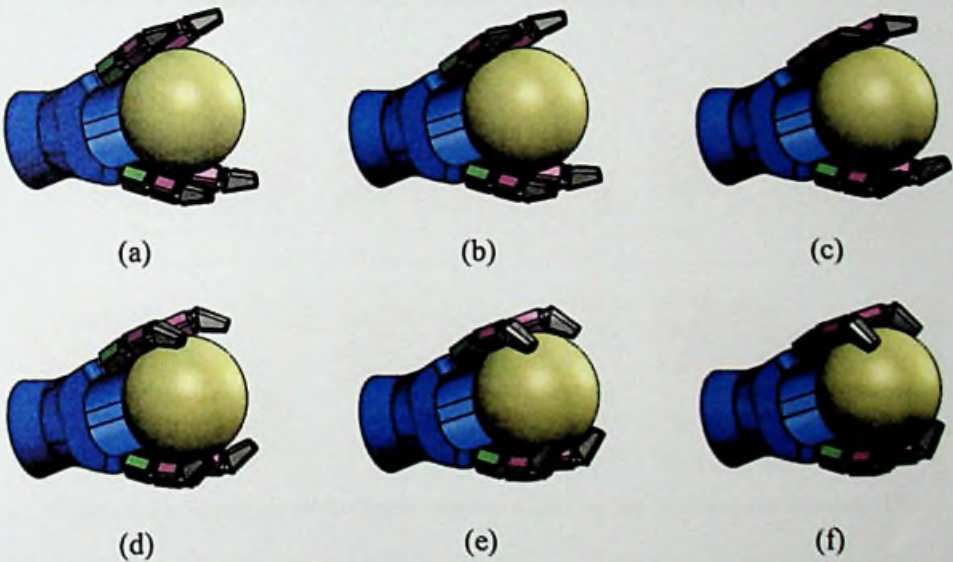


Figure 5.18: Grasp sequence of large sphere

(a) - (f) Initial step to final step

5.5 Experimental Results

The designed finger mechanism was experimentally investigated to ensure the expected functionality and finger motions. The sequences of the finger motions were recorded during the experimental investigations. Figure 5.19 and Figure 5.20 demonstrate the sequence of the finger motions with respect to change of distance DG and CD

respectively. Figure 5.21 demonstrate sequence of the finger motions with respect to change of distances both CD and DG simultaneously.

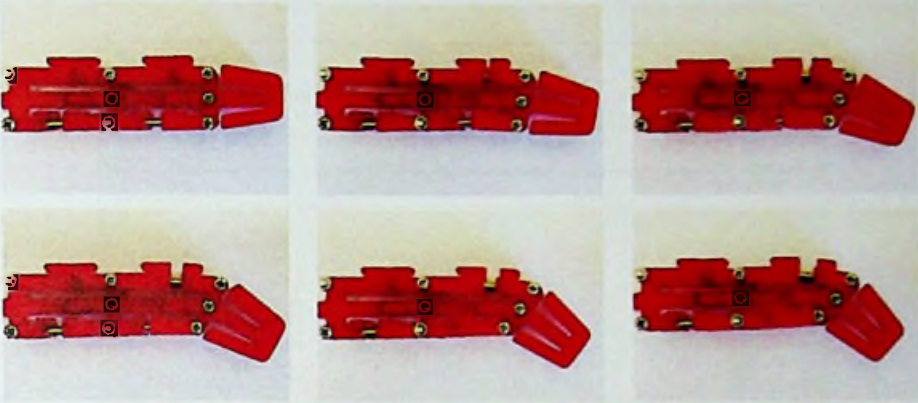


Figure 5.19: Sequence of the finger motion with respect to change of distance DG

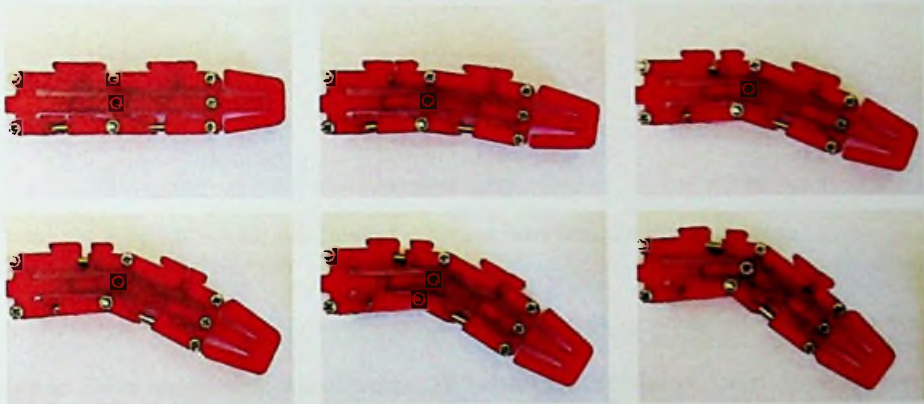


Figure 5.20: Sequence of the finger motion with respect to change of distance CD

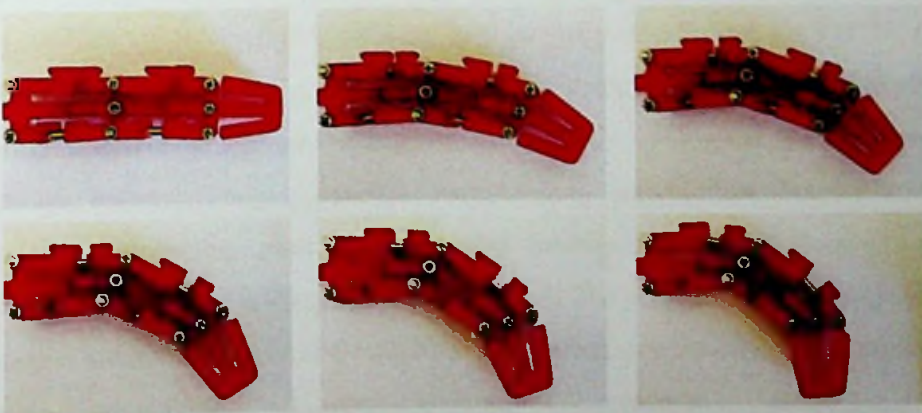


Figure 5.21: Sequence of the finger motion with respect to change of distance both CD and DG

In addition DIP and PIP joint angles were measured with respect to different CD and DG distances with the aid of Fiji ImageJ software package.

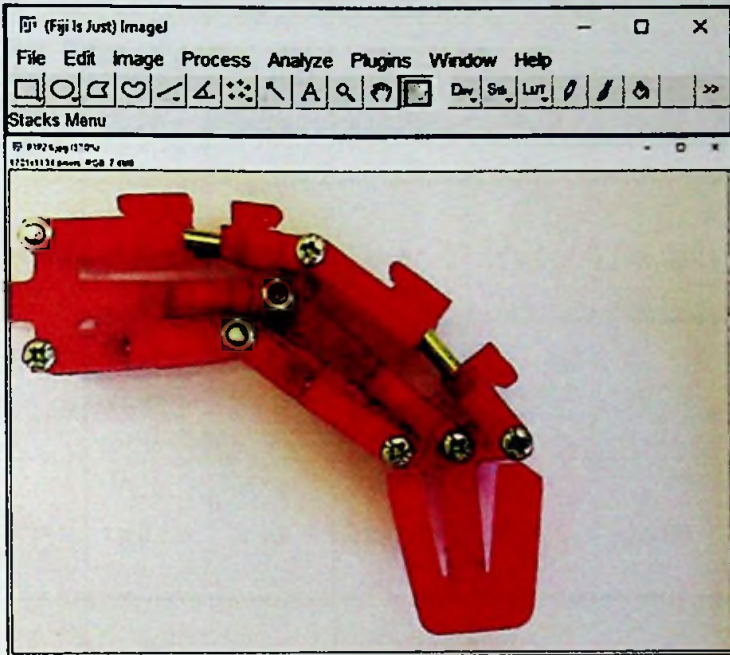








Figure 5.22: Fiji ImageJ software interface during measuring

Fiji is an open source image processing package based on ImageJ. The software is capable to solve many image processing and analysis problems, from three-dimensional live-cell imaging to radiological image processing, multiple imaging system data comparisons to automated hematology systems. ImageJ can calculate area and pixel value statistics of user-defined selections and intensity-thresholded objects. Further it measures distances and angles and creates density histograms and line profile plots. It supports standard image processing functions such as logical and arithmetical operations between images, contrast manipulation, convolution, Fourier analysis, sharpening, smoothing, edge detection, and median filtering. It does geometric transformations such as scaling, rotation, and flips. The program supports any number of images simultaneously, limited only by available memory. Experimental results were compared with the Solidworks motion simulations as presented in Table 5.3.




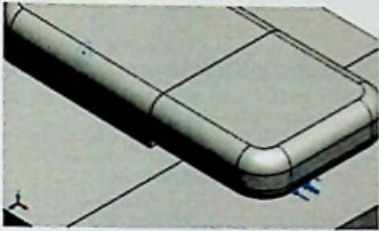
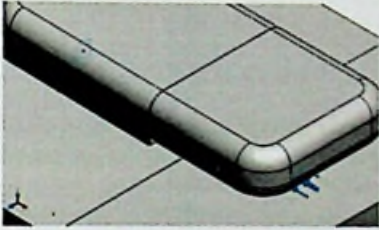


Table 5.3: Comparison for experimental and simulation results for distance and angle measurements

Experimental Segment	CD Distance (mm)	DG Distance (mm)	PIP Joint Angle ($180^\circ - \theta_1$)		DIP Joint Angle ($180^\circ - \theta_2$)	
			Experimental	Simulation	Experimental	Simulation
	38.98	39.96	172.96	174.12	179.28	179.78
	36.57	39.93	158.26	159.90	178.83	179.60
	39.99	36.55	177.98	179.93	159.23	159.78
	39.87	34.68	178.39	179.25	146.95	147.65
	35.95	36.98	154.35	156.07	160.54	162.43
	33.98	33.99	141.53	142.51	140.86	142.64

5.6 FEA Simulation

Designed prosthesis finger mechanism is expected to carry 20N payload at distal phalanx. Mechanical structure of the prosthesis is design to bear the maximum payload and the weight of the links and actuators of the mechanical design. In addition to the play load it is assumed that 5N is applied by the elastics rubber loops as a spring effect. Further the tension of nylon strings is taken as 10N where it applies a pull on the PPB2 and IPB2. SolidWorks motion study indicated that with those loads the finger mechanism performs as expected. Table 5.4 outline the details of the loads and fixtures considered for FEA simulation.

Table 5.4: Load and fixtures for FEA simulation

Load / Fixtures	Load / Fixture Image	Load / Fixture Details
Play load at distal phalanx		Entities: 1 face(s) Type: Apply normal force Value: 20 N
Spring effect between PPT1 and PPT2		Entities: 2 face(s) Type: Apply normal force Value: 5 N
Spring effect between IPT1 and IPT2		Entities: 2 face(s) Type: Apply normal force Value: 5 N
Pull load apply by nylon strings on PPB2 and IPB2		Entities: 2 face(s) Type: Apply normal force Value: 10 N
Connection to palm		Entities: 4 face(s) Type: Fixed Geometry

PLA Plastic is used as material for 3D printed parts and copper is for linear guides. The material properties considers for simulation are defined in Table 5.5.

Table 5.5: Material properties for FEA simulation

Components	Material Name	Material Properties
PPT1, PPT2, PPM1, PPM2, PPB1, PPB2, IPT1, IPT2, IPM1, IPM2, IPB1, IPB2, DP1, DP2	PLA	Model type: Linear Elastic Isotropic Model type: Linear Elastic Isotropic Default failure criterion: Max von Mises Stress Yield strength: $7e+007 \text{ N/m}^2$ Tensile strength: $7.3e+007 \text{ N/m}^2$ Elastic modulus: $3.5e+009 \text{ N/m}^2$ Poisson's ratio: 0.36 Mass density: 1252 kg/m^3 Shear modulus: $3.189e+008 \text{ N/m}^2$
LGs	Copper	Model type: Linear Elastic Isotropic Yield strength: $2.58646e+008 \text{ N/m}^2$ Tensile strength: $3.9438e+008 \text{ N/m}^2$ Elastic modulus: $1.1e+011 \text{ N/m}^2$ Poisson's ratio: 0.37 Mass density: 8900 kg/m^3 Shear modulus: $4e+010 \text{ N/m}^2$ Thermal expansion coefficient: $2.4e-005$ /Kelvin

Von misses stress, resultant displacement and equivalent strain is of the finger is tested using the FEA package in Solidworks Simulations. According to the results, the designed finger has a maximum von Mises Stress of $3.35889e+007 \text{ N/m}^2$, maximum resultant displacement of 1.5538 mm and maximum equivalent strain of 0.00811427. The minimum factor of safety is determined as 2.08402. Accordingly, the results proves the finger mechanism will not fail during operation. The mesh information and simulation results are presented in Table 5.6.

Table 5.6: Mesh information and FEA results

Mesh type	Solid Mesh
Jacobian points	4 Points
Element Size	2.5 mm
Total Nodes	53545
Total Elements	31673
Minimum von Mises Stress	33.8091 N/m ² Node: 10290
Maximum von Mises Stress	3.35889e+007 N/m ² Node: 12608
Minimum Resultant Displacement	0 mm Node: 9176
Maximum Resultant Displacement	1.5538 mm Node: 44465
Minimum Equivalent Strain	3.64539e-008 Element: 6328
Maximum Equivalent Strain	0.00811427 Element: 6309
Minimum Factor of Safety	2.08402 Node: 12608
Maximum Factor of Safety	2.07045e+006 Node: 10290

Model name: Finger
 Study name: (Static 1) Default 1
 Plot type: Static model stress (stress)
 Deformation scale: 6.31433

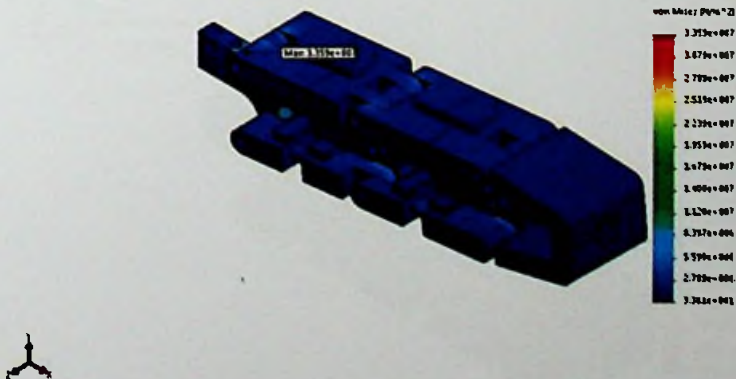


Figure 5.23: Von mises stress of finger

Model name: Finger
 Study name: Static 11 (Default)
 Plot type: Static displacement Displacement2
 Deformation scale: 8.57433

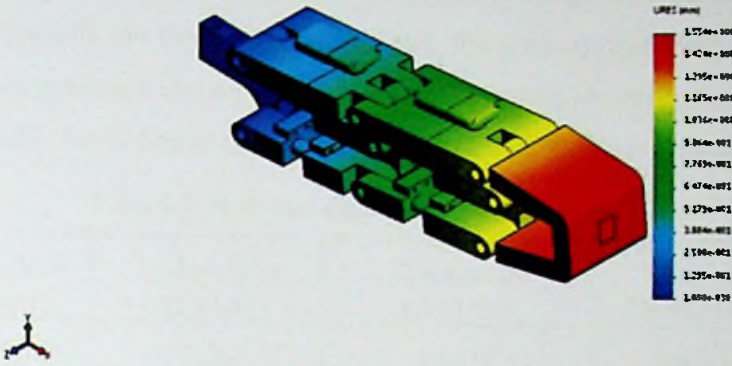


Figure 5.24: Resultant displacement of finger

Model name: Finger
 Study name: Static 11 (Default)
 Plot type: Static Strain Strain1
 Deformation scale: 8.57433

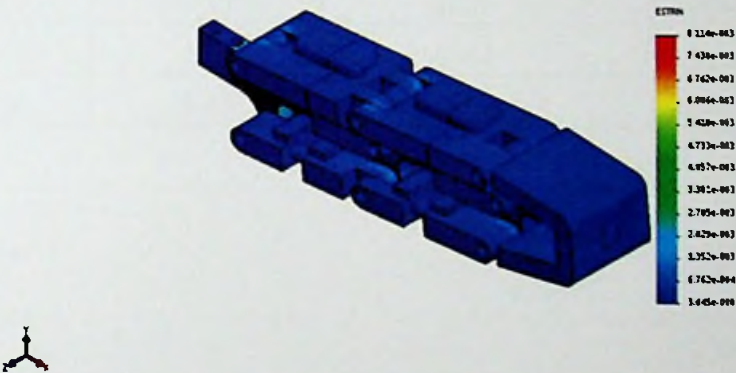


Figure 5.25: Equivalent strain of the finger

Model name: Finger
 Study name: Static 11 (Default)
 Plot type: Factor of Safety Factor of Safety1
 Criterion: Automatic
 Factor of safety distribution: Min FOS = 2.1

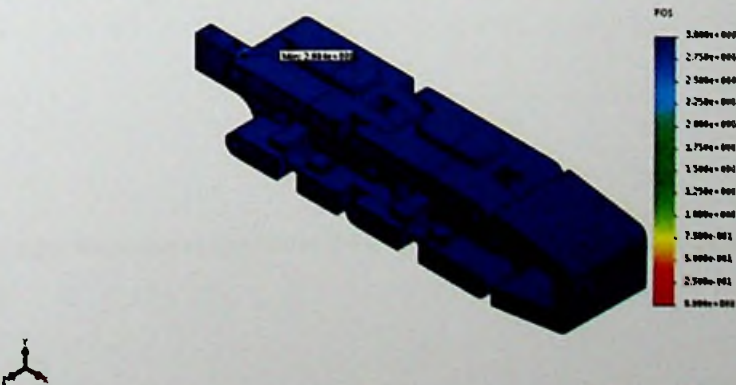


Figure 5.26: Factor of safety of the finger

Convergence is a universal concept in finite element analysis, when the model contains non-linearity. Consequently, iterations are essential to check whether the results are converging towards the finer mesh size. Thus, the convergence analysis has been carried out for randomly chosen mesh sizes and the results are presented in Table 5.7 and Figure 5.27. According to the polynomial curve, the results are converging.

Table 5.7: Mesh size, number of elements and stress

Mesh Size (mm)	1/Mesh Size (1/mm)	Total no of Elements	Maximum Stress (N/m ²)
5.00	0.20	16429	2.40E+07
4.70	0.21	17864	2.48E+07
4.00	0.25	18606	2.81E+07
3.50	0.29	20561	3.00E+07
3.00	0.33	24081	3.29E+07
2.60	0.38	30044	3.35E+07
2.50	0.40	31673	3.36E+07

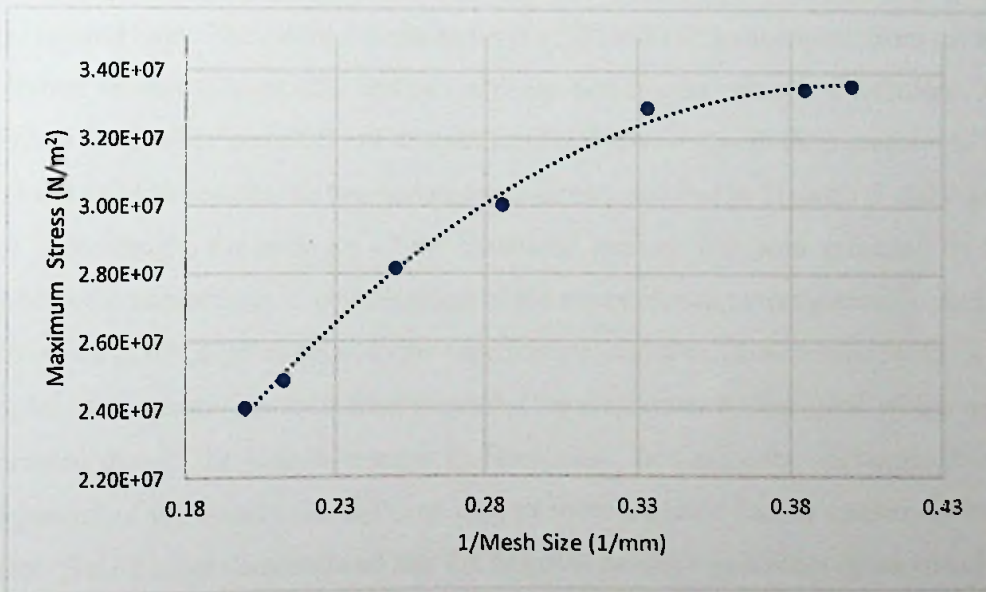


Figure 5.27: Variation of maximum stress with respect to the one over mesh size

CHAPTER 06: DISCUSSION

Although the Chebychev–Grübler–Kutzbach criterion has limitations to analysis parallel robots, the simplification of the kinematic representation has been effective to analysis the mobility of the proposed linkage mechanism. However, it will demonstrate the effective DoF for finger actuation, which will not give a clear understanding about the friction of the mechanism. According to the mobility analysis the proposed mechanism has two degrees of freedom. Consistent with the proposed self-adaptive mechanism, the finger can be actuated by a single linear actuator. Hence, the presented linkage finger mechanism is competent as an underactuated mechanism since the number of actuators required are less than the achievable degrees of freedom. The explicated two-step kinematic analysis, first generating the relationships between the link lengths and the joint angles, then D-H conversion towards the forward kinematics is an impeccable approach to analysis the systems, which are developed as a hybrid of series and parallel links. The presented two-step approach eliminates the limitations of D-H conversion method to analysis the robotics systems with both series and parallel links. The values calculated for the DIP and PIP joint angles, from the two different methods, kinematic analysis and the Solidworks motion simulations, are slightly different at lower CD or DG links lengths. However, with the increment of the CD and DG link lengths the two curves coincide as presented in Figure 5.5 and Figure 5.6. Accordingly, the accuracy of the kinematic analysis has been validated by the Solidworks simulations. In consideration of the experimental investigations, there is a difference of two degrees between the experimental and simulation results for the joint angles. One reason for such error might be the play between the links, which were occurred due to the high tolerances in fabrication. Secondly the variations in the alignment of the camera the different images were captured can be caused for such error. The FEA has demonstrated that the finger is having a minimum factor of safety of 2.084, while applying a 20N finger contact force. Thus, it can be assumed that all four fingers can apply 80N grip on an object without any failure, which will be good enough for a grown male. However, there is a possibility to fail the nylon strings during such a high workload. Hence, the nylon strings can be replaced with cables having a high tensile strength, for example carbon fibre.

CHAPTER 07: CONCLUSION

This thesis proposes a transradial prosthetic hand for upper limb amputees, which is designed by considering the anthropometric data of the Sri Lankan population. In order to accomplish power grasp a novel finger mechanism is developed and tested. The prosthesis terminal device is made of four identical fingers where the Chebychev–Grübler–Kutzbach criterion for a planar mechanism has proved that the DoF of the linkage finger mechanism is two. Accordingly, the terminal device generates eight DoF in all with the flexion and extension of each finger.

Kinematic analysis based on the Denavit-Hartenberg (DH) parameter approach has demonstrated the relationship between the length of the CD link and the PIP joint angle, in the same way the relationship between the length of the DG link and the DIP joint angle. The maximum flexion where, both PIP and DIP joint angle equals to 134.5° is obtained once the CD and DG length are moved to its minimum of 33mm. Furthermore, the motion simulations have verified that the equations derived in the kinematic analysis are accurate.

The proposed finger mechanism is evaluated and it proved the mechanism is free of mechanical constraints due to joints collision or links collision. The motion study simulation in Solidworks demonstrated that the expected motion patterns of the finger mechanism are accomplished by the design. Accordingly, the hand is capable of grasping a cylinder having a diameter from 75mm to 100mm. Further it is demonstrated that the ability to grasp a sphere having a diameter from 85mm to 110mm. The finite element analysis in Solidworks Simulations has demonstrated that the finger is sturdy to withstand the standard finger forces. In addition, the experimental testing has verified the functionality of the novel linkage mechanism, which is designed in order to perform power grasping.

Fingertip trajectories and the work envelope are two key outcomes of the motion study. Those findings will be beneficial for future research towards developing control algorithms for finger actuation. As the next step of the research, a mechanism should be improved to reduce the friction between joints.

PUBLICATIONS

1. H. M. C. M. Herath, R. A. R. C. Gopura, Thilina D. Lalitharatne, Prosthetic Hand with a Linkage Finger Mechanism for Power Grasping Applications, IEEE Life Sciences Conference, Sydney, Australia, 13-15 December 2017. [Submitted]
2. H. M. C. M. Herath, R. A. R. C. Gopura, Thilina D. Lalitharatne, An Underactuated Linkage Finger Mechanism and its Kinematic Analysis, Journal of Mechanisms and Robotics. [Submitted]

REFERENCES

- [1] E. Peña-Pitarch, N. T. Falguera, J. A. L. Martinez, A. A. Omar and I. A. Larrión, "Driving device for a hand movement without external force," *Mechanism and Machine Theory*, vol. 105, pp. 388-396, 2016.
- [2] D. S. V. Bandara, R. A. R. C. Gopura, K. T. M. U. Hemapala and K. Kiguchi, "A multi-DoF anthropomorphic transradial prosthetic arm," in *IEEE RAS/EMBS International Conference on Biomedical Robotics and Biomechatronics*, São Paulo, Brazil, 2014.
- [3] D. G. K. Madusanka, L. N. S. Wijayasingha, K. Sanjeevan, M. A. R. Ahamed, J. C. W. Edirisooriya and R. A. R. C. Gopura, "A 3DOF transtibial robotic prosthetic limb," in *7th International Conference on Information and Automation for Sustainability*, Colombo, Sri Lanka, 2014.
- [4] V. Ramos, "Introduction to Prosthetic Limbs," *The Kabod*, vol. 2, no. 1, pp. 1-11, 2015.
- [5] R. Niska, F. Bhuiya and J. Xu, "National Hospital Ambulatory Medical Care Survey: 2007 emergency department summary," National health statistics reports, 2010.
- [6] V. Ivan, F. Dario and C. A. Oskar, "New developments in prosthetic arm systems," *Orthopedic Research and Reviews*, vol. Rev 8, pp. 31-39, 2016.
- [7] B. Grunert, C. Smith, C. Devine and B. Fehring, "Early psychological aspects of severe hand injury," *Journal of Hand Surgery: British & European Volume*, vol. 13, no. B(2), pp. 177-180, 1988.
- [8] M. Grob, N. Papadopulos, A. Zimmermann, E. Biemer and L. Kovacs, "The psychological impact of severe hand injury," *Journal of Hand Surgery (European Volume)*, vol. 33, no. 3, pp. 358-362, 2008.
- [9] V. Putti, "Historical Prostheses," *Journal of Hand Surgery (British and European Volume)*, vol. 30, no. 3, pp. 310-325, 2005.

- [10] D. Merrill, J. Lockhart, P. Troyk, R. Weir and D. Hankin, "Development of an implantable myoelectric sensor for advanced prosthesis control," *Artif Organs*, vol. 35, no. 3, pp. 249-252, 2011.
- [11] P. P. H. Perera, "History of Prosthetics and Orthotics in Sri Lanka," Sri Lanka Association for Prosthetics and Orthotics, Colombo, 2017, [Online]. Available: <http://www.slapo.lk>. [Accessed: 20-09-2016].
- [12] K. M. Norton, "A Brief History of Prosthetics," Amputee Coalition, Manassas, 2017.
- [13] N. Wiener, *Cybernetics or Control and Communication in the Animal and the Machine*, vol. 25, MIT Press, 1965.
- [14] R. Atkins and D. Meier, "Functional Restoration of Adults and Children with Upper Extremity Amputation," *Res Trends for the Twenty-First Century*, vol. 30, no. 30, pp. 353-360, 2004.
- [15] Arms Within Reach Foundation, "Six Prosthetic Options," [Online]. Available: <http://www.armswithinreach.org>. [Accessed: 11-09-2016].
- [16] M. Demello, "Feet and footwear: A cultural Encyclopedia," ABC-CLIO, 2009.
- [17] M. M. Lusardi, M. Jorge and C. C. Nielsen, *Orthotics & prosthetics in rehabilitation*, Elsevier Health Sciences, 2013.
- [18] A. Freivalds, *Biomechanics of the Upper Limbs: mechanics, modeling and musculoskeletal injuries*, CRC Press LLC, 2004.
- [19] P. Gigis and K. Kuczynski, "The distal interphalangeal joints of the human," *Journal of Hand Surgery*, vol. 7, no. 2, pp. 76–182, 1982.
- [20] Levangie, K. Pamela and C. Norkin, *Joint structure and function: a comprehensive analysis*, FA Davis, 1992.
- [21] M. Batmanabane and S. Malathi, "Movements at the carpometacarpal and metacarpophalangeal joints of the hand and their effect on the dimensions of the articular ends of the metacarpal bones," *The Anatomical Record*, vol. 213, no. 1, pp. 102–110, 1985.

- [22] A. Steindler, *Kinesiology of the human body under normal and pathological conditions*, vol. 63, Springfield: CC Thomas, 1995.
- [23] Y. Youm, R. McMurty, A. Flatt and T. Gillespie, "Kinematics of the wrist. I. An experimental study of radial-ulnar deviation and flexion-extension," *Journal of Bone and Joint Surgery*, vol. 60, no. 4, pp. 424–431, 1978.
- [24] W. His, W. Spalteholz and L. F. Barker, *Hand Atlas of Human Anatomy*, Bibliolife DBA of Bilibio Bazaar, 2015.
- [25] D. Sanjaya, "Development of an Anthropomorphic Transhumeral Prosthetic Arm for Upper-Arm Amputees," M.Phil dissertation: University of Moratuwa, Katubedda 2014.
- [26] A. D. Astin, "Finger force capability: measurement and prediction using anthropometric and myoelectric measures," Ph.D. dissertation: Virginia Polytechnic Institute and State University, Blacksburg, Virginia, 1999.
- [27] C. Pylatiuk, S. Schulz and L. Döderlein, "Results of an Internet survey of myoelectric prosthetic hand users," *Prosthet Orthot Int*, vol. 31, no. 04, pp. 362-370, 2007.
- [28] K. Mirza and E. David, "General Formulation for Force Distribution in Power Grasp," in *IEEE International Conference on Robotics and Automation*, San Diego, 1994.
- [29] Nottingham University, "Ergonomics Data for use in the Design of Safer Products," DTI Publications, London, 2000.
- [30] D. G. Kamper, E. G. Cruz and M. P. Siegel, "Stereotypical fingertip trajectories during grasp," *Journal of neurophysiology*, vol. 90, no. 6, pp. 3702-3710, 2003.
- [31] Y. Kamata, T. Nakamura, S. Sueda, M. Tada, D. K. Pai, T. Nagura and Y. Toyama, "Motion analysis of fingertip trajectory under different levels of lumbrical muscle activation," *ORS Annual Meeting*, 2012.
- [32] C. Arunesh, C. Pankaj and D. Surinder, "Analysis of Hand Anthropometric Dimensions of Male Industrial Workers of Haryana State," *International Journal of Engineering (IJE)*, vol. 5, no. 3, pp. 242-256, 2011.

- [33] J. Damascene, A. Anthony and S. Houshang, "Body Size Data of Sri Lankan Workers and Their Comparison with Other Populations in the World: It's Impact on the Use of Imported Goods," *Journal of human ergology*, vol. 16, no. 2, pp. 193-208, 1987.
- [34] N. Jarrassé, M. Maestrutti, G. Morel and A. Roby-Brami, "Robotic Prosthetics : Moving Beyond Technical Performance," *IEEE Technology and Society Magazine*, vol. 34, no. 2, pp. 71 - 79, 2015.
- [35] I. Dudkiewicz, R. Gabrielov, I. Seiv-Ner, G. Zelig and M. Heim, "Evaluation of prosthetic usage in upper limb amputees," *Disability & Rehabilitation*, vol. 26, no. 1, pp. 60-63, 2004.
- [36] D. Atkins, D. Heard and W. Donovan, "Epidemiologic overview of individuals with upper-limb loss and their reported research priorities," *JPO: Journal of Prosthetics and Orthotics*, vol. 8, no. 1, pp. 2-11, 1996.
- [37] J. Belter, J. Segil, A. Dollar and R. Weir, "Mechanical design and performance specifications of anthropomorphic prosthetic hands: A review," *Journal of Rehabilitation Research & Development*, vol. 50, no. 5, pp. 599-618, 2013.
- [38] B. Maat, G. Smit, D. Plettenburg and P. Breedveld, "Passive prosthetic hands and tools: A literature review," *Prosthetics and Orthotics International*, pp. 1-9, 2017.
- [39] J. Pillet, "The aesthetic hand prosthesis," *The Orthopedic Clinics of North America*, vol. 12, no. 4, pp. 961-969, 1981.
- [40] T. A. Kuiken, G. Li, B. A. Lock, R. D. Lipschutz and M. L. A, "Targeted muscle reinnervation for real-time myoelectric control of multifunction artificial arms," *Journal of American Medical Association*, vol. 301, no. 6, pp. 619-628, 2009.
- [41] L. Hochberg, D. Bacher, B. Jarosiewicz, N. Masse, G. Simeral, J. Vogel and S. Haddadin, "Reach and grasp by people with tetraplegia using a neurally controlled robotic arm," *Nature*, vol. 485, no. 7398, pp. 372-375, 2012.
- [42] C. Antfolk, A. Björkman, S. O. Frank, F. Sebelius, G. Lundborg and B. Rosen, "Sensory feedback from a prosthetic hand based on air-mediated pressure from

- the hand to the forearm skin," *Journal of Rehabilitation Medicine*, vol. 44, no. 8, pp. 702-707, 2012.
- [43] M. Stanisa, F. Capogrosso, M. Petrini, M. Bonizzato, J. Rigosa, G. Di Pino and J. Carpaneto, "Restoring natural sensory feedback in real-time bidirectional hand prostheses," *Science Translational Medicine*, vol. 2, no. 222, pp. 19-222, 2014.
- [44] P. U. Jeethesh, N. P. Sarath, R. Sidharth, A. P. Kumar, S. Pramod and G. Udupa. "Design and manufacture of 3D printed myoelectric multi-fingered hand for prosthetic application," in *International Conference on Robotics and Automation for Humanitarian Applications (RAHA)*, Kerala, India, 2016.
- [45] M. S. Çelik, C. Tepe, H. Baş and İ. Eminoğlu, "Multifunctional hand prosthesis setup design," in *Medical Technologies National Congress (TIPTEKNO)*, Antalya, Turkey, 2016.
- [46] C. L. Semasinghe, J. L. B. Prasanna, H. M. Kandamby, R. K. P. S. Ranaweera, D. G. K. Madusanka and R. A. R. C. Gopura , "Transradial prostheses: Current status and future directions," in *Manufacturing & Industrial Engineering Symposium (MIES)*, Colombo, Sri Lanka, 2016.
- [47] R. A. M. Abayasiri, D. G. K. Madhusanka, N. M. P. Arachige, A. T. S. Silva and R. A. R. C. Gopura, "MoBio: A 5 DOF trans-humeral robotic prosthesis," in *2017 International Conference on Rehabilitation Robotics (ICORR)*, London, UK, 2017.
- [48] R. A. R. C. Gopura, D. S. V. Bandara, G. N. P. A, H. V. H and B. S. Ariyaratna, "A prosthetic hand with self-adaptive fingers Control," in *2017 3rd International Conference on Automation and Robotics (ICCAR)*, Nagoya, Japan, 2017.
- [49] S. Farah, D. G. Anderson and R. Langer, "Physical and mechanical properties of PLA, and their functions in widespread applications - A comprehensive review," *Advanced Drug Delivery Reviews*, vol. 107, pp. 367-392, 2016.
- [50] G. Gogu, "Chebychev–Grübler–Kutzbach's criterion for mobility calculation of multi-loop mechanisms revisited via theory of linear transformations," *European Journal of Mechanics - A/Solids*, vol. 24, no. 3, pp. 427-441, 2005.

- [51] J. S. Dai, Z. Huang and H. Lipkin, "Mobility of Overconstrained Parallel Mechanisms," *Journal of Mechanical Design*, vol. 128, no. 1, pp. 220-229, 2004.
- [52] F. C. Chen, S. Appendino, A. Battezzato, A. Favetto, M. Mousavi and F. Pescarmona, "Human Finger Kinematics and Dynamics," in *New Advances in Mechanisms, Transmissions and Applications*, Springer, pp. 115-122, 2014.
- [53] W. Licheng, K. Yanxuan and L. Xiali, "A fully rotational joint underactuated finger mechanism and its kinematics analysis," *International Journal of Advanced Robotic Systems*, vol. 13, no. 5, pp. 1-9, 2016.
- [54] K. H. Hunt, A. E. Samuel and P. R. McAree, "Special configurations of multi-finger multi-freedom grippers—A kinematic study," *The International Journal of Robotics Research*, vol. 10, no. 2, pp. 123-134, 1991.
- [55] C. R. Rocha, C. P. Tonetto and A. Dias, "A comparison between the Denavit–Hartenberg and the screw-based methods used in kinematic modeling of robot manipulators," *Robotics and Computer-Integrated Manufacturing*, vol. 27, no. 4, pp. 723-728, 2011.
- [56] P. I. Corke, "A simple and systematic approach to assigning Denavit–Hartenberg parameters," *IEEE transactions on robotics*, vol. 23, no. 3, pp. 590-594, 2007.
- [57] S. Singh, A. Singla, A. Singh, S. Soni and S. Verma, "Kinematic modelling of a five-DOFs spatial manipulator used in robot-assisted surgery," *Perspectives in Science*, vol. 8, pp. 550-553, 2016.
- [58] J. Dupuis, C. Holst and H. Kuhlmann, "Improving the kinematic calibration of a coordinate measuring arm using configuration analysis," *Precision Engineering*, vol. 50, pp. 171-182, 2017.
- [59] Z. Du, W. Yang and W. Dong, "Kinematics modeling of a notched continuum manipulator," *Journal of Mechanisms and robotics*, vol. 7, no. 4, pp. 1-9, 2015.
- [60] P. Boscarriol, A. Gasparetto, L. Scalera and R. Vidoni, "Efficient closed-form solution of the kinematics of a tunnel digging machine," *Journal of Mechanisms and Robotics*, vol. 9, no. 3, pp. 1-13, 2017.

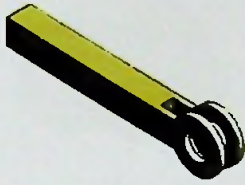
- [61] J. Li, L. D. Yu, J. Q. Sun and H. J. Xia, "A kinematic model for parallel-joint coordinate measuring machine," *Journal of Mechanisms and Robotics*, vol. 5, no. 4, pp. 1-4, 2013.
- [62] H. Lipkin, "A note on Denavit-Hartenberg notation in robotics," in *ASME International Design Engineering Technical Conferences and Computers and Information in Engineering Conference*, California, USA, 2005.

APPENDIX I

Appendix I: Components of the linkage mechanism



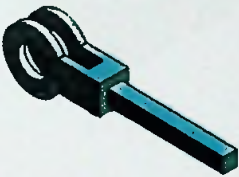
PPT1



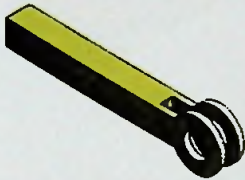
PPT2



PPM



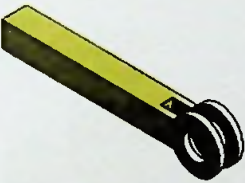
PPB1



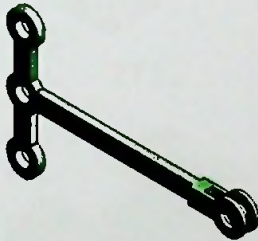
PPB2



IPT1



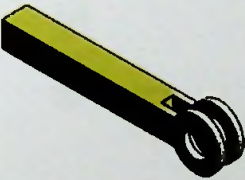
IPT2



IPM



IPB1



IPB2



DP

APPENDIX II

Appendix II: Components of the finer mechanism



PPT1



PPT2



PPM1



PPM2



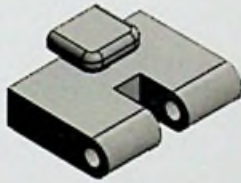
PPB1



PPB2



IPT1



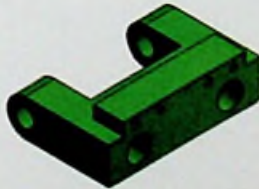
IPT2



IPM1



IPM2



IPB1



IPB2



DP1



DP2



LG

APPENDIX III

Appendix III: Matlab codes used to generate 3D plots

Matlab code to determine X coordinate of Point D:

```
[CD,DG] = meshgrid(33:.2:40);
AB=40;
AC=10;
BD=10;
BH=40;
GH=10;
HJ=30;
JK=9;
A1=((CD.^2-AB.^2-AC.^2-BD.^2)/((-2)*BD*(sqrt(AB.^2+AC.^2))));
D1=atan(AC/AB);
T1=asin(A1)-D1;
A2=((DG.^2-BH.^2-BD.^2-GH.^2)/((-2)*GH*(sqrt(BH.^2+BD.^2))));
D2=atan(BD/BH);
T2=asin(A2)-D2;
XD=(-BD*sin(T1))+AB;
surf(CD,DG,XD)
xlabel('CD Distance, mm')
ylabel('DG Distance, mm')
zlabel('X Coordinate of Point D')
```

Matlab code to determine Y coordinate of Point D:

```
[CD,DG] = meshgrid(33:.2:40);
AB=40;
AC=10;
BD=10;
BH=40;
GH=10;
HJ=30;
JK=9;
A1=((CD.^2-AB.^2-AC.^2-BD.^2)/((-2)*BD*(sqrt(AB.^2+AC.^2))));
D1=atan(AC/AB);
T1=asin(A1)-D1;
A2=((DG.^2-BH.^2-BD.^2-GH.^2)/((-2)*GH*(sqrt(BH.^2+BD.^2))));
D2=atan(BD/BH);
T2=asin(A2)-D2;
YD=(BD*cos(T1));
surf(CD,DG,YD)
xlabel('CD Distance, mm')
ylabel('DG Distance, mm')
zlabel('Y Coordinate of Point D')
```

Matlab code to determine X coordinate of Point G:

```

[CD,DG] = meshgrid(33:.2:40);
AB=40;
AC=10;
BD=10;
BH=40;
GH=10;
HJ=30;
JK=9;
A1=((CD.^2-AB.^2-AC.^2-BD.^2)/((-2)*BD*(sqrt(AB.^2+AC.^2))));
D1=atan(AC/AB);
T1=asin(A1)-D1;
A2=((DG.^2-BH.^2-BD.^2-GH.^2)/((-2)*GH*(sqrt(BH.^2+BD.^2))));
D2=atan(BD/BH);
T2=asin(A2)-D2;
XG=(-GH*sin(T1+T2))+(BH*cos(T1))+AB;
surf(CD,DG,XG)
xlabel('CD Distance, mm')
ylabel('DG Distance, mm')
zlabel('X Coordinate of Point G')

```

Matlab code to determine Y coordinate of Point G:

```

[CD,DG] = meshgrid(33:.2:40);
AB=40;
AC=10;
BD=10;
BH=40;
GH=10;
HJ=30;
JK=9;
A1=((CD.^2-AB.^2-AC.^2-BD.^2)/((-2)*BD*(sqrt(AB.^2+AC.^2))));
D1=atan(AC/AB);
T1=asin(A1)-D1;
A2=((DG.^2-BH.^2-BD.^2-GH.^2)/((-2)*GH*(sqrt(BH.^2+BD.^2))));
D2=atan(BD/BH);
T2=asin(A2)-D2;
YG=(GH*cos(T1+T2))+(BH*sin(T1));
surf(CD,DG,YG)
xlabel('CD Distance, mm')
ylabel('DG Distance, mm')
zlabel('Y Coordinate of Point G')

```

Matlab code to determine X coordinate of Point K:

```

[CD,DG] = meshgrid(33:.2:40);
AB=40;
AC=10;
BD=10;
BH=40;

```




```

GH=10;
HJ=30;
JK=9;
A1=((CD.^2-AB.^2-AC.^2-BD.^2)/((-2)*BD*(sqrt(AB.^2+AC.^2))));
D1=atan(AC/AB);
T1=asin(A1)-D1;
A2=((DG.^2-BH.^2-BD.^2-GH.^2)/((-2)*GH*(sqrt(BH.^2+BD.^2))));
D2=atan(BD/BH);
T2=asin(A2)-D2;
XK=(HJ*cos(T1+T2))-(JK*sin(T1+T2))+(BH*cos(T1))+AB;
surf(CD,DG,XK)
xlabel('CD Distance, mm')
ylabel('DG Distance, mm')
zlabel('X Coordinate of Point K')

```

Matlab code to determine Y coordinate of Point K:

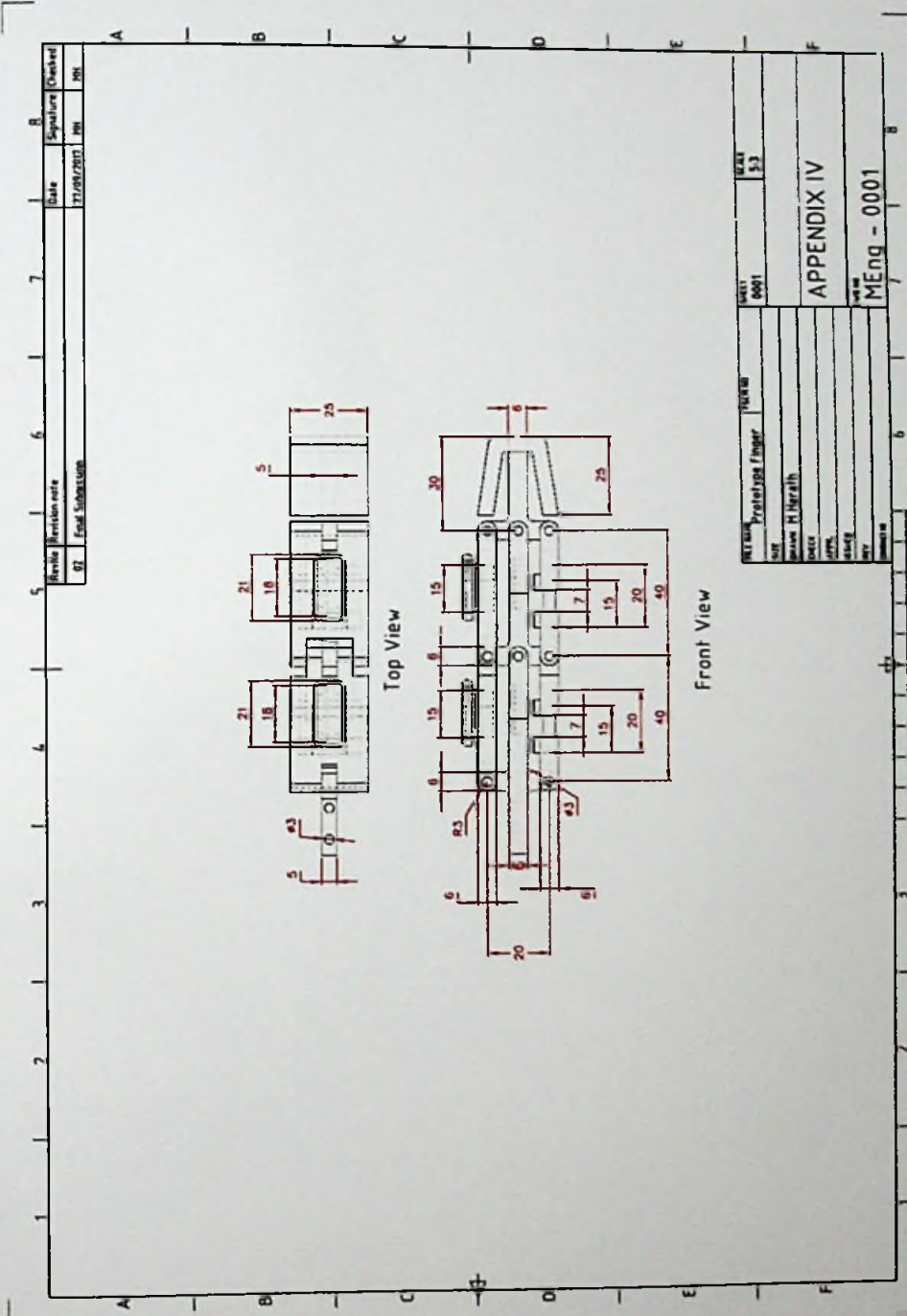
```

[CD,DG] = meshgrid(33:.2:40);
AB=40;
AC=10;
BD=10;
BH=40;
GH=10;
HJ=30;
JK=9;
A1=((CD.^2-AB.^2-AC.^2-BD.^2)/((-2)*BD*(sqrt(AB.^2+AC.^2))));
D1=atan(AC/AB);
T1=asin(A1)-D1;
A2=((DG.^2-BH.^2-BD.^2-GH.^2)/((-2)*GH*(sqrt(BH.^2+BD.^2))));
D2=atan(BD/BH);
T2=asin(A2)-D2;
YK=(HJ*sin(T1+T2))+(JK*cos(T1+T2))+(BH*sin(T1));
surf(CD,DG,YK)
xlabel('CD Distance, mm')
ylabel('DG Distance, mm')
zlabel('Y Coordinate of Point K')

```

APPENDIX IV

Appendix IV: Detail drawing of the finger



Revisio	Revisio	Revisio	Revisio	Revisio	Revisio	Revisio	Revisio
01	02	03	04	05	06	07	08
Final Submissio							
Date	Signature	Date	Signature	Date	Signature	Date	Signature
17/09/2013							

Project Name	Project No	Scale
Prototype Finger	0001	1:1
Author	Checked	Drawn
Shanm R Ngrath		
Checked	Approved	Project No
		APPENDIX IV
Checked	Approved	Project No
		MEng - 0001

